The Role of OPDA Signaling in Induced Systemic Defenses Against Biotic and Abiotic Stresses

by

Simrandeep Kaur

A thesis submitted to the Graduate Faculty of
Auburn University
in partial fulfillment of the
requirements for the Degree of
Master of Science

Auburn, Alabama
August 3, 2024

Keywords: plant growth-promoting rhizobacteria, plant defense, induced systemic resistance, OPDA, circadian rhythm, growth and defense tradeoff.

Approved by

Dr. Sang-Wook Park, Chair, Associate professor of Plant Pathology
Dr. Aaron Rashotte, Professor of Biology Sciences
Dr. Sung-Hwan Kang, Assistant professor of Plant Pathology

Abstract

Plants are vulnerable to a range of biotic and abiotic stressors, which hinder their growth and reduce agricultural yield. Existing management strategies fall short, lacking durable resistant/tolerant cultivars and nontoxic, low-cost pesticides, necessitating an urgent breakthrough, which is not necessarily forthcoming due to an incomplete understanding of plant defense mechanisms and plant growth and defense tradeoffs, a major problem in genetic engineering for plant stress resilience. To understand if and how plants co-ordinate growth and defense responses, we exploited the role and mode of plant growth-promoting rhizobacteria (PGPR)-mediated 'induced systemic resistance (ISR) and tolerance (IST),' phenomena capable of priming broad-spectrum durable resistances without the usually accompanied growth penalty to biotic and abiotic stresses, respectively. This study describes that 12-oxophytodienoic acid (OPDA) acts as ***i***) local defense and ***ii***) long-distance phloem-mobile systemic defense signals in ISR, stimulating the cyclophilin 20-3 (CYP20-3)-mediated activation of two-component system, consisting of glutaredoxin transcriptional regulators (e.g., GRX480) and TGA transcription factors (e.g., TGA2, TGA5, TGA6). The GRX/TGA pathway then recruits the *nonexpresser of PR1 (NPR1)* and conveys both OPDA and salicylic acid (SA) signaling, which prime disease resistance in local and systemic tissues against a broad range of pathogens, including bacterial and fungal microbes and plant parasitic nematodes. Besides biotic stresses, the crosstalk between OPDA and SA signaling simultaneously runs 'growth and defense machinery' against abiotic stresses, especially drought. Recently, we have identified two drought-responsive genes, *RESPONSIVE TO DESICCATION 29 (RD29)A and RD29B,* which are located downstream of the GRX/TGA system, playing an important

role in IST development. In the present study, we also found −for the first time− that plants can coordinate cellular multitasking by the circadian rhythmic expression of *RD29A*, which acts as a noncanonical esterase/hydrolase, and relay CYP20-3/OPDA signaling in priming IST against drought. Although *RD29B* is also induced by PGPR, we found it to be physiologically distinct from *RD29A*, acting as a constitutive gene positioned upstream and controlling RD29A-dependent/independent defense responses. Together, we hypothesize CYP20-3-dependent OPDA signaling as a key node helping balance growth and defense against various stresses, synergistically optimizing plant fitness.

Acknowledgments

I would like to extend my gratitude to my major advisor, Dr. Sang-Wook Park, for giving me the opportunity to pursue a master's degree at Auburn University and for providing invaluable guidance and knowledge throughout my graduate studies. It has been a privilege to learn and conduct research under his supervision. I would also like to thank my committee members, Dr. Aaron Rashotte and Dr. Sung Hwan Kang, for their insightful guidance, support, and critical feedback on my research. Additionally, I extend my thanks to my colleagues who have assisted me with experimental procedures and my friends for their encouragement throughout the journey. Finally, I would like to express my deepest gratitude to my parents, Jaspal Singh and Rajwinder Kaur, and my brother, Gagandeep Singh, for their unwavering support throughout this journey. This thesis is dedicated to my mom and dad; your endless love, encouragement, and sacrifices mean the world to me. Thank you for being my pillars of strength.

Table of Contents

List of Tables

List of Figures

CHAPTER 1: INTRODUCTION AND REVIEW OF LITERATURE

Annual crop losses to plant pathogens, estimated at about $220 billion USD, pose a significant challenge in meeting the food demands of a fast-growing population, which is projected to increase by 50% by 2050 (FAO 2022). This challenge largely stems from the extensive use of traditional introgressive breeding methods in the past century of monoculture, incorporating resistance (R) genes from wild plants into commercial crops (Huang et al., 2023). However, this resistance isn't durable as pathogens evolve rapidly, overcoming resistance conferred by individual R genes (Miller et al., 2017). Additionally, plant defense responses to pathogens are often accompanied by growth retardation, a major pitfall in the genetic engineering of disease resistance (He et al., 2022). Chemical pesticides, with their toxic properties and high costs that far outweigh their benefits, aren't viable solutions either (Rani et al., 2021). Therefore, understanding the plant's basic defense mechanism is crucial for upgrading the plant's defense response for effective, long-term, durable disease management against rapidly evolving pathogens without growth penalty.

Plants possess two main types of innate immune responses: local and systemic resistance. The local resistance is the intrinsic development of disease resistance at the site of infections. It begins with plant pattern recognition receptors detecting conserved microbial features, known as pathogen-associated molecular patterns (PAMPs), leading to PAMP-triggered immunity (PTI), the first line of defense (Schwessinger et al., 2008). Pathogens, in turn, secrete virulence-associated molecules called the effectors to suppress host PTI. Nevertheless, plants' immune systems have evolved to recognize these effectors by R protein, activating effector-triggered immunity (ETI), the second layer of immunity leading to a hypersensitive response, which is a rapid development of necrosis at the site of infections limiting pathogen growth and spread (Cui et al., 2015). In contrast, systemic resistance is the state of enhanced defensive capacity in the unaffected tissues developed throughout a whole plant when appropriately primed. It is of two types- Systemic Acquired Resistance (SAR) triggered by pathogenic microbes and Induced Systemic Resistance (ISR) elicited by beneficial microbes (Kamle et al., 2020).

This review will focus on understanding systemic plant resistance, as it provides long-lasting and broad-spectrum disease resistance compared to local resistance.

SAR was discovered in 1961 as a "whole plant" resistance response against a wide range of pathogens triggered by prior localized exposure to pathogenic microbes (Ross et al., 1961). This defense mechanism majorly relies on salicylic acid (SA), involving SA accumulations in both the infected primary tissue and systemic tissues along with the activation of pathogenic-related (PR) genes, which relies on *NONEXPRESSOR OF PR1* (*NPR1*), a well-known transcription activator of SA signaling pathway (Ali et al., 2018). Subsequently, several long-distance mobile signals were identified for inducing SAR that travel from infected to systemic tissue via the phloem to prime systemic tissue against future infections by a broad spectrum of pathogens, such as azelaic acid, dehydroabietinal, glycerol-3-P, methyl salicylate, and pipecolic acid (Klessig et al., 2018). In contrast, ISR by beneficial microbes was first discovered in 1991 (ALSTRÖM et al., 1991; Kloepper et al., 1991; Van Peer et al., 1991). Since beneficial microbes promote plant growth along with inducing systemic resistance, ISR helps coordinate the plants' growth and defense responses, which involves Jasmonic acid (JA) and ethylene (ET) signaling pathways (Naik et al., 2019; Pieterse et al., 1998). Surprisingly, *NPR1,* crucial for SA signaling and SAR, was also critical for ISR development, while SA biosynthesis plays no role in ISR (Pieterse et al., 1998). This enigma has long puzzled researchers, compounded by the absence of a known long-distance mobile signal molecule for ISR priming systemic tissues. However, recent studies conducted by our team and Wang et al. (2020a,b) have shed light on the emerging role of OPDA, which can serve as a potential mobile signal for ISR and can induce *NPR1*-dependent SA signaling pathway independent of SA.

While the phenomenon of SAR has been extensively explored, with numerous reviews available, limited attention has been given to reviewing and identifying research gaps in the known molecular signaling mechanism of ISR. Thus, our review highlights current developments and points out significant knowledge gaps about this phenomenon. It focuses on the direct and indirect mechanisms of beneficial microbes inducing ISR in promoting plant growth, ISR priming, and long-distance ISR signaling. Additionally, it explores the role of transcription factors, iron-deficiency response, key signaling

molecules such as OPDA, JA, ET, and *NPR1* in ISR development. The review provides insights into the relevance of ISR for plant defense and growth, with implications for agricultural practices.

1.1. What is Induced Systemic Resistance (ISR)

ISR is a physiological state of enhanced defensive capacity induced by beneficial microbes whereby the plant's innate defenses are potentiated against subsequent biotic challenges without the usually accompanied growth penalty. It is mostly induced by plant growth-promoting microbes (PGPMs) that are further classified into plant growth-promoting rhizobacteria (PGPR) and plant growth-promoting fungi (PGPF) (Olowe et al., 2020).

1.2. ISR inducers

1.2.1. Plant-growth-promoting rhizobacteria (PGPR)

Bacteria that inhabit plant roots are classified based on their location relative to the roots. The categories include (1) rhizosphere bacteria, dwelling in the soil surrounding the roots; (2) rhizoplane bacteria, colonizing the surface of the roots; (3) endophytes, occupying spaces between root cortical cells; (4) rhizobia or Frankia sp., residing within cells in specialized root structures, or nodules (Glick 1995). Regardless of their category and if they contribute to plant growth, these bacteria are identified as PGPR and are mostly gram-positive, soil-borne bacteria. Vessey (2003) proposed a different classification, suggesting that the first three groups be referred to as extracellular PGPR (ePGPR), for example, *Bacillus, Caulobacter, Pseudomonas, Serratia,* and the fourth group would be referred to as intracellular PGPR (iPGPR), including, for example, *Rhizobium* and *Bradyrhizobium.*

PGPR enhances plant growth through both direct and indirect mechanisms. Direct mechanisms involve improving the uptake of soil nutrients, such as nitrogen, phosphorus, and iron, which mostly exist in insoluble, immobilized, or inaccessible forms in the soil or atmosphere, posing challenges for plant absorption (Parewa et al., 2014). PGPR fixes nitrogen to ammonia form via nodule formation using the nitrogenase enzyme, chelates

iron by forming siderophores, and solubilizes inorganic phosphate to monobasic and dibasic forms via the phosphatase enzyme, which is readily assimilated by plants (Hider et al., 2010; Smith et al., 2004; Vessey et al., 2003). Additionally, it generates plant growth hormones like cytokinin, auxin, and gibberellins (Khan et al., 2020). Certain PGPR strains also possess the 1-aminocyclopropane-1-carboxylate (ACC) deaminase enzyme, which breaks down the ethylene precursor ACC into ammonia and α-ketobutyrate, helping plants counteract the adverse effects of ethylene stress, fostering plant growth (Gamalero et al., 2015).

On the other hand, indirectly, it prevents soil-borne phytopathogens by generating antimicrobial metabolites and hydrolytic enzymes like chitinase, protease, and lipase, facilitating the lysis of pathogenic bacteria and fungi (Khalil et al., 2002). It also strengthens plants without altering the plant's genome against various abiotic stresses like heat, salt, cold, drought, and flooding, called induced systemic tolerance, and against biotic stresses, including pathogens and insects, called induced systemic resistance (Sarma et al., 2012; Pieterse et al., 2014).

Research has demonstrated that certain PGPRs that enhance root growth cannot induce IST against drought (Liu et al., 2020). Additionally, Arabidopsis mutants and ISR-defective mutants exhibit similar alterations in root morphology when exposed to PGPR (Zamioudis et al., 2013). Together, this suggests the independence of IST or ISR mechanisms and root growth promotion.

1.2.2. Plant Growth Promoting Fungi (PGPF)

Plant growth-promoting fungi (PGPFs) are a heterogeneous group of non-pathogenic naturally occurring saprophytic fungi that can be obtained in the rhizosphere, at the root surfaces, or inside the roots of plants (Hossain et al., 2017). These fungi can also establish symbiotic relationships with the plant's roots, forming mycorrhiza, which can be ectomycorrhizae (forming a sheath around the root) or endomycorrhizal (penetrating the root cells) (López-Ráez et al., 2012). Examples are Gliocladium, Penicillium, Phoma, Phytophthora, Rhizoctonia, Talaromyces, Arbuscular mycorrhizal fungi, and *Trichoderma* (Hossain et al., 2024). Like PGPR, PGPF also stimulates the growth and development of plants by producing growth hormone, ACC deaminase,

siderophore, secondary metabolites, better solubilization of nutrients, and inducing ISR in plants (Adedayo et al., 2023).

1.3. What do we know about jasmonate and SA pathways so far?

Two key defense hormones, JA and SA, play crucial roles in plant defense mechanisms against various stresses (**Fig 1.1**). SA primarily defends against biotrophic and semi-biotrophic pathogens (Chen et al., 2019). Its biosynthesis initiates in the chloroplast, where chorismate is converted via isochorismate synthase and phenylalanine ammonia-lyase pathways, yielding isochorismate and phenylalanine. These compounds then form physiologically active SA (Lefevere et al., 2020). SA then activates and monomerizes *NPR1*, the transcription activator of the SA signaling pathway, in the cytosol, allowing them to travel to the nucleus. It further activates TGA transcription factors, which induce SA-dependent defense gene expressions, including *PR1, PR2*, and *PR5* (Johnson et al., 2003).

In contrast, JA biosynthesis is activated by necrotrophic pathogens, insect pests, and abiotic stresses and occurs via the octadecanoid pathway (Macioszek et al., 2023). When stressed, trienoic-fatty acids from chloroplast membranes like linolenic acid (18:3) undergo lipase-mediated oxidation to 12-oxo-phytodienoic acid (OPDA), that travels to peroxisomes and undergoes β-oxidations to form JA. JA is further released to the cytosol, conjugating to isoleucine to form jasmonic acid-isoleucine (JA-Ile) (Griffiths et al., 2020). Only JA-Ile and OPDA are physiologically active as signals among all the jasmonates (Dave et al., 2012; Howe et al., 2001). JA-Ile binds to its receptor, CORONATINE INSENSITIVE 1 (COI1), forming a complex that further binds and ubiquitinates jasmonate ZIM-domain (JAZ) proteins, which are negative transcription regulators of JA-responsive genes (JRGs). Thus, JAZ degradation by 26S proteasomes enables MYC activators to interact directly with MED25, which frees transcription factors and allows subsequent gene expressions (Chini et al., 2009). On the other hand, our group has shown that some OPDA can bind to its receptor, Cyclophilin 20-3, activating OPDA-responsive defense gene activation (Park et al., 2013).

1.4. Current understanding of the signaling mechanism of ISR

In contrast to SAR, very little information is known about the signaling mechanism of the ISR. About 25 years ago, one breakthrough study revealed that ISR and SAR employ different cellular mechanisms, and on top of that, ISR uses a jasmonate-dependent, SA-independent, *NPR1* signaling pathway. This study demonstrated the absence of ISR triggered by *P. fluorescens* WCS417r in Arabidopsis mutants defective in JA signaling, *jar1,* and ethylene (ET)-signaling, *etr1,* when challenged with *P. syringae* pv tomato (Pieterse et al., 1998). This shows the importance of JA and ET signaling in ISR induction, which is confirmed by subsequent research using various PGPR across different crop species like Arabidopsis, rice, and tomato (De Vleesschauwer et al., 2008; Hase et al., 2008; Lavicoli et al., 2003; Stein et al., 2008; Yan et al., 2002). Moreover, Methyl Jasmonate application didn't protect *etr1-1* plants, but ethylene precursor 1-aminocyclopropane-1-carboxylic acid (ACC) treatment induced resistance in the *jar1*, suggesting that jasmonate signaling acts upstream of ethylene signaling to initiate a defense reaction. Surprisingly, ISR was induced in the SA biosynthesis mutant, *NahG,* but not in the SA signaling mutant, *npr1.* Hence, unlike SAR, SA accumulation is not required in ISR; instead, the defense reaction is regulated by *NPR1*, a widely known transcriptional co-activator of SA-responsive genes in SAR (Pieterse et al., 1998). However, the *PR1* gene, whose expression is dependent on NPR1, was not induced after PGPR inoculation. Nevertheless, later studies demonstrated various ISR-inducing PGPR strains that also activate PR1 promoters in transgenic tobacco lines expressing the β-glucuronidase gene, which was later found to induce resistance independent of salicylic acid (Park et al., 2000; Zhang et al., 2002). Additional research has further demonstrated that PGPMs can induce *NPR1*-dependent *PR1* gene expression (Ilham et al., 2019; Samaras et al., 2021; Tjamos et al., 2005). This SA-independent activation of *NPR1*-dependent SA signaling has set the scientific community abuzz. However, the mode is not known yet, though their study clearly suggests that *NPR1* is a molecular hub for ISR and SAR development, although they probably use different molecular pathways.

There are some exceptions to this study where the beneficial microbes, especially Trichoderma, triggered ISR independent of JA and ET but dependent on SA accumulations (Contreras-Cornejo et al., 2011; Hossain et al., 2017; Martínez-Medina et

al., 2013; van de Mortel et al., 2012; Yuan et al., 2019). These PGPMs are likely expected to follow a SAR signaling mechanism (Pieterse et al., 2014). On the other hand, other studies have claimed that PGPR can produce SA that can trigger systemic resistance (Maurhofer et al., 1998). However, later studies demonstrated that PGPR-produced SA becomes part of siderophores containing SA moieties under iron-limiting conditions, rendering it unavailable to trigger a defense response (Audenaert et al., 2002; Djavaheri et al., 2012; Press et al., 1997). Interestingly, the combined activation of SAR and ISR pathways had an additive effect against *P. syringae* pv tomato in a manner dependent on *NPR1*, indicating both pathways do not compete for *NPR1* (Van Wees et al., 2000). Nevertheless, no progress has been made so far on how JA or ET can activate *NPR1* in an SA-independent manner.

1.5. ISR priming: an inconspicuous preparation for future infections in systemic tissue

ISR enhances the defensive capacity of the whole plant on PGPM inoculations, preparing systemic tissues for subsequent pathogen or insect attacks, resulting in stronger and faster activation of cellular defenses. This process is known as priming (Conrath et al., 2006). For instance, it has been found that ISR induction by PGPR leads to the potentiated expression of Jasmonate and ethylene-responsive genes and their transcriptional regulators from the AP2/ERF family upon subsequent pathogen infections (Van der Ent et al., 2009; Van Wees et al., 1999; Verhagen et al., 2004). Enhanced induction of *HEL* and *PDF1.2* was particularly observed in ISR-induced Arabidopsis upon following attack by ISR-sensitive herbivore *Spodoptera exigua* compared to ISR-non-sensitive *Pieris rapae* (Oosten et al., 2008). PGPR treatment is also known to induce structural barriers upon pathogen attack; for example, treatment of *P. fluorescens* and *Bacillus subtilis* leads to enhanced callose depositions and stomata closure in Arabidopsis against *Hyaloperonospora arabidopsidis* and *P. syringae* pv tomato, respectively (Van der Ent et al., 2009; Kumar et al., 2012). Studies indicate that the expenses associated with this priming are less than those of constitutively activated defenses due to growth and defense trade-offs (van Hulten et al., 2006).

1.6. Mobile signaling in ISR

Numerous long-distance signaling molecules governing SAR have been uncovered, yet the mystery of long-distance signaling in ISR remains to be unraveled (Klessig et al., 2018). Different root-specific genes and molecules have been discovered in the quest for identifying mobile signals. For instance, the R2R3 type transcription factor, *MYB72*, was demonstrated to be essential for ISR induction at the root interface (Verhagen et al., 2004). Its expression is strongly induced in local root tissue after treatment with *P. fluorescens* and *Trichoderma*, and the absence of *MYB72* in the knockout (KO) mutant leads to defective ISR development (Alizadeh et al., 2013; Segarra et al., 2009; Van der Ent et al., 2008). However, the overexpression of MYB72 did not enhance the ISR response, suggesting that MYB72 alone is insufficient or requires other components to induce ISR. *MYB72* is typically induced in root tissues under iron-limiting conditions; however, even when plants are not experiencing iron stress, ISR-inducing *Pseudomonas* strains trigger the induction of iron deficiency marker genes (Palmer et al., 2013). This contrasts with wild-type plants treated with non-ISR inducer *P. fluorescens* WCS374r or ISR defective-*myb72* mutants treated with ISR-inducing *Pseudomonas* strains. Hence, it should be explored if *MYB72* or iron deficiency response plays a role in the generation or transduction of ISR mobile signal.

Another study has demonstrated that ISR specifically requires functional ethylene signaling in the roots or at the site of PGPR inoculation, as indicated by the absence of ISR in *eir1-1* and *axr1-12* mutants, which have impaired ethylene perception in roots but normal signaling in leaves. Additionally, ISR was induced when PGPR was pre-inoculated in the systemic tissue/ leaves in *eir1-1*, in contrast to roots where pre-inoculation of PGPR did not induce ISR in systemic leaf tissue (Knoester et al., 1999). ACC treatment on leaves induced ISR in WT but not in ethylene-insensitive mutant, *etr1*, highlighting the necessity of ethylene signaling in systemic tissue also for ISR development. This together suggests that ethylene signaling may directly or indirectly contribute to generating a mobile signal of ISR. However, ET biosynthesis or hormone-responsive genes were not induced in the root or leaf tissues following PGPR treatment but were activated after pathogen treatment, suggesting ET signaling might not be necessary to develop a primed state just after PGPR treatment, which requires the movement of a mobile signal from

primary to systemic tissues, but is required to develop ISR after a pathogen challenge to initiate a defense response (Pieterse et al., 1998; Van der Ent et al., 2009). This implies that it itself may not function as a mobile signal. However, similar to SAR, it is also possible that ISR involves more than one mobile signal.

1.6.1. Can JA activate ET or NPR1-mediated signaling transduction pathway?

NPR1 is known to regulate JA-signaling negatively by physically interacting with MYC2, which disrupts its binding with the MED25 Mediator subunit, leading to the suppression of JA-responsive genes (Nomoto et al., 2021; Spoel et al., 2003). This indicates an inverse relationship between NPR1 and JA. Surprisingly, MeJA, a derivative of JA, also inhibits the ET pathway (Clay et al., 2009), whereas OPDA, a JA precursor, activates it, inducing ethylene biosynthesis and receptor genes (Varsani et al., 2019). These findings suggest that JA might not play a role in triggering ET or NPR1-mediated signaling after PGPR inoculation.

1.6.2. OPDA is a new kid on the block!

Wang et al. (2020a,b) proposed that OPDA, rather than JA, may serve as the mobile signal for ISR, priming the systemic tissues. It was induced in the roots, leaves, and xylem tissues of ISR-positive maize plants but not in ISR-negative mutants when treated with ISR-inducible PGPF, T*richoderma virens* WT (*Tv*WT), and *TvΔsir1,* compared to non-ISR inducible PGPF, *TvΔsm1*. Also, OPDA deficiency in *lox10-3* mutant leads to defects in ISR development against *Colletotrichum graminicola.* At the same time, transfusion of the sap supplemented with increasing OPDA concentrations in the WT maize plants led to increased resistance in a dose-dependent manner. This OPDA-enriched sap could also restore ISR in ISR-defective *lox10-3* maize mutants when treated with *Tv*WT or *TvΔsm1*. In fact, pre-treating leaves with OPDA has been shown to provide resistance to various pathogens and herbivores, indicating that OPDA is capable of priming resistance against a broad range of biotic stresses (Fernández-Crespo et al., 2017; Scalschi et al., 2015; Varsani et al., 2019; Wang et al., 2020b). Conversely, transfusion with JA led to enhanced susceptibility, and the JA-deficient mutant could still

induce ISR. Henceforth, OPDA steps into the spotlight as a long-distance signal for ISR, revolutionizing our understanding.

1.6.2.1 Can insights from monocot long-distance signaling apply to other crops?

The caveat in the maize study by Wang et al. (2020a,b) is that maize is a monocot, which doesn't have a well-developed vascular system that may not completely be able to explain phloem movement of long-distance signals in most of the crop systems that are dicots (Zimmermann et al. 1972). Scattered vascular bundles throughout the stem in monocots complicate the tracing of the signal.

1.6.2.2 OPDA: A Mobile Signal in Dicots Activating NPR1-dependent SA Signaling Pathway

Interestingly, our recent research sheds light on the role of OPDA as a mobile signaling molecule in ISR in dicot model plant systems as well. We observed that local root tissues of both Arabidopsis and cotton plants induce and activate OPDA and JA-Ile signaling, as well as trigger SA signaling, without producing SA. Meanwhile, systemic leaf tissues activate OPDA (but not JA-Ile) and SA signaling, yet there is no de-novo synthesis of OPDA, JA-Ile, or SA. Indeed, OPDA hormone was enriched in phloem sap after PGPR treatment. These results suggest that OPDA produced in root tissues travels via phloem cells to leaf tissues, activating OPDA signaling without converting to JA/JA-Ile. Furthermore, we also found that OPDA, but not JA, upregulates SA-independent SA signaling marker genes via the *NPR1*-dependent pathway through GRX transcriptional regulators and TGA transcriptional factors. In fact, Arabidopsis mutants *cyp20-3, npr1,* and *grx480,* but not *NahG*, were also defective in ISR development. We also found *jar1* plants have a negative feedback loop suppressing OPDA and JA-Ile biosynthesis after PGPR treatment. Consequently, the ISR deficiency observed in *jar1* mutants by various researchers may stem from their inability to induce OPDA after PGPR treatment.

This discovery resolves a longstanding mystery about how PGPR can activate SA signaling without triggering its biosynthesis. Hence, it reveals that ISR relies on the accumulation of OPDA in local tissues, which moves to systemic tissues to activate GRX-mediated OPDA and SA response pathways. OPDA induces phloem-localized resistance

against corn leaf aphids in dicots by enhancing the sieve element's callose deposition, also suggesting the phloem's role in ISR signal transmission (Varsani et al., 2019). OPDA, but not JA, has also been found to act as a mobile signal in wounding from shoot-to-root transportation, indicating this hormone can move basipetally and acropetally (Schulze et al., 2019).

1.7. CONCLUSION AND FUTURE DIRECTIONS

Since the discovery in 1991 that certain PGPMs can trigger systemic resistance, a significant amount of information about the ISR has been amassed over the past three decades. It has been well-established that PGPM-induced ISR can help coordinate growth and defense trade-offs. This opens up prospects of exploring its mechanism further, as it offers opportunities for natural biological control, increased food production with reduced fertilizer and pesticide use, and the potential to genetically engineer crops for durable disease resistance without hindering growth. Yet, various questions still need to be answered regarding how PGPMs can potentiate whole plants against future infections. Initial progress has been achieved in deciphering the molecular communication between plant's systemic tissues and roots colonizing-ISR-triggering microbes, which have suggested the important role of NPR1, jasmonate, and ET pathways in ISR. It is also proposed that OPDA is a node of convergence potentially acting as a mobile signal in the ISR signaling pathway in both monocots and dicots triggered by different PGPMs. Nevertheless, substantial gaps remain to be addressed. For instance, conducting a grafting study using mutants with defects in various hormonal biosynthesis pathways as rootstock and wild-type scions could determine the importance of OPDA generation in roots for ISR development in systemic tissue and verify OPDA's movement to systemic tissues. Also, after PGPR inoculation, OPDA-responsive genes are induced in systemic tissue even without de-novo biosynthesis of jasmonates; however, JA or ET-responsive genes are potentiated after the challenge inoculation. So, it would be interesting to test if OPDA, accumulated in systemic tissue after PGPR inoculation, is converted to JA, inducing JA and ET signaling following a pathogen attack. Biochemical studies exploring interactions between OPDA and GRX or TGA transcription

factors could reveal how OPDA regulates the activation of SA-responsive genes through GRX.

1.8. REFERENCES

Adedayo, A.A., & Babalola, O.O. (2023). Fungi that promote plant growth in the rhizosphere boost crop growth. Journal of Fungi, 9(2), 239.

Ali, A., Shah, L., Rahman, S., Riaz, M.W., Yahya, M., Xu, Y.J., Liu, F., Si, W., Jiang, H., & Cheng, B. (2018). Plant defense mechanism and current understanding of salicylic acid and *NPRs* in activating SAR. Physiological and molecular plant pathology, 104, 15-22.

Alizadeh, H., Behboudi, K., Ahmadzadeh, M., Javan-Nikkhah, M., Zamioudis, C., Pieterse, C.M., & Bakker, P.A. (2013). Induced systemic resistance in cucumber and *Arabidopsis thaliana* by the combination of *Trichoderma harzianum* Tr6 and *Pseudomonas* sp. Ps14. Biological control, 65(1), 14-23.

ALSTRÖM, S. (1991). Induction of disease resistance in common bean susceptible to halo blight bacterial pathogen after seed bacterization with rhizosphere pseudomonads. The Journal of General and Applied Microbiology, 37(6), 495-501.

Audenaert, K., Pattery, T., Cornelis, P., & Höfte, M. (2002). Induction of systemic resistance to *Botrytis cinerea* in tomato by *Pseudomonas aeruginosa* 7NSK2: role of salicylic acid, pyochelin, and pyocyanin. Molecular Plant-Microbe Interactions, 15(11), 1147-1156.

Chen, H., Clinton, M., Qi, G., Wang, D., Liu, F., & Fu, Z.Q. (2019). Connecting the dots: a new and complete salicylic acid biosynthesis pathway. Molecular Plant, 12(12), 1539-1541.

Chini, A., Boter, M., & Solano, R. (2009). Plant oxylipins: COI1/JAZs/MYC2 as the core jasmonic acid-signalling module. The FEBS journal, 276(17), 4682-4692.

Clay, N.K., Adio, A.M., Denoux, C., Jander, G., & Ausubel, F.M. (2009). Glucosinolate metabolites required for an Arabidopsis innate immune response. Science, 323(5910), 95-101.

Conrath, U., Beckers, G.J., Flors, V., García-Agustín, P., Jakab, G., Mauch, F., Newman, M.A., Pieterse, C.M.J., Poinssot, B., Pozo, M.J., Pugin, A., Schaffrath, U., Ton, J.,

Wendehenne, D., Zimmerli, L., & Mauch-Mani, B. (2006). Priming: getting ready for battle. Molecular plant-microbe interactions, 19(10), 1062-1071.

Contreras-Cornejo, H.A., Macías-Rodríguez, L., Beltrán-Peña, E., Herrera-Estrella, A., & López-Bucio, J. (2011). Trichoderma-induced plant immunity likely involves both hormonal-and camalexin-dependent mechanisms in *Arabidopsis thaliana* and confers resistance against necrotrophic fungi *Botrytis cinerea*. Plant signaling & behavior, 6(10), 1554-1563.

Cui, H., Tsuda, K., & Parker, J.E. (2015). Effector-triggered immunity: from pathogen perception to robust defense. Annual review of plant biology, 66, 487-511.

Dave, A., & Graham, I.A. (2012). Oxylipin signaling: a distinct role for the jasmonic acid precursor cis-(+)-12-oxo-phytodienoic acid (cis-OPDA). Frontiers in plant science, 3, 42.

De Vleesschauwer, D., Djavaheri, M., Bakker, P.A., & Höfte, M. (2008). *Pseudomonas fluorescens* WCS374r-induced systemic resistance in rice against *Magnaporthe oryzae* is based on pseudobactin-mediated priming for a salicylic acid-repressible multifaceted defense response. Plant physiology, 148(4), 1996-2012.

Djavaheri, M., Mercado-Blanco, J., Versluis, C., Meyer, J.M., Van Loon, L.C., & Bakker, P.A. (2012). Iron-regulated metabolites produced by *Pseudomonas fluorescens* WCS 374r are not required for eliciting induced systemic resistance against *Pseudomonas syringae* pv. tomato in Arabidopsis. Microbiology Open, 1(3), 311-325.

FAO. (2022). FAO's Plant Production and Protection Division. Rome. https://doi.org/10.4060/cc2447en

Fernández-Crespo, E., Navarro, J.A., Serra-Soriano, M., Finiti, I., García-Agustín, P., Pallás, V., & González-Bosch, C. (2017). Hexanoic acid treatment prevents systemic MNSV movement in Cucumis melo plants by priming callose deposition correlating SA and OPDA accumulation. Frontiers in Plant Science, 8, 1793.

Gamalero, E., & Glick, B.R. (2015). Bacterial modulation of plant ethylene levels. Plant physiology, 169(1), 13-22.

Glick, B.R. (1995). The enhancement of plant growth by free-living bacteria. Canadian journal of microbiology, 41(2), 109-117.

Griffiths, G. (2020). Jasmonates: biosynthesis, perception and signal transduction. Essays in Biochemistry, 64(3), 501-512.

Hase, S., Takahashi, S., Takenaka, S., Nakaho, K., Arie, T., Seo, S., Ohashi, Y., & Takahashi, H. (2008). Involvement of jasmonic acid signalling in bacterial wilt disease resistance induced by biocontrol agent *Pythium oligandrum* in tomato. Plant Pathology, 57(5), 870-876.

He, Z., Webster, S., & He, S.Y. (2022). Growth–defense trade-offs in plants. Current Biology, 32(12), R634-R639.

Hider, R.C., & Kong, X. (2010). Chemistry and biology of siderophores. Natural product reports, 27(5), 637-657.

Hossain, M.M. (2024). Upscaling plant defense system through the application of plant growth-promoting fungi (PGPF). In Microbial Technology for Agro-Ecosystems (pp. 61-95). Academic Press.

Hossain, M.M., Sultana, F., & Hyakumachi, M. (2017). Role of ethylene signalling in growth and systemic resistance induction by the plant growth-promoting fungus *Penicillium viridicatum* in Arabidopsis. Journal of Phytopathology, 165(7-8), 432-441.

Hossain, M.M., Sultana, F., & Islam, S. (2017). Plant growth-promoting fungi (PGPF): phytostimulation and induced systemic resistance. Plant-Microbe Interactions in Agro-Ecological Perspectives: Volume 2: Microbial Interactions and Agro-Ecological Impacts, 135-191.

Howe, G.A. (2001). Cyclopentenone signals for plant defense: remodeling the jasmonic acid response. Proceedings of the National Academy of Sciences, 98(22), 12317-12319.

Huang, K., Jahani, M., Gouzy, J., Legendre, A., Carrere, S., Lázaro-Guevara, J.M., González Segovia, E.G., Todesco, M., Mayjonade, B., Rodde, N., Cauet, S., Dufau, I., Staton, S.E., Pouilly, N., Boniface, M.C., Tapy, C., Mangin, B., Duhnen, A., Gautier, V., Poncet, C., Donnadieu, C., Mandel, T., Hübner, S., Burke, J.M., Vautrin, S., Bellec, A., Owens, G.L., Langlade, N., Muños, S., & Rieseberg, L.H. (2023). The genomics of linkage drag in inbred lines of sunflower. Proceedings of the National Academy of Sciences, 120(14), e2205783119.

Iavicoli, A., Boutet, E., Buchala, A., & Métraux, J.P. (2003). Induced systemic resistance in *Arabidopsis thaliana* in response to root inoculation with *Pseudomonas fluorescens* CHA0. Molecular plant-microbe interactions, 16(10), 851-858.

Ilham, B., Noureddine, C., Philippe, G., Mohammed, EG., Brahim, E., Sophie, A., & Muriel, M. (2019). Induced systemic resistance (ISR) in *Arabidopsis thaliana* by *Bacillus amyloliquefaciens* and *Trichoderma harzianum* used as seed treatments. Agriculture, 9(8), 166.

Johnson, C., Boden, E., & Arias, J. (2003). Salicylic acid and *NPR1* induce the recruitment of trans-activating TGA factors to a defense gene promoter in Arabidopsis. The Plant Cell, 15(8), 1846-1858.

Kamle, M., Borah, R., Bora, H., Jaiswal, A. K., Singh, R.K., & Kumar, P. (2020). Systemic acquired resistance (SAR) and induced systemic resistance (ISR): role and mechanism of action against phytopathogens. Fungal biotechnology and bioengineering, 457-470.

Khalil, M.S.M., Hassan, M.H.A.R., Mahmoud, A.F., & Morsy, K.M.M. (2022). Involvement of secondary metabolites and extracellular lytic enzymes produced by plant growth promoting rhizobacteria in inhibiting the soilborne pathogens in *Faba Bean* Plants. Jurnal Hama dan Penyakit Tumbuhan Tropika, 22(2), 100-108.

Khan, N., Bano, A., Ali, S., & Babar, M.A. (2020). Crosstalk amongst phytohormones from planta and PGPR under biotic and abiotic stresses. Plant Growth Regulation, 90, 189-203.

Klessig, D.F., Choi, H.W., & Dempsey, D.M.A. (2018). Systemic acquired resistance and salicylic acid: past, present, and future. Molecular plant-microbe interactions, 31(9), 871-888.

Kloepper, J.W., Tuzun, S., & Wei, G. (1991). Induction of Systemic Resistant of Cucumber to Colletrotichum orbicular by Select Strain of Plant Growth-Promoting Rhizobacteria. Pathology. Tersedia dalam: http://www.bashanfoundation. Org.

Knoester, M., Pieterse, C.M., Bol, J.F., & Van Loon, L.C. (1999). Systemic resistance in Arabidopsis induced by rhizobacteria requires ethylene-dependent signaling at the site of application. Molecular Plant-Microbe Interactions, 12(8), 720-727.

Kumar, A. S., Lakshmanan, V., Caplan, J.L., Powell, D., Czymmek, K.J., Levia, D.F., & Bais, H.P. (2012). Rhizobacteria *Bacillus subtilis* restricts foliar pathogen entry through stomata. The Plant Journal, 72(4), 694-706.

Iavicoli, A., Boutet, E., Buchala, A., & Métraux, J.P. (2003). Induced systemic resistance in *Arabidopsis thaliana* in response to root inoculation with *Pseudomonas fluorescens* CHA0. Molecular plant-microbe interactions, 16(10), 851-858.

Lefevere, H., Bauters, L., & Gheysen, G. (2020). Salicylic acid biosynthesis in plants. Frontiers in plant science, 11, 521987.

Liu, W., Sikora, E., & Park, S.W. (2020). Plant growth-promoting rhizobacterium, *Paenibacillus polymyxa* CR1, upregulates dehydration-responsive genes, *RD29A* and *RD29B*, during priming drought tolerance in arabidopsis. Plant Physiology and Biochemistry, 156, 146-154.

López-Ráez, J.A., Bouwmeester, H., & Pozo, M.J. (2012). Communication in the rhizosphere, a target for pest management. Agroecology and strategies for climate change, 109-133.

Macioszek, V.K., Jęcz, T., Ciereszko, I., & Kononowicz, A.K. (2023). Jasmonic acid as a mediator in plant response to necrotrophic fungi. Cells, 12(7), 1027.

Martínez-Medina, A., Fernández, I., Sánchez-Guzmán, M.J., Jung, S.C., Pascual, J.A., & Pozo, M.J. (2013). Deciphering the hormonal signalling network behind the systemic resistance induced by *Trichoderma harzianum* in tomato. Frontiers in Plant Science, 4, 206.

Maurhofer, M., Reimmann, C., Schmidli-Sacherer, P., Heeb, S., Haas, D., & Défago, G. (1998). Salicylic acid biosynthetic genes expressed in *Pseudomonas fluorescens* strain P3 improve the induction of systemic resistance in tobacco against tobacco necrosis virus. Phytopathology, 88(7), 678-684.

Miller, R.N.G., Costa Alves, G.S., & Van Sluys, M.A. (2017). Plant immunity: unravelling the complexity of plant responses to biotic stresses. Annals of Botany, 119(5), 681-687.

Naik, K., Mishra, S., Srichandan, H., Singh, P.K., & Sarangi, P.K. (2019). Plant growth promoting microbes: Potential link to sustainable agriculture and environment. Biocatalysis and Agricultural Biotechnology, 21, 101326.

Nomoto, M., Skelly, M.J., Itaya, T., Mori, T., Suzuki, T., Matsushita, T., Tokizawa, M., Kuwata, K., Mori, H., Yamamoto, Y.Y. Higashiyama, T., Tsukagoshi, T., Spoel, & S.H., Tada, Y. (2021). Suppression of MYC transcription activators by the immune cofactor *NPR1* fine-tunes plant immune responses. Cell reports, 37(11).

Olowe, O. M., Akanmu, A. O., & Asemoloye, M. D. (2020). Exploration of microbial stimulants for induction of systemic resistance in plant disease management. Annals of Applied Biology, 177(3), 282-293.

Palmer, C.M., Hindt, M.N., Schmidt, H., Clemens, S., & Guerinot, M.L. (2013). MYB10 and MYB72 are required for growth under iron-limiting conditions. PLoS genetics, 9(11), e1003953.

Parewa, H.P., Yadav, J., Rakshit, A., Meena, V.S., & Karthikeyan, N. (2014). Plant growth promoting rhizobacteria enhance growth and nutrient uptake of crops. Agric Sustain Dev, 2(2), 101-116.

Park, K.S., & Kloepper, J.W. (2000). Activation of PR-1a promoter by rhizobacteria that induce systemic resistance in tobacco against *Pseudomonas syringae* pv. tabaci. Biological Control, 18(1), 2-9.

Park, S.W., Li, W., Viehhauser, A., He, B., Kim, S., Nilsson, A.K., Andersson, M.X., Kittle, J.D., Ambavaram, M.M., Luan, S. Esker, A.R., Tholl, D., Cimini, D., Ellerström, M., Coaker, G., Mitchell, T.K., Pereira, A., Dietz, K.J., & Lawrence, C.B. (2013). Cyclophilin 20-3 relays a 12-oxo-phytodienoic acid signal during stress responsive regulation of cellular redox homeostasis. Proceedings of the National Academy of Sciences, 110(23), 9559-9564.

Pieterse, C.M., Van Pelt, J.A., Ton, J., Parchmann, S., Mueller, M.J., Buchala, A.J., Métraux, J.P., & Van Loon, L.C. (2000). Rhizobacteria-mediated induced systemic resistance (ISR) in Arabidopsis requires sensitivity to jasmonate and ethylene but is not accompanied by an increase in their production. Physiological and molecular plant pathology, 57(3), 123-134.

Pieterse, C.M., Van Wees, S.C., Van Pelt, J.A., Knoester, M., Laan, R., Gerrits, H., Weisbeek, P.J., & Van Loon, L.C. (1998). A novel signaling pathway controlling induced systemic resistance in Arabidopsis. The Plant Cell, 10(9), 1571-1580.

Pieterse, C.M., Zamioudis, C., Berendsen, R.L., Weller, D.M., Van Wees, S.C., & Bakker, P.A. (2014). Induced systemic resistance by beneficial microbes. Annual review of phytopathology, 52, 347-375.

Press, C.M., Wilson, M., Tuzun, S., & Kloepper, J.W. (1997). Salicylic acid produced by *Serratia marcescens* 90-166 is not the primary determinant of induced systemic resistance in cucumber or tobacco. Molecular Plant-Microbe Interactions, 10(6), 761-768.

Rani, L., Thapa, K., Kanojia, N., Sharma, N., Singh, S., Grewal, A.S., Srivastav, A.L., & Kaushal, J. (2021). An extensive review on the consequences of chemical pesticides on human health and environment. Journal of cleaner production, 283, 124657.

Ross, A. F. (1961). Systemic acquired resistance induced by localized virus infections in plants. Virology, 14(3), 340-358.

Samaras, A., Roumeliotis, E., Ntasiou, P., & Karaoglanidis, G. (2021). *Bacillus subtilis* MBI600 promotes growth of tomato plants and induces systemic resistance contributing to the control of soilborne pathogens. Plants, 10(6), 1113.

Sarma, B.K., Yadav, S.K., Singh, D.P., & Singh, H.B. (2012). Rhizobacteria mediated induced systemic tolerance in plants: prospects for abiotic stress management. Bacteria in agrobiology: stress management, 225-238.

Scalschi, L., Sanmartín, M., Camañes, G., Troncho, P., Sánchez-Serrano, J.J., García-Agustín, P., & Vicedo, B. (2015). Silencing of *OPR3* in tomato reveals the role of OPDA in callose deposition during the activation of defense responses against *Botrytis cinerea*. The Plant Journal, 81(2), 304-315.

Schulze, A., Zimmer, M., Mielke, S., Stellmach, H., Melnyk, C.W., Hause, B., & Gasperini, D. (2019). Wound-induced shoot-to-root relocation of JA-Ile precursors coordinates Arabidopsis growth. Molecular plant, 12(10), 1383-1394.

Schwessinger, B., & Zipfel, C. (2008). News from the frontline: recent insights into PAMP-triggered immunity in plants. Current opinion in plant biology, 11(4), 389-395.

Segarra, G., Van der Ent, S., Trillas, I., & Pieterse, C.M.J. (2009). MYB72, a node of convergence in induced systemic resistance triggered by a fungal and a bacterial beneficial microbe. Plant biology, 11(1), 90-96.

Smith, B.E., Richards, R.L., & Newton, W.E. (Eds.). (2004). Catalysts for nitrogen fixation: nitrogenases, relevant chemical models and commercial processes (Vol. 1). Springer Science & Business Media.

Spoel, S.H., Koornneef, A., Claessens, S.M., Korzelius, J.P., Van Pelt, J.A., Mueller, M.J., Buchala, A.J., Métraux, J.P., Brown, R., Kazan, K., & Van Loon, L.C. (2003). NPR1 modulates cross-talk between salicylate-and jasmonate-dependent defense pathways through a novel function in the cytosol. The Plant Cell, 15(3), 760-770.

Stein, E., Molitor, A., Kogel, K. H., & Waller, F. (2008). Systemic resistance in Arabidopsis conferred by the mycorrhizal fungus *Piriformospora indica* requires jasmonic acid signaling and the cytoplasmic function of *NPR1*. Plant and cell physiology, 49(11), 1747-1751.

Tjamos, S.E., Flemetakis, E., Paplomatas, E.J., & Katinakis, P. (2005). Induction of resistance to *Verticillium dahliae* in *Arabidopsis thaliana* by the biocontrol agent K-165 and pathogenesis-related proteins gene expression. Molecular Plant-Microbe Interactions, 18(6), 555-561.

van de Mortel, J.E., de Vos, R.C., Dekkers, E., Pineda, A., Guillod, L., Bouwmeester, K., van Loon, J.J., Dicke, M., & Raaijmakers, J.M. (2012). Metabolic and transcriptomic changes induced in Arabidopsis by the rhizobacterium *Pseudomonas fluorescens* SS101. Plant Physiology, 160(4), 2173-2188.

Van der Ent, S., Van Hulten, M., Pozo, M.J., Czechowski, T., Udvardi, M.K., Pieterse, C. M., & Ton, J. (2009). Priming of plant innate immunity by rhizobacteria and β-aminobutyric acid: differences and similarities in regulation. New Phytologist, 183(2), 419-431.

Van der Ent, S., Verhagen, B.W., Van Doorn, R., Bakker, D., Verlaan, M.G., Pel, M.J., Joosten, R.G., Proveniers, M.C., Van Loon, L.C., Ton, J., & Pieterse, C.M. (2008). MYB72 is required in early signaling steps of rhizobacteria-induced systemic resistance in Arabidopsis. Plant Physiology, 146(3), 1293-1304.

van Hulten, M., Pelser, M., Van Loon, L.C., Pieterse, C.M., & Ton, J. (2006). Costs and benefits of priming for defense in Arabidopsis. Proceedings of the National Academy of Sciences, 103(14), 5602-5607.

Van Peer, R., Niemann, G. J., & Schippers, B. (1991). Induced resistance and phytoalexin accumulation in biological control of Fusarium wilt of carnation by *Pseudomonas* sp. strain WCS 417 r. Phytopathology, 81(7), 728-734.

Van Wees, S.C., De Swart, E.A., Van Pelt, J.A., Van Loon, L.C., & Pieterse, C.M. (2000). Enhancement of induced disease resistance by simultaneous activation of salicylate-and jasmonate-dependent defense pathways in *Arabidopsis thaliana.* Proceedings of the National Academy of Sciences, 97(15), 8711-8716.

Van Wees, S.C., Luijendijk, M., Smoorenburg, I., Van Loon, L.C., & Pieterse, C.M. (1999). Rhizobacteria-mediated induced systemic resistance (ISR) in Arabidopsis is not associated with a direct effect on expression of known defense-related genes but stimulates the expression of the jasmonate-inducible gene *Atvsp* upon challenge. Plant molecular biology, 41, 537-549.

Varsani, S., Grover, S., Zhou, S., Koch, K.G., Huang, P.C., Kolomiets, M.V., Williams, W.P., Heng-Moss, T., Sarath, G., Luthe, D.S. Jander, G., & Louis, J. (2019). 12-Oxo-phytodienoic acid acts as a regulator of maize defense against corn leaf aphid. Plant physiology, 179(4), 1402-1415.

Verhagen, B.W., Glazebrook, J., Zhu, T., Chang, H.S., Van Loon, L.C., & Pieterse, C.M. (2004). The transcriptome of rhizobacteria-induced systemic resistance in Arabidopsis. Molecular Plant-Microbe Interactions, 17(8), 895-908.

Vessey, J. K. (2003). Plant growth promoting rhizobacteria as biofertilizers. Plant and soil, 255, 571-586.

Wang, K.D., Borrego, E.J., Kenerley, C.M., & Kolomiets, M.V. (2020a). Oxylipins other than jasmonic acid are xylem-resident signals regulating systemic resistance induced by *Trichoderma virens* in maize. The Plant Cell, 32(1), 166-185.

Wang, K.D., Gorman, Z., Huang, P.C., Kenerley, C.M., & Kolomiets, M.V. (2020b). *Trichoderma virens* colonization of maize roots triggers rapid accumulation of 12-oxophytodienoate and two $_{\gamma}$-ketols in leaves as priming agents of induced systemic resistance. Plant signaling & behavior, 15(9), 1792187.

Yan, Z., Reddy, M.S., Ryu, C.M., McInroy, J.A., Wilson, M., & Kloepper, J.W. (2002). Induced systemic protection against tomato late blight elicited by plant growth-promoting rhizobacteria. Phytopathology, 92(12), 1329-1333.

Yuan, M., Huang, Y., Ge, W., Jia, Z., Song, S., Zhang, L., & Huang, Y. (2019). Involvement of jasmonic acid, ethylene and salicylic acid signaling pathways behind the systemic resistance induced by *Trichoderma longibrachiatum* H9 in cucumber. BMC genomics, 20, 1-13.

Zamioudis, C., Mastranesti, P., Dhonukshe, P., Blilou, I., & Pieterse, C.M. (2013). Unraveling root developmental programs initiated by beneficial *Pseudomonas* spp. bacteria. Plant Physiology, 162(1), 304-318.

Zhang, S., Moyne, A.L., Reddy, M.S., & Kloepper, J.W. (2002). The role of salicylic acid in induced systemic resistance elicited by plant growth-promoting rhizobacteria against blue mold of tobacco. Biological control, 25(3), 288-296.

Zimmermann, M.H., & Tomlinson, P.B. (1972). The vascular system of monocotyledonous stems. Botanical Gazette, 133(2), 141-155.

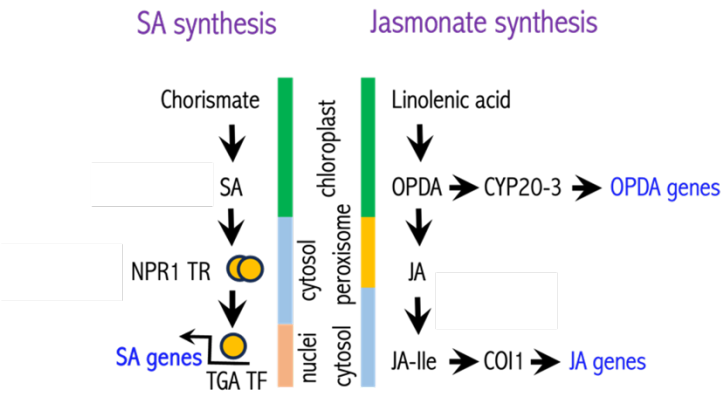

Figure 1.1. Scheme of Salicylic Acid and Jasmonate biosynthesis and signaling pathway in *A. thaliana.*

Jasmonates are biosynthesized from linolenic acid, which breaks down into 12-oxo-phytodienoic acid (OPDA) in the chloroplast; OPDA then travels to peroxisomes for β-oxidation to form Jasmonic acid (JA), which is released to the cytosol and conjugated to JA-isoleucine (JA-Ile). Among all the jasmonates, OPDA and JA-Ile are biologically active as signals (Howe et al., 2001) which bind to their own receptors, Cyclophilin (CYP)20-3 and CORONATINE INSENSITIVE 1 (COI1) to activate OPDA and JA responsive gene expressions. On the other hand, Salicylic Acid (SA) is biosynthesized from chorismate (Lefevere et al., 2020). SA subsequently activates the *NONEXPRESSOR OF PATHOGENESIS-RELATED PROTEINS1* (*NPR1),* a transcriptional regulator (TR) of SA signaling, causing its cytosol monomerization and facilitating nuclear translocation. This process also triggers TGA transcription factors (TF), initiating the expression of SA-dependent defense genes (Johnson et al., 2003).

CHAPTER 2: 12-OXOPHYTODIENOIC ACID: A MOBILE SIGNAL PRIMING INDUCED SYSTEMIC RESISTANCE IN PLANTS AND BALANCING PLANT GROWTH AND DEFENSE

2.1. ABSTRACT

In plants, growth and defense trade-offs have been a major pitfall for the genetic engineering of disease resistance. To understand if and how plants co-ordinate growth and defense responses, we exploit the role and mode of plant growth-promoting rhizobacteria (PGPR)-mediated 'induced systemic resistance (ISR),' a phenomenon capable of priming broad-spectrum durable disease resistances without the usually accompanied growth penalty. However, the mobile signal for ISR has been elusive. In this study, we identified PGPR strains, *Pseudomonas oryzahabitans,* and *Bacillus subtilis,* that are able to develop ISR in Arabidopsis and cotton plants. During ISR activations, our transcriptional and metabolomic analyses reconstituted that ***i***) Local root tissues induce and activate OPDA and JA-Ile signaling, as well as trigger *NPR1*-dependent signaling without SA productions. In the meantime, ***ii***) Systemic leaf tissues activate OPDA (but not JA-Ile) and SA signaling. Since leaf tissues do not de novo synthesize OPDA, JA-Ile, and SA, these results delineate that OPDA produced in root tissues travels via phloem cells to leaf tissues, where they activate OPDA signaling. In support of this scenario, we observed that ***iii***) OPDA (but not JA-Ile) can upregulate SA signaling marker genes via NPR1-dependent pathway, i.e., via GRX transcriptional regulators and TGA transcriptional factors. Consistent with our hypothesis, mutant plants deficient in *CYP20-3*, *NPR1*, *GRX480*, and *TGAs* exhibited impaired ISR development. Together, we propose that ISR requires the accumulation of OPDA in local tissues that moves to systemic tissues where it activates GRX-mediated OPDA and SA response defense gene expression pathways to prime disease resistance.

2.2. INTRODUCTION

Annual crop losses to plant pathogens, costing $220 billion USD, pose a significant threat to food security, especially as the global population is projected to increase by 50%

by 2050 (FAO 2022). The rapid evolution of pathogens has rendered traditional resistance breeding methods largely ineffective. Additionally, plant defense responses are often accompanied by growth retardation, hindering genetic engineering for disease resistance (He et al., 2022). Chemical pesticides are not a viable solution either due to their high toxicity and cost (Rani et al., 2021). Therefore, it is crucial to understand plant defense mechanisms to develop effective and durable disease management strategies that do not compromise plant growth.

Plant defense responses involve both local and systemic levels to limit pathogen growth and spread. Locally, they often initiate hypersensitive responses, developing regulated necrosis at the site of infections; systemic tissues consequently develop a state of enhanced defensive capacity called systemic acquired resistance (SAR) if triggered by pathogenic microbes or induced systemic resistance (ISR) if elicited by plant growth-promoting rhizobacteria (PGPR) or fungi (Maithani et al., 2012). SAR mostly relies on salicylic acid (SA) and the activation of *PATHOGENIC-RELATED* (*PR*) genes, mediated by *NONEXPRESSOR OF PR1 (NPR1)*, a well-known transcription activator of SA signaling (Ali et al., 2018). To prime disease resistance throughout the plant, a signal from the infected tissue must travel through the phloem to the systemic tissues. Several such mobile signals are identified for inducing SAR, including azelaic acid, dehydroabietinal, glycerol-3-P, methyl salicylate, and pipecolic acid (Chaturvedi et al., 2012; Návarová et al., 2012; Park et al., 2007; Chanda et al., 2011; Jung et al., 2009). Conversely, to date, no mobile signal has been identified for ISR, prompting our study on the ISR signaling mechanism. ISR is like acquired immunity in being systemic and durable and like innate immunity in providing broad-spectrum resistance to subsequent infections without the usually accompanied growth penalty (Pieterse et al., 2014; Van Loon et al., 1998). It is known to be majorly dependent on Jasmonic acid (JA), which functions upstream of ethylene (ET) and *NPR1*-dependent SA signaling pathways. Surprisingly, the activation of *NPR1* signaling occurs independently of SA, a mechanism that has remained largely enigmatic until now (Pieterse et al., 2014; Pieterse et al., 1998).

These two major phytodefense hormones have completely independent biosynthesis and signaling pathways. Jasmonate biosynthesis begins with the oxygenation of linolenic acid into 12-oxo-phytodienoic acid (OPDA) by the sequential

action of lipoxygenase (LOX), allene oxide synthase (AOS), and allene oxide cyclase (AOC) in the chloroplast; OPDA then travels to peroxisomes for β-oxidation to form JA via 12-oxophytodienoic acid reductase (OPR3), which is released to the cytosol and conjugated to JA-isoleucine (JA-Ile). OPDA and JA-Ile are biologically active as signals (Howe et al., 2001; Sasaki et al., 2001). OPDA binds to its receptor, CYP20-3, activating OPDA-responsive gene expressions (ORGs) such as *GLUTAREDOXIN 480 (GRX480)* and *Cytochrome P450 (CYP81D11)* in Arabidopsis (Park et al., 2013). While JA-Ile binds to CORONATINE INSENSITIVE 1 (COI1), forming a complex that ubiquitinates jasmonate ZIM-domain proteins, which releases transcription factors to activate JA-responsive genes (JRGs), like *THIONIN (Thi)2.1* in Arabidopsis (Bohlmann et al., 1998). On the other hand, SA biosynthesis starts in the chloroplast with the conversion of chorismate via isochorismate synthase (ICS1) and phenylalanine ammonia-lyase (PAL) pathways, producing isochorismate and phenylalanine, which then forms SA (Lefevere et al., 2020). SA activates and monomerizes *NPR1* in cytosol, allowing it to move to the nucleus and activates TGA transcription factors, inducing SA-dependent defense genes (SRGs), like *PATHOGENESIS-RELATED GENE (PR)1* and *PR5* (Johnson et al., 2003).

Interestingly, recent studies have shown that MeJA, a derivative of JA, inhibits the ET pathway (Clay et al., 2009), whereas OPDA, a JA precursor, activates it, inducing ethylene biosynthesis and receptor genes (Varsani et al., 2019). Moreover, an inverse relationship between *NPR1* and JA signaling has been observed, with *NPR1* negatively regulating JA signaling (Nomoto et al., 2021; Spoel et al., 2003). These studies suggest that OPDA, rather than JA, might be a key player in ISR priming. In fact, a recent study by Wang et al. (2020a, b) proposed OPDA as the mobile signal for ISR in maize because it triggers plant defense responses when applied, is induced in the roots, leaves, and xylem tissues of ISR-positive but not ISR-negative mutants, and its deficiency impairs ISR development, which is restored dose-dependently by OPDA supplementation in increasing concentrations in the xylem sap. Conversely, transfusion with JA led to enhanced susceptibility, and the JA-deficient mutant could still induce ISR. The caveat here is that maize, a monocot, doesn't have a well-developed vascular system that may not completely explain phloem movement of long-distance signals in most of the crop systems that are dicots (Zimmermann et al. 1972).

Henceforth, to further characterize the long-distance mobile signaling in ISR, this study first established a standard ISR assay using bacteria, *Pseudomonas syringae,* in the dicot model plant system, *Arabidopsis thaliana,* and fungi, *Corynespora cassiicola,* in cotton. We then conducted transcription marker gene and hormone analyses to determine the mobile signal and the mechanism of SA-independent *NPR1*-signaling activation in ISR. Notably, we identified OPDA as a potential mobile signal capable of activating SA signaling independently of SA, mediated by GRX transcription regulators and TGA transcription factors. Consistent with this, KO mutant plants with disrupted *CYP20-3, NPR1, GRX,* and *TGA* genes exhibited impaired ISR. These findings suggest that OPDA is a critical mobile inducer of PGPR-mediated systemic resistance in plants.

2.3. RESULTS AND DISCUSSION

2.3.1. *Bacillus subtilis* and *Pseudomonas oryzahabitans* induce ISR in Arabidopsis and Cotton

To elucidate the molecular nodes and mechanisms by which PGPR induces ISR, we first identified PGPR capable of triggering ISR, *P. oryzihabitans,* and *B. subtilis,* which significantly primed disease resistance against bacteria, *P. syringae* in Arabidopsis, demonstrated using bacterial leaf infiltration assay (**Fig 2.2B**) and fungi, *C. cassiicola* in cotton shown using detached leaf assay (**Fig 2.3A**). ISR is evident as reduced bacterial growth or percentage of fungal infection in systemic leaves after secondary *P. syringae* or *C. cassiicola* infections on plants that received a primary PGPR inoculation relative to those that received a primary mock inoculation. The reduction in bacterial growth or fungal infection occurs because ISR induced by primary PGPR inoculation enhances the plant's ability to limit pathogen growth and spread during subsequent encounters. Note that our previous study found these PGPRs ineffective in priming-induced systemic tolerance to drought, indicating this phenomenon involves different signaling cascades than ISR (Liu et al. 2020). We then examined the duration of ISR after PGPR inoculation by treating *B. subtilis* 1, 3, 5, and 7 days before *Pseudomonas syringae* secondary inoculation. We found that ISR can be sustained for over a week after PGPR inoculations, but as early as one day was enough time to develop ISR (**Fig 2.2A**).

2.3.2. ISR-inducing PGPR stimulates jasmonate production in roots but only increases OPDA levels in the phloem and systemic tissue without triggering local hormone biosynthesis

To clarify the role of jasmonates and other important phytodefense hormones like SA and understand long-distance signaling in ISR, we did a transcription analysis of marker genes involved in the defense signaling pathways of major plant defense hormones SA, JA, and OPDA (Monte et al., 2023) in local inoculated and systemic uninoculated tissues after treating plant roots with ISR-inducible PGPR in both cotton and Arabidopsis. Since JA and OPDA-specific signaling marker genes are unknown in cotton, we first identified them by examining the differential expression of analogs of jasmonate-responsive genes from Arabidopsis in cotton following OPDA and MeJA treatments. We discovered that *HEAT SHOCK PROTEIN (HSP)17.0* is specifically induced by OPDA but not MeJA, designating it as an OPDA-responsive gene. In contrast, *MYC2* and *GLUTATHIONE TRANSFERASE (GST)8* were induced by both jasmonates, designating them as JA-responsive genes (**Fig 2.1**).

In fact, PGPR inoculations of *B. subtilis and P. oryzahabitans* in both Arabidopsis (**Fig 2.2C**) and cotton (**Fig 2.3B**) root tissues activate the entire jasmonate biosynthesis and signaling pathway. These included the activation of jasmonate biosynthesis marker genes (JBGs; *AOC1, OPR3* in Arabidopsis*,* and *G. hirsutum (Gh)LOX1, GhOPR3* in cotton) along with OPDA and JA signaling marker genes such as ORGs (*GRX480, CYP81D1* in Arabidopsis*,* and *GhHSP17* in cotton*)* and JRGs *(Thi2.1* in Arabidopsis*,* and *GhMYC2, GhGST8* in cotton). However, these inoculations did not induce SA biosynthesis marker genes (SBGs; *ICS1* in Arabidopsis*,* and *GhPAL* in cotton). Despite this, there was still robust induction of SA signaling marker genes *PR1 and PR5*.

On the other hand, leaves or uninoculated systemic tissues showed little to no activation of JBGs and SBGs following root inoculation with *B. subtilis and P. oryzihabitan*s, suggesting an absence of hormone biosynthesis. Nevertheless, there were drastic increases in ORGs and SRGs, with minimal induction of selective JRGs (**Fig 2.2C** and **2.3C**). Collectively, this indicates that the OPDA or SA hormone signal might have translocated from root to leaf tissues. This is most likely OPDA, but not SA, because there is no SA accumulation in root tissues.

Consistent with transcriptional analysis, our metabolic analysis of the WT Arabidopsis plant root tissue after PGPR treatment showed elevated levels of all jasmonates—OPDA, JA, and JA-Ile—without a corresponding rise in SA (**Fig 2.2D**). However, in phloem exudates and systemic leaf tissues, we detected a subsequent rise in only OPDA hormone levels, while SA, JA, and JA-Ile levels remained unchanged in both phloem and systemic tissues (**Fig 2.2D**). Together, this proposes that OPDA may be involved in long-distance signaling in ISR development, moving from the root to the systemic leaf tissues via the phloem following PGPR inoculation.

2.3.3. OPDA hormone is critical for ISR development

We then performed ISR assays to validate if OPDA signaling is required for ISR development with various Arabidopsis KO mutants by treating PGPR, *B. subtilis*, and *P. oryzihabitans* before secondary inoculation by *P. syringae.* Indeed, *cyp20-3* KO disrupting OPDA signaling (Park et al., 2013) was defective in ISR development against *P. syringae* infections compared to WT, suggesting that OPDA signaling is critical for ISR development (**Fig 2.4A**). However, our ISR assays in the Arabidopsis system showed, like previous studies (De Vleesschauwer et al., 2008; Hase et al., 2008; Lavicoli et al., 2003; Stein et al., 2008; Yan et al., 2002, Pieterse et al., 1998), that *jar1* that doesn't produce JA-Ile (Staswick et al., 2004) also impairs ISR development (**Fig 2.4A**). Thus, to test if ISR needs both JA-Ile and OPDA, we tested if the *jar1* mutant maintains normal OPDA biosynthesis and signaling in response to PGPR treatment. However, we discovered a negative feedback loop within *jar1*, whereby *jar1,* unlike other mutants, inhibits not only JA-Ile production but also OPDA biosynthesis in root tissue on PGPR treatment as seen by marker gene expression, suggesting that *jar1* is impaired in ISR development, possibly due to a lack of OPDA biosynthesis after PGPR treatment (**Fig 2.4B**). This further supports our hypothesis that OPDA plays a key role in priming disease resistance in ISR.

2.3.4. Activation of GRX480 by OPDA signaling bypasses the SA signaling pathway, resulting in *NPR1*-dependent expression of *PR1* independent of SA

A caveat is that PGPR induces *NPR1*-dependent SRGs- *PR1* and *PR5*, in both root and leaf tissue in Arabidopsis and cotton but not SA biosynthesis (**Fig 2.3** and **2.4**), raising a question of how PGPR induces SA signaling without SA accumulations. In fact, this SA-independent activation of *NPR1*-dependent signaling is crucial for ISR development as the SA signaling mutant, *npr1* (Cao et al., 1994), showed impaired ISR development, in accordance with previous studies (**Fig 2.4A**) (Nie et al., 2017; Ramírez et al., 2010; Ahn et al., 2007; Pieterse et al., 1998). To see if any hormone other than SA could induce *PR1* gene expression, we treated Arabidopsis leaves with 75 µM each of OPDA, MeJA, and SA and cotton leaves with 1 mM SA and 0.1 mM each of MeJA and OPDA. Indeed, OPDA but not JA can induce PR1 expression in both Arabidopsis and cotton, as does SA– suggesting that PGPR induces OPDA, which, in turn, upregulates SRGs (**Fig 2.5A**). So, we tested whether OPDA can activate SA biosynthesis to trigger the SA signaling pathway. However, OPDA did not activate SBGs, indicating that OPDA activates SA signaling independently of the SA biosynthesis pathway (**Fig 2.5B**).

The immediate candidate regulator for OPDA and SA signaling pathways is Glutaredoxin or GRX, a transcriptional regulator known to be upregulated by both OPDA and SA and suppressed from JA (Park et al., 2013; Ndamukong et al., 2007). GRX further regulates TGA transcription factors, which interact with *NPR1* and are important in SA-dependent gene expression (Ndamukong et al., 2007). Notably, in Arabidopsis, GRX480 binds to and regulates TGA2 and TGA6, mediating both *NPR1*-dependent SA defense gene expression and CYP20-3-dependent OPDA-responsive gene expression (Park et al., 2013; Mueller et al., 2008; Ndamukong et al., 2007). Indeed, in cotton, both OPDA and SA were able to induce GRX, although both of them induce different isoforms of GRX, i.e., OPDA induces GRX1 while SA induces GRX3, which in turn upregulates expression of TGA transcription factors, thereby activating the SA signaling pathway (**Fig 2.5D**). Similarly, in Arabidopsis, both OPDA and SA induced GRX 480 and GRXS13 (**Fig 2.5C**). However, neither SA nor OPDA upregulated class II TGA transcription factors, TGA 2 and 6, which are crucial for SA-mediated gene expression (Zhang et al., 2003). This is expected because SA treatment doesn't alter TGA protein levels but enhances NPR1-

mediated TGA binding to PR-1 promotor (Johnson et al., 2003), leading to upregulation of PR1 gene expression (**Fig 2.5A**). So, we hypothesize that activation of GRX480 by OPDA signaling may bypass the SA signaling pathway to activate the TGA transcription factor and *NPR1*-dependent SA-independent PR1 expression pathway.

To further validate if OPDA-induced GRX-mediated SA signaling is critical for ISR development, we conducted an ISR assay using various Arabidopsis mutants, including *GRX480* KO CRISPR line and *tga2/5/6* KO Arabidopsis plants (Zhang et al., 2003) (**Fig 2.5E**). Considering that TGA transcription factors negatively regulate GRXS13 but positively regulate GRX480 and that GRXS13, unlike GRX480, is not involved in PR1 gene expression, we used the GRXS13 knockout CRISPR line as a negative control (La Camera et al., 2011). Indeed, both *grx480* and *tga2,5,8* KO Arabidopsis plants, but not *grxs13,* were defective in ISR development, indicating activation of SA signaling by OPDA via GRX and TGA is important for ISR development (**Fig 2.5F**).

2.4. CONCLUSION

Our findings argue that OPDA acts as a long-distance phloem-mobile ISR signal as i) PGPR induces the production of jasmonates, including OPDA and JA, but not SA, in local root tissues (**Fig 2.2C, 2.2D,** and **2.2B**); ii) OPDA levels consequently increase in phloem exudates post-PGPR treatment on roots, unlike SA and JA (**Fig 2.2D**); ii) Systemic leaf tissues also upregulates OPDA, not SA and JA, levels activating OPDA signaling without de novo synthesizing OPDA, JA-Ile, or SA (**Fig 2.2C, 2.2D** and **2.3C**); iii) SA signaling is induced in both local and systemic tissues without SA biosynthesis, with OPDA, but not JA, upregulating SA signaling marker genes via SA-independent *NPR1*-dependent pathway involving GRX transcription regulator and TGA transcription factors (**Fig 2.2C, 2.2D, 2.3B, 2.3C, 2.5A-D**); v) Arabidopsis mutants lacking GRX, TGA, *NPR1*, or OPDA signaling showed impaired ISR development (**Fig 2.4A** and **2.5E**). Together, these results hint that OPDA that's biosynthesized in the root tissue travels as a long-distance mobile signal via phloem cells to the systemic tissue, activating GRX-mediated SA and OPDA-responsive genes priming systemic resistance (**Fig 2.6**).

This discovery resolves a longstanding mystery about long-distance signaling in ISR and how PGPR can activate *NPR1* dependent-SA signaling without triggering its

biosynthesis, revealing a key mechanism of ISR by which plants coordinate growth and defense. Additionally, this finding suggests that OPDA is a node of convergence, potentially serving as a mobile signal in the ISR signaling pathway in both monocots (Wang et al. 2020a, b) and dicots triggered by different PGPMs. It has been found that OPDA, but not JA, acts as a mobile signal in wounding, transporting from shoot to root, indicating that this hormone can move both basipetally and acropetally (Schulze et al., 2019). Interestingly, the combined activation of SAR and ISR pathways had an additive effect against *P. syringae* pv tomato in a manner dependent on *NPR1*, suggesting no competition for *NPR1* (Van Wees et al., 2000). This indicates that simultaneous activation of the *NPR1*-signaling pathway by SA and OPDA enhances the response without competition. Future biochemical studies exploring interactions between OPDA and GRX or TGA transcription factors could reveal how OPDA regulates the activation of SA-responsive genes through GRX.

2.5. MATERIALS AND METHODS

2.5.1. Plant growth conditions

Cotton (*Gossypium hirsutum*), wild-type Arabidopsis (*A. thaliana* Col-0), and Arabidopsis mutants (*jar1, npr1, cyp20-3*, ∆*trx, roxy18, roxy19*) were grown in a growth chamber maintained at 22°C, with a 12-hour light/dark cycle and relative humidity ranging from 60-80%.

2.5.2. Inoculation of PGPR

8 mL of PGPR cell suspension of *Bacillus subtilis* and *Pseudomonas oryzahabitans* (10^8 colony forming units (CFU)/mL) was drenched around the roots of 3-wk-old Arabidopsis and cotton plants in pots for ISR induction. Plants were then subjected to the challenge-inoculation with the bacterial phytopathogen *Pseudomonas syringae* pathovar tomato (*Pst)* DC3000 and the fungal phytopathogen *Corynespora cassiicola,* respectively. For expression analysis and hormone quantification, 1 ml of 10^8 CFU cell suspension was used for inoculation.

2.5.3. Bacterial Pathogen Infection Assay

A bacterial leaf infiltration assay was conducted to evaluate resistance, as described previously, with slight modifications (Liu et al., 2015). In brief, *Pst* DC3000 culture grown overnight in 4 ml of liquid KB medium at 28°C, 250 rpm was resuspended in 10 mM $MgCl_2$ and diluted to 10^5 CFU/ml (OD_{600} of 0.0002), which was syringe-infiltrated into the marked leaves. After 3 days, a leaf disc was punched from two infected leaves of each of three individual plants per genotype to measure bacterial growth, expressed as colony-forming units per disc. The experiment was performed with three technical replicates for each sample.

2.5.4. Fungal detached leaf assay

The inoculant was prepared by suspending spores of *Corynespora cassiicola* from the 7-d-old cultures on PDA plates in sterile distilled water with 0.05% Tween 20. The resulting spore suspension was quantified to count spores using a hemacytometer for detached leaf assays. Leaves were detached from cotton plants 1 and 3 days after primary root inoculation of *B. subtilis* and *P. oryzahabitans*. Control plants did not receive any PGPR inoculations. Leaves were then slightly wounded using a sterilized needle, and an equivalent number of spores were applied to the wounded areas of the leaves. Subsequently, the inoculated leaves were placed in sterile Petri plates and incubated in the dark at room temperature for 15 days. The percentage of infection was recorded.

2.5.5. Quantitative RT-PCR

Total RNA was extracted from leaves of 3–4-wk-old Arabidopsis and cotton plants using TRIzol reagent (Invitrogen) and the Direct-zol RNA Kit (Zymo Research) following the manufacturer's instructions. The quality of the RNA was assessed via agarose gel electrophoresis and NanoDrop spectrophotometry, ensuring A260/A280 > 1.8 and A260/A230 > 2.0 (Udvardi et al., 2008). Reverse transcription reactions were conducted using an oligo(dT) primer and qScript reverse transcriptase (QuantaBio). Quantitative PCR was performed with PerfeCT® SYBR® Green Fast Mix® Reaction Mixes (QuantaBio) on a CFX96 Touch™ PCR system (Bio-Rad), with 40 cycles using gene-specific primers (**Table 2.1** and **2.2**) and an annealing temperature of 53°C. To quantify

target transcripts, cDNA levels were compared to the housekeeping gene POLYUBIQUITIN-C (UBC, Czechowski et al., 2005), and relative transcript abundance was calculated using the $2^{-\Delta\Delta Ct}$ method, where $-\Delta Ct = (Ct,gene - Ct,UBC)$.

2.5.6. Hormone treatments

3-wk-old cotton plants were spray-inoculated with 1 mM SA, 0.1 mM MeJA, and 0.1 mM OPDA in 0.01% Triton X-100. On the other hand, 3-wk-old Arabidopsis plants were treated with 75 µM each of SA, MeJA, and OPDA in 0.01% Triton X-100 with leaf samples collected at 0, 3, 6, 12, and 24 hours after treatment.

2.5.7. Collection of phloem exudate

Leaf exudate was collected as described by Park et al., 2007. In brief, leaf petioles were cut under 1 mM EGTA (pH 7.0) and placed in vials with EGTA solution. The leaves were incubated in continuous light at 20°C and 100% humidity.

2.5.8. Hormone Quantification

Plant material for phytohormone analysis was collected simultaneously with RNA extraction samples to ensure correspondence with transcriptomic data. Roots and leaves of Arabidopsis WT were harvested at 0, 3, 6, 12, and 24 hours after PGPR treatment. Samples were immediately flash-frozen in liquid nitrogen with three biological replicates taken at each time point (approximately 50 mg of roots and 200 mg of leaves). These samples were then stored at −80°C until phytohormone analysis was determined, according to Gutierrez-Larruscain et al. (2022). The tissue was homogenized using zirconium beads and a FastPrep-24 instrument in a 50% acetonitrile/water extraction buffer with internal standards. After thorough mixing and a 30-minute incubation at 4°C, the mixture was centrifuged at 30,000g for 20 minutes. The supernatant was then applied to an SPE Oasis HLB 96-well plate. The remaining pellet was re-extracted with more extraction buffer, centrifuged again, and the supernatants were combined. A 5 µl sample of this combined extract was injected into an LCMS system. Phytohormones were separated on a Kinetex EVO C18 column. Hormone analysis was conducted on an Agilent LCMS system in MRM mode, with data processed using Mass Hunter software.

2.6. REFERENCES:

Aadil, H.N., Jha, S., Parekh, V., Rajkumar, B.K., Ramani, H.R., Kapadiya, C., & Singh, D. (2020). Dissection of phenylpropanoid pathway during salt stress in cotton (*Gossypium hirsutum* L.). IJCS, 8(1), 21-29.

Ahn, I.P., Lee, S.W., & Suh, S.C. (2007). Rhizobacteria-induced priming in Arabidopsis is dependent on ethylene, jasmonic acid, and *NPR1*. Molecular Plant-Microbe Interactions, 20(7), 759-768.

Ali, A., Shah, L., Rahman, S., Riaz, M.W., Yahya, M., Xu, Y.J., Liu, F., Si, W., Jiang, H., & Cheng, B. (2018). Plant defense mechanism and current understanding of salicylic acid and *NPRs* in activating SAR. Physiological and molecular plant pathology, 104, 15-22.

Bohlmann, H., Vignutelli, A., Hilpert, B., Miersch, O., Wasternack, C., & Apel, K. (1998). Wounding and chemicals induce expression of the *Arabidopsis thaliana* gene *Thi2.1*, encoding a fungal defense, via the octadecanoid pathway. FEBS letters, 437(3), 281-286.

Cao, H., Bowling, S.A., Gordon, A.S., & Dong, X. (1994). Characterization of an Arabidopsis mutant that is nonresponsive to inducers of systemic acquired resistance. The Plant Cell, 6(11), 1583-1592.

Chanda, B., Xia, Y.E., Mandal, M.K., Yu, K., Sekine, K.T., Gao, Q.M., Selote, D., Hu, Y., Stromberg, A., Navarre, D. and Kachroo, A. & Kachroo, P. (2011). Glycerol-3-phosphate is a critical mobile inducer of systemic immunity in plants. Nature genetics, 43(5), 421-427.

Chaturvedi, R., Venables, B., Petros, R.A., Nalam, V., Li, M., Wang, X., Takemoto, L.J. & Shah, J. (2012). An abietane diterpenoid is a potent activator of systemic acquired resistance. The Plant Journal, 71(1), 161-172.

Clay, N.K., Adio, A.M., Denoux, C., Jander, G., & Ausubel, F.M. (2009). Glucosinolate metabolites required for an Arabidopsis innate immune response. Science, 323(5910), 95-101.

De Vleesschauwer, D., Djavaheri, M., Bakker, P.A., & Höfte, M. (2008). *Pseudomonas fluorescens* WCS374r-induced systemic resistance in rice against *Magnaporthe*

oryzae is based on pseudobactin-mediated priming for a salicylic acid-repressible multifaceted defense response. Plant physiology, 148(4), 1996-2012.

FAO. 2022. FAO's Plant Production and Protection Division. Rome. https://doi.org/10.4060/cc2447en

Hase, S., Takahashi, S., Takenaka, S., Nakaho, K., Arie, T., Seo, S., Ohashi, Y., & Takahashi, H. (2008). Involvement of jasmonic acid signalling in bacterial wilt disease resistance induced by biocontrol agent *Pythium oligandrum* in tomato. Plant Pathology, 57(5), 870-876.

He, Z., Webster, S., & He, S.Y. (2022). Growth–defense trade-offs in plants. Current Biology, 32(12), R634-R639.

Howe, G.A. (2001). Cyclopentenone signals for plant defense: remodeling the jasmonic acid response. Proceedings of the National Academy of Sciences, 98(22), 12317-12319.

Hu, Q., Zhu, L., Zhang, X., Guan, Q., Xiao, S., Min, L., & Zhang, X. (2018). *GhCPK33* negatively regulates defense against *Verticillium dahliae* by phosphorylating *GhOPR3.* Plant Physiology, 178(2), 876-889.

Iavicoli, A., Boutet, E., Buchala, A., & Métraux, J.P. (2003). Induced systemic resistance in *Arabidopsis thaliana* in response to root inoculation with *Pseudomonas fluorescens* CHA0. Molecular plant-microbe interactions, 16(10), 851-858.

Johnson, C., Boden, E., & Arias, J. (2003). Salicylic acid and *NPR1* induce the recruitment of trans-activating TGA factors to a defense gene promoter in Arabidopsis. The Plant Cell, 15(8), 1846-1858.

Jung, H.W., Tschaplinski, T.J., Wang, L., Glazebrook, J., & Greenberg, J.T. (2009). Priming in systemic plant immunity. Science, 324(5923), 89-91.

La Camera, S., L'Haridon, F., Astier, J., Zander, M., Abou-Mansour, E., Page, G., Thurow, C., Wendehenne, D., Gatz, C., Métraux, J.P. & Lamotte, O. (2011). The glutaredoxin *ATGRXS13* is required to facilitate *Botrytis cinerea* infection of *Arabidopsis thaliana* plants. The Plant Journal, 68(3), 507-519.

Lefevere, H., Bauters, L., & Gheysen, G. (2020). Salicylic acid biosynthesis in plants. Frontiers in plant science, 11, 521987.

Li, Z.K., Chen, B., Li, X.X., Wang, J.P., Zhang, Y., Wang, X.F., Yan, Y.Y., Ke, H.F., Yang, J., Wu, J.H., Wang, G.N., Zhang, G.Y., Wu, L.Q., Wang, X.Y. & Ma, Z.Y. (2019). A newly identified cluster of *glutathione S-transferase* genes provides Verticillium wilt resistance in cotton. The Plant Journal, 98(2), 213-227.

Liu, T., Song, T., Zhang, X., Yuan, H., Su, L., Li, W., Xu, J., Liu, S., Chen, L., Chen, T., Zhang, M., Gu, L., Zhang, B., & Dou, D. (2014). Unconventionally secreted effectors of two filamentous pathogens target plant salicylate biosynthesis. Nature communications, 5(1), 4686.

Liu, W., Sikora, E., & Park, S.W. (2020). Plant growth-promoting rhizobacterium, *Paenibacillus polymyxa* CR1, upregulates dehydration-responsive genes, *RD29A* and *RD29B*, during priming drought tolerance in arabidopsis. Plant Physiology and Biochemistry, 156, 146-154.

Maithani, D., Singh, H., & Sharma, A. (2021). Stress alleviation in plants using SAR and ISR: Current views on stress signaling network. Microbes and signaling biomolecules against plant stress: strategies of plant-microbe relationships for better survival, 7-36.

Monte, I. (2023). Jasmonates and salicylic acid: Evolution of defense hormones in land plants. Current Opinion in Plant Biology, 76, 102470.

Mueller, S., Hilbert, B., Dueckershoff, K., Roitsch, T., Krischke, M., Mueller, M.J., & Berger, S. (2008). General detoxification and stress responses are mediated by oxidized lipids through TGA transcription factors in Arabidopsis. The Plant Cell, 20(3), 768-785.

Návarová, H., Bernsdorff, F., Döring, A.C., & Zeier, J. (2012). Pipecolic acid, an endogenous mediator of defense amplification and priming, is a critical regulator of inducible plant immunity. The Plant Cell, 24(12), 5123-5141.

Ndamukong, I., Abdallat, A.A., Thurow, C., Fode, B., Zander, M., Weigel, R., & Gatz, C. (2007). SA-inducible Arabidopsis glutaredoxin interacts with TGA factors and suppresses JA-responsive *PDF1. 2* transcription. The Plant Journal, 50(1), 128-139.

Nie, P., Li, X., Wang, S., Guo, J., Zhao, H., & Niu, D. (2017). Induced systemic resistance against *Botrytis cinerea* by *Bacillus cereus* AR156 through a JA/ET-and *NPR1*-

dependent signaling pathway and activates PAMP-triggered immunity in *Arabidopsis*. Frontiers in Plant Science, 8, 247629.

Nomoto, M., Skelly, M.J., Itaya, T., Mori, T., Suzuki, T., Matsushita, T., Tokizawa, M., Kuwata, K., Mori, H., Yamamoto, Y.Y. Higashiyama, T., Tsukagoshi, H., Spoel, S.H., & Tada, Y. (2021). Suppression of MYC transcription activators by the immune cofactor *NPR1* fine-tunes plant immune responses. Cell reports, 37(11).

Park, S.W., Kaimoyo, E., Kumar, D., Mosher, S., & Klessig, D.F. (2007). Methyl salicylate is a critical mobile signal for plant systemic acquired resistance. Science, 318(5847), 113-116.

Park, S.W., Li, W., Viehhauser, A., He, B., Kim, S., Nilsson, A.K., Andersson, M.X., Kittle, J.D., Ambavaram, M.M., Luan, S., Esker, A.R., Tholl, D., Cimini, D., Ellerström, M., Coaker, G., Mitchell, T.K., Pereira, A., Dietz, K.J., & Lawrence, C.B. (2013). Cyclophilin 20-3 relays a 12-oxo-phytodienoic acid signal during stress responsive regulation of cellular redox homeostasis. Proceedings of the National Academy of Sciences, 110(23), 9559-9564.

Pieterse, C.M., Van Pelt, J.A., Verhagen, B.W., Ton, J., Van Wees, S.A.S.K.I.A., Leon-Kloosterziel, K.M., & Van Loon, L.C. (2003). Induced Systemic Resistance by Plant Growth-Promoting Rhizobacteria. Symbiosis, 35, 39–54.

Pieterse, C.M., Van Wees, S.C., Van Pelt, J.A., Knoester, M., Laan, R., Gerrits, H., Weisbeek, P.J., & Van Loon, L.C. (1998). A novel signaling pathway controlling induced systemic resistance in Arabidopsis. The Plant Cell, 10(9), 1571-1580.

Ramírez, V., Van der Ent, S., García-Andrade, J., Coego, A., Pieterse, C.M., & Vera, P. (2010). OCP3 is an important modulator of *NPR1*-mediated jasmonic acid-dependent induced defenses in Arabidopsis. BMC plant biology, 10, 1-13.

Rani, L., Thapa, K., Kanojia, N., Sharma, N., Singh, S., Grewal, A.S., Srivastav, A.L., & Kaushal, J. (2021). An extensive review on the consequences of chemical pesticides on human health and environment. Journal of cleaner production, 283, 124657.

Sasaki, Y., Asamizu, E., Shibata, D., Nakamura, Y., Kaneko, T., Awai, K., Amagai, M., Kuwata, C., Tsugane, T., Masuda, T. and Shimada, H., Takamiya, K.I., Ohta, H., & Tabata, S. (2001). Monitoring of methyl jasmonate-responsive genes in

Arabidopsis by cDNA macroarray: self-activation of jasmonic acid biosynthesis and crosstalk with other phytohormone signaling pathways. Dna Research, 8(4), 153-161.

Schulze, A., Zimmer, M., Mielke, S., Stellmach, H., Melnyk, C.W., Hause, B., & Gasperini, D. (2019). Wound-induced shoot-to-root relocation of JA-Ile precursors coordinates Arabidopsis growth. Molecular plant, 12(10), 1383-1394.

Spoel, S.H., Koornneef, A., Claessens, S.M., Korzelius, J.P., Van Pelt, J.A., Mueller, M.J., Buchala, A.J., Métraux, J.P., Brown, R., Kazan, K., & Van Loon, L.C. (2003). NPR1 modulates cross-talk between salicylate-and jasmonate-dependent defense pathways through a novel function in the cytosol. The Plant Cell, 15(3), 760-770.

Staswick, P.E., & Tiryaki, I. (2004). The oxylipin signal jasmonic acid is activated by an enzyme that conjugates it to isoleucine in Arabidopsis. The Plant Cell, 16(8), 2117-2127.

Stein, E., Molitor, A., Kogel, K.H., & Waller, F. (2008). Systemic resistance in Arabidopsis conferred by the mycorrhizal fungus *Piriformospora indica* requires jasmonic acid signaling and the cytoplasmic function of *NPR1*. Plant and cell physiology, 49(11), 1747-1751.

Van Loon, L.C., Bakker, P.A.H.M., & Pieterse, C.M.J. (1998). Systemic resistance induced by rhizosphere bacteria. Annual review of phytopathology, 36(1), 453-483.

Van Wees, S.C., De Swart, E.A., Van Pelt, J.A., Van Loon, L.C., & Pieterse, C.M. (2000). Enhancement of induced disease resistance by simultaneous activation of salicylate-and jasmonate-dependent defense pathways in *Arabidopsis thaliana.* Proceedings of the National Academy of Sciences, 97(15), 8711-8716.

Varsani, S., Grover, S., Zhou, S., Koch, K.G., Huang, P.C., Kolomiets, M.V., Williams, W.P., Heng-Moss, T., Sarath, G., Luthe, D.S. Jander, G., & Louis, J. (2019). 12-Oxo-phytodienoic acid acts as a regulator of maize defense against corn leaf aphid. Plant physiology, 179(4), 1402-1415.

Wang, K.D., Borrego, E.J., Kenerley, C.M., & Kolomiets, M.V. (2020a). Oxylipins other than jasmonic acid are xylem-resident signals regulating systemic resistance induced by *Trichoderma virens* in maize. The Plant Cell, 32(1), 166-185.

Wang, K.D., Gorman, Z., Huang, P.C., Kenerley, C.M., & Kolomiets, M.V. (2020b). *Trichoderma virens* colonization of maize roots triggers rapid accumulation of 12-oxophytodienoate and two $_{\gamma}$-ketols in leaves as priming agents of induced systemic resistance. Plant signaling & behavior, 15(9), 1792187.

Yan, Z., Reddy, M.S., Ryu, C.M., McInroy, J.A., Wilson, M., & Kloepper, J.W. (2002). Induced systemic protection against tomato late blight elicited by plant growth-promoting rhizobacteria. Phytopathology, 92(12), 1329-1333.

Zhang, Y., Gao, Y., Liang, Y., Dong, Y., Yang, X., & Qiu, D. (2019). *Verticillium dahliae* PevD1, an Alt a 1-like protein, targets cotton PR5-like protein and promotes fungal infection. Journal of experimental botany, 70(2), 613-626.

Zhang, Y., Tessaro, M.J., Lassner, M., & Li, X. (2003). Knockout analysis of Arabidopsis transcription factors TGA2, TGA5, and TGA6 reveals their redundant and essential roles in systemic acquired resistance. The Plant Cell, 15(11), 2647-2653.

Zhu, Y., Hu, X., Wang, P., Gao, L., Pei, Y., Ge, Z., Ge, X., Li, F. & Hou, Y. (2021). *GhPLP2* positively regulates cotton resistance to verticillium wilt by modulating fatty acid accumulation and jasmonic acid signaling pathway. Frontiers in Plant Science, 12, 749630.

Zimmermann, M.H., & Tomlinson, P.B. (1972). The vascular system of monocotyledonous stems. Botanical Gazette, 133(2), 141-155.

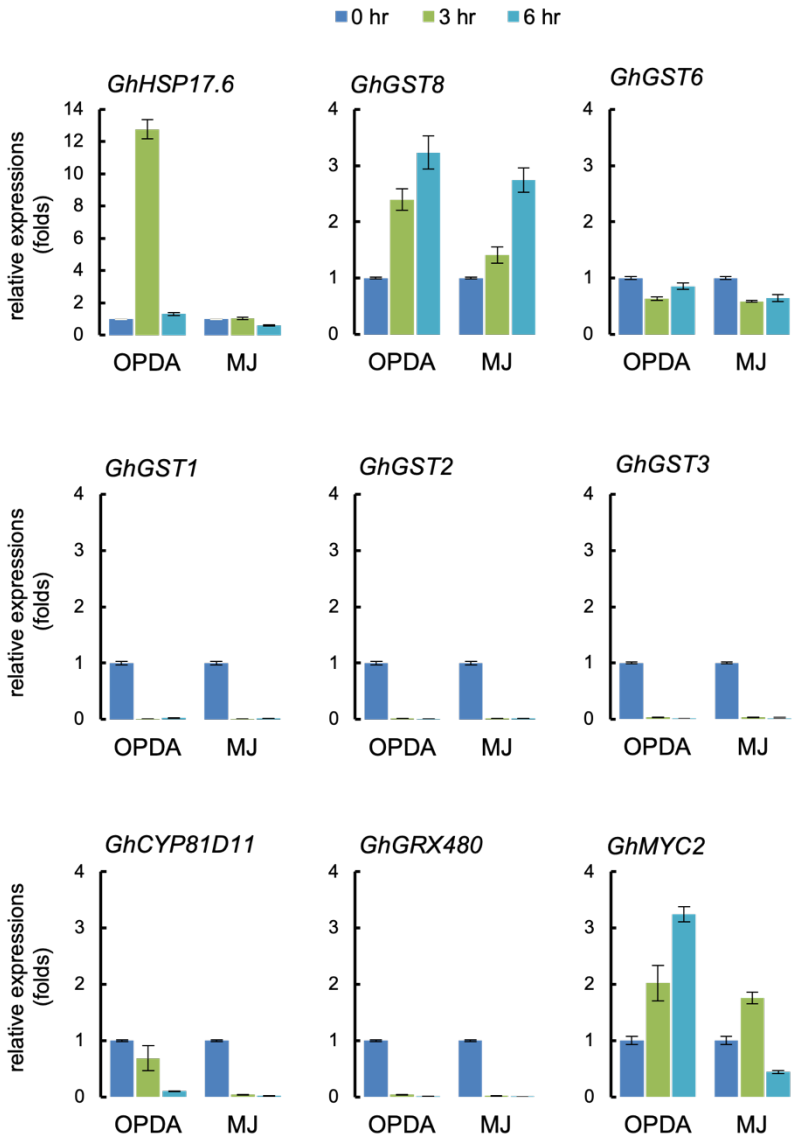

Figure 2.1. Identification of *MYC2* and *GST8* as marker genes for Jasmonic signaling and *HSP17.6* as a marker gene for OPDA signaling in cotton.

Time-resolved qRT-PCR analysis on genes in *Gossypium hirsutum* (Cotton) WT plants that are homologous to known jasmonate-responsive genes in Arabidopsis to evaluate them as potential marker genes for cotton, including *HEAT SHOCK PROTEIN (HSP)17.6, GLUTATHIONE TRANSFERASE (GST)8, GST1, GST2, GST3, CYTOCHROME P450 (CYP81D11), GLUTAREDOXIN (GRX)480,* and *MYC2.* Total RNAs were prepared from leaves at 0, 3, and 6-h post-treatment with 12-Oxophytodienoic acid (OPDA) or Methyl Jasmonate (MeJA) (*B. subtilis* and *P. oryzihabitans*). Values were normalized to POLYUBIQUITIN expression (mean ± SD; n = 3).

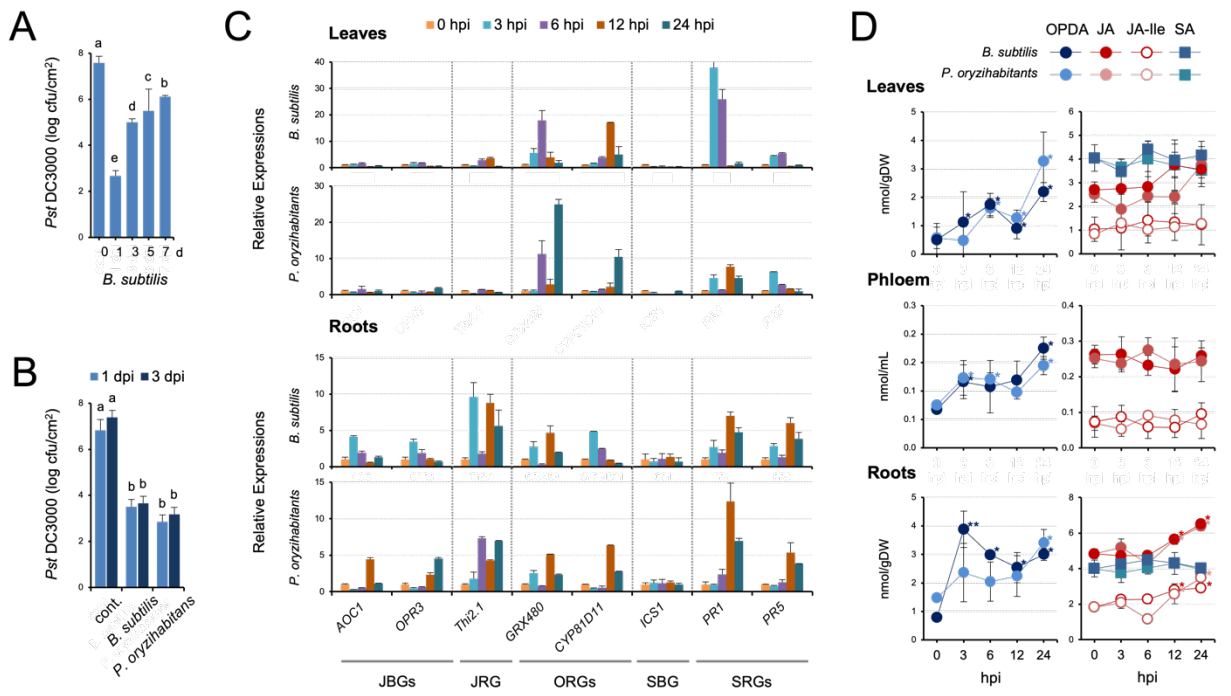

Figure 2.2. ISR-inducing PGPR stimulates jasmonate (OPDA and JA) biosynthesis in roots but elevates only OPDA levels in phloem and systemic leaf tissues without inducing local biosynthesis of these hormones.

(***A, B***) ISR activations were measured by infecting *Pseudomonas syringae* pv tomato (*Pst*) DC3000 to 3-wk-old Arabidopsis WT (Col-0) at 1, 3, 5 and/or 7 d-post inoculation (dpi) with *Bacillus subtilis* or *P. oryzihabitans.* Bacterial growth was shown as log colony forming units (cfu) per cm^2 of leaf disk. Statistically significant differences between treatments are indicated by different letters (Fisher's LSD test; α = 0.05). (***C***) Time-resolved qRT-PCR analysis in Arabidopsis WT plants of Jasmonate Biosynthesis genes (JBGs; *ALLENE OXIDE CYCLASE 1 (AOC1),* and *OPDA REDUCTASE 3 (OPR3)*), Jasmonic acid (JA)-responsive gene (JRG; *THIONIN 2.1 (Thi2.1)*), OPDA-responsive gene (ORGs; *GLUTAREDOXIN 480 (GRX480), Cytochrome P450* gene *(CYP81D11)*), Salicylic acid (SA)-Biosynthesis genes (SBG; *Isochorismate (ICS1)*) and SA responsive genes (SRGs; *Pathogenesis-related protein (PR)1, PR5*). Total RNAs were prepared from roots and leaves at 0, 3, 6, 12, and 24 hpi. Values were normalized to the expression of POLYUBIQUITIN (mean ± SD; n = 3). (***D***) Hormone quantification of OPDA, JA, JA-Isoleucine (JA-Ile), and SA was conducted in leaves, phloem exudates, and root of

Arabidopsis WT (Col-0) plants at 0, 3, 6, 12, and 24 hpi. The asterisks denote statistically significant differences (*p ≤0.05, **p ≤0.01) according to the student's t-test.

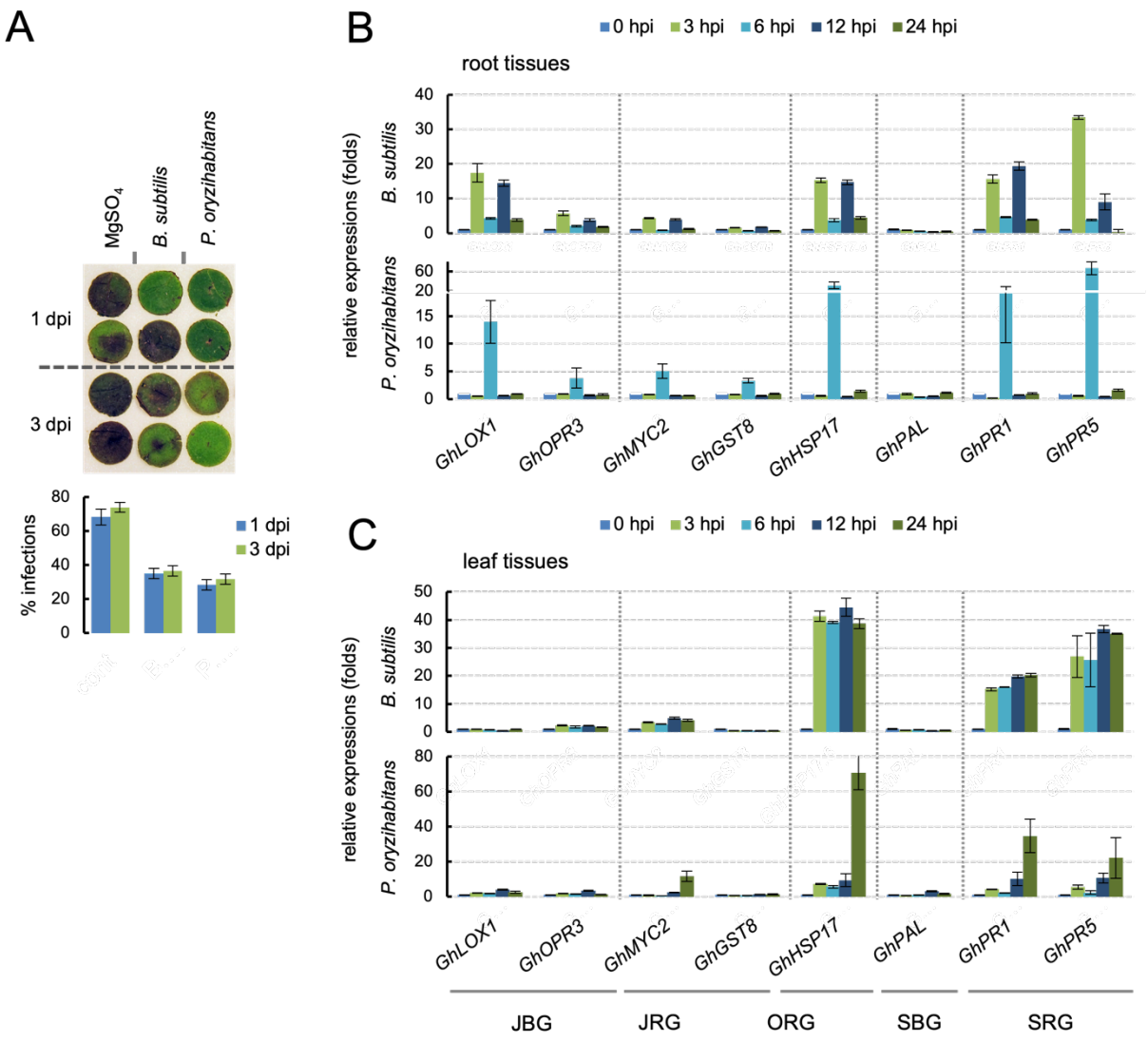

Figure 2.3. ISR-inducing PGPR primes cotton disease resistance against *C. casiicola* by enhancing jasmonate (OPDA and JA) production in roots but elevating only OPDA and SA signaling in systemic leaves without locally producing these hormones.

(***A***) Detached leaf assay for antifungal activity. 3-wk-old Cotton WT plants received a secondary inoculation with *Corynespora casiicola* at 1 and 3 days post-primary inoculation (dpi) with B*acillus subtilis* and *Pseudomonas oryzihabitans*. Leaves were then detached and inoculated with equal spore concentrations on sterile plates, and fungal growth was assessed at 7 days post-secondary infection. The percentage of infection in each treatment with PGPR inoculation was determined compared to the positive control, which received no primary inoculation. (***B-C***) Time-resolved qRT-PCR analysis in

Arabidopsis WT plants of Jasmonate Biosynthesis genes (JBGs; *LIPOXYGENASE (LOX1)*, and *12-OXOPHYTODIENOATE REDUCTASE 3 (OPR3)*), Jasmonic acid (JA)-responsive gene (JRG; *MYC2* and *GLUTATHIONE S-TRANSFERASE (GST)8*), 12-Oxo-Phytodienoic Acid (OPDA)-responsive gene (ORGs; *HEAT SHOCK PROTEIN (HSP)17*), Salicylic acid (SA)-Biosynthesis genes (SBG; *PHENYLALANINE AMMONIA-LYASE (PAL)*) and SA responsive genes (SRGs; Pathogenesis-related protein *(PR)1*, *PR5*). Total RNAs were prepared from roots (***B***) and leaves (***C***) of a 3-wk-old Arabidopsis plant at 0, 3, 6, 12, and 24-h post-PGPR (*Bacillus subtilis* and *Pseudomonas oryzihabitans*) inoculation (hpi). Values were normalized to the expression of *POLYUBIQUITIN* (mean ± SD; n = 3).

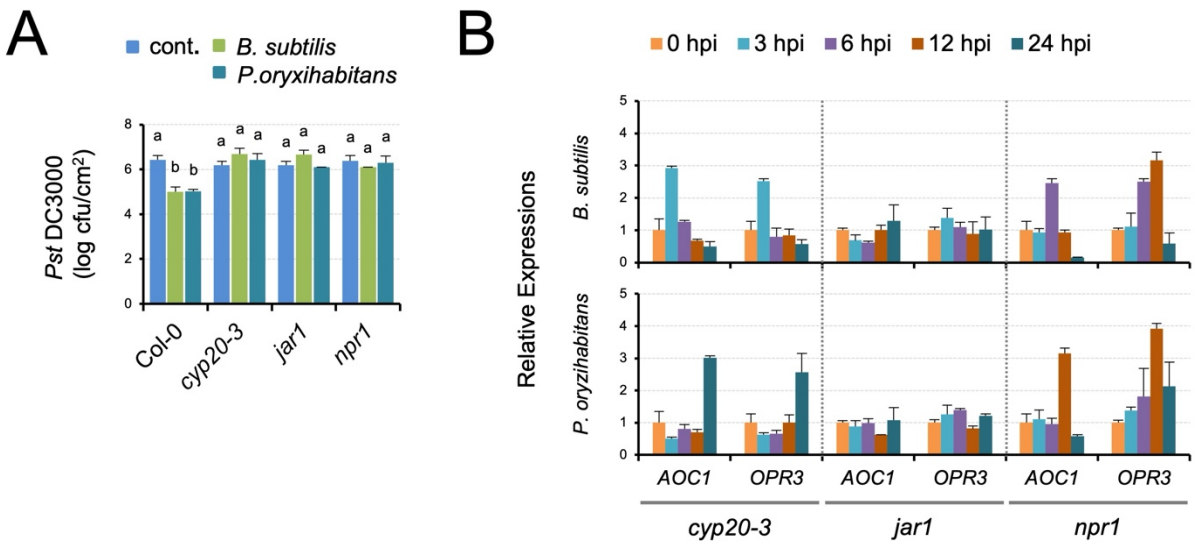

Figure 2.4. OPDA signaling is critical for ISR development, and impaired OPDA biosynthesis in *cyp20-3* and *jar1* mutants hinders ISR following PGPR treatment. (***A***) ISR assays by infecting *Pst* DC3000 to 3-wk-old Arabidopsis WT (Col-0) at 1 dpi with *Bacillus subtilis* or *P. oryzihabitans.* 3-wk-old Arabidopsis WT (Col-0) and mutant (*cyp20-3, jar1,* and *npr1*) plants received a secondary inoculation with *Pst* DC3000 at 1-d post-primary inoculation with *B. subtilis* and *P. oryzihabitans*. Bacterial growth was shown as log colony forming units (cfu) per cm^2 of leaf disk relative to control plants. Statistically significant differences between treatments are indicated by different letters (Fisher's LSD test; α = 0.05). (***B***) Time-resolved qRT-PCR analysis of JBGs *AOC1* and *OPR3* in Arabidopsis mutant plants. Total RNAs were prepared from roots at 0, 3, 6, 12, and 24 hpi with PGPR (*B. subtilis* and *P. oryzihabitans*). Values were normalized to *POLYUBIQUITIN* expression (mean ± SD; n = 3).

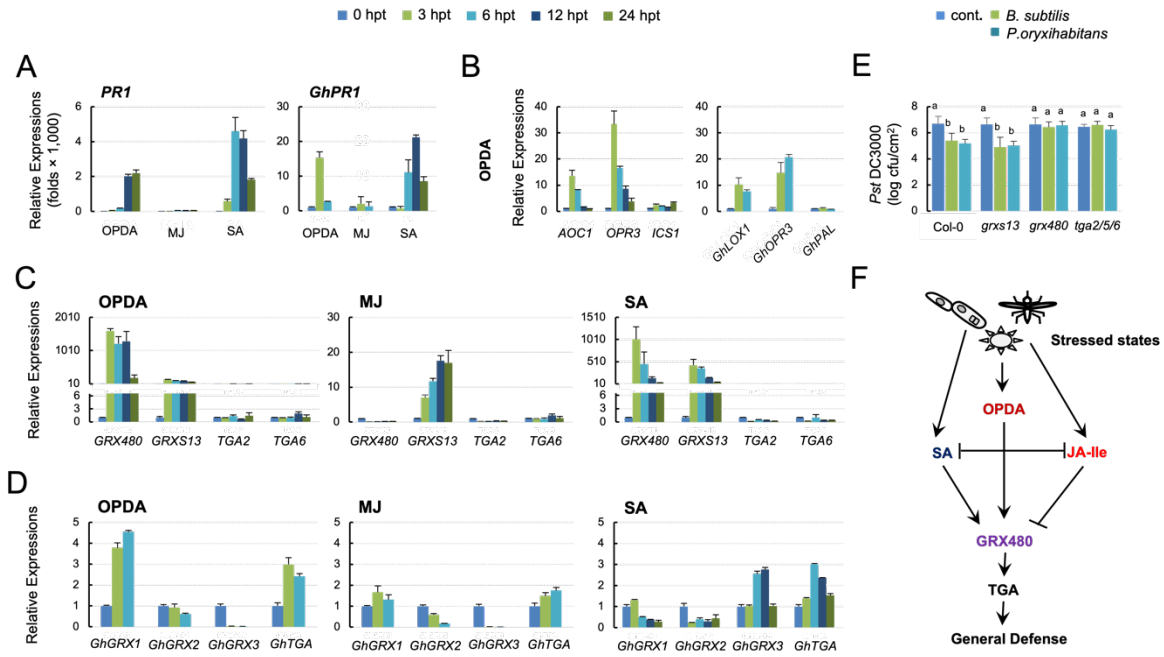

Figure 2.5. Activation of GRX480 by OPDA signaling might circumvent the SA signaling pathway, leading to the activation of the TGA transcription factor and *NPR1*-dependent expression of *PR1* independent of SA.

(***A-D***) Time-resolved qRT-PCR analysis of SRG *(Arabidopsis thaliana PR1* and *Gossypium hirsutum (Gh)PR1*), JBG *(AOC1*, *GhLOX1, OPR3* and *GhOPR3),* SBG *(ICS1* and *PAL), Glutaredoxin (GRX480, GRXS13, GhGRX1, GhGRX2,* and *GhGRX3)* and TGA *(TGA2, 6 and GhTGA)* genes in Arabidopsis WT (Col-0) (***A left, B left,*** and ***D***) and cotton (***A right, B right,*** and ***C***) plants after treatment with OPDA (***A-D***), MeJA, and SA (***A, C,*** and ***D***). Total RNAs were prepared from leaves at 0, 3, 6, 12, and 24-h post-hormone inoculation (hpi). Values were normalized to POLYUBIQUITIN expression (mean ± SD; n = 3). (***E***) ISR assays by infecting *Pst* DC3000 to 3-wk-old Arabidopsis WT (Col-0), CRISPR *grx480* and *grxS13,* and t-DNA insertion KO *tga2/5/6* plants at 1 dpi with *Bacillus subtilis* or *P. oryzihabitans. Pst* DC3000 growth was determined at 3 days post-secondary infection in log cfu per cm^2 of leaf disk. (***F***) Proposed model of activation of SA signaling pathway by OPDA via GRX transcription regulator and TGA transcription factors. GRX480 levels increase in response to SA induced by biotrophic pathogens, as well as OPDA produced in response to necrotrophic microbes, pests, and various abiotic stresses such as salinity, oxidative stress, light exposure, and mechanical injury, but are suppressed by JA. GRX480 then functions as a transcription regulator that binds and

activates TGA transcription factors, which further convey the *nonexpressor of pathogenesis-related protein 1 (NPR1)*-dependent salicylic acid (SA) defense gene expressions.

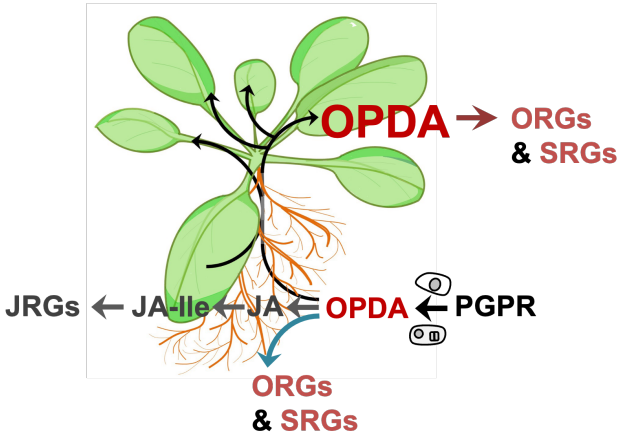

Figure 2.6. Proposed ISR signaling pathway.

In the primary inoculated root tissue, PGPR inoculations induce JA biosynthesis, activating JA-responsive genes (JRGs) and OPDA biosynthesis, activating OPDA-responsive genes (ORGs), which in turn induce GRX-mediated SA-responsive genes (SRGs). OPDA acts as a long-distance signal, traveling via phloem to uninoculated systemic tissues, where it continues to activate ORGs and GRX-mediated SRGs, thereby priming disease resistance across the entire plant.

Table 2.1. Oligonucleotides used in this study for Arabidopsis.

Name	Direction	Sequence, 5′ to 3′
AtPR1·Fw	Forward	GGGACTAACACGGCTTATGG
AtPR1·Rev	Reverse	CCTGGCAGTTGCTCTTTAAT
AtPR5·Fw	Forward	GGAGACTGTGGCGGTCTAAG
AtPR5·Rev	Reverse	CGGATGGTCTTATCCCCAGC
AtICS1·Fw	Forward	GAACTCAAATCTCAACCTCC
AtICS1·Rev	Reverse	ACTGCGACGAGAGAAGAAAC
AtCYP81D11·Fw	Forward	CTCTCAACATGGGTTTGTGA
AtCYP81D11·Rev	Reverse	GCTAACAACTACCTCGGCAA
AtGRX480·Fw	Forward	TGATTGTGATTGGACGGAGA
AtGRX480·Rev	Reverse	TAAACCGCCGGTAACTTCAC
AtThi2.1·Fw	Forward	CTCAGCTGATGCTACCAATGAGC
AtThi2.1·Rev	Reverse	GCTCCATTCACAATTTCACTTGC
AtOPR3·Fw	Forward	CACATGACGGCGGCACAAGG
AtOPR3·Rev	Reverse	TCAGAGGCGGGAAAAAGGA
AtAOC3·Fw	Forward	TCCAGACCAAGTAAGATCCA
AtAOC3·Rev	Reverse	TGTTTGTGAATGGGACGAGATC
AtGRXS13·Fw	Forward	CATACGAGTCACCGTGGAC
AtGRXS13·Rev	Reverse	GGAGTGGCCATTAATATGA
AtTGA2·Fw	Forward	CGGTGGTTGGAAGAAAAGAA
AtTGA2·Rev	Reverse	ACCGAGCCACAAGAAACATC
AtTGA6·Fw	Forward	CACTCACGATGGCTTGAAGA
AtTGA6·Rev	Reverse	AGAAACATCGCTCAGCTGGT
AtUBC·Fw	Forward	CTGCGACTCAGGGAATCTTCTAA
AtUBC·Rev	Reverse	TTGTGCCATTGAATTGAACCC

Table 2.2. Oligonucleotides used in this study for cotton.

Name	Direction	Sequence, 5′ to 3′	Reference
GhPR1·Fw	Forward	CTTGTCTCGTGGGGTTAGTC	Liu et al., 2014
GhPR1·Rev	Reverse	TGTGAGCGTTGAGGTAGTCT	Liu et al., 2014
GhPR5·Fw	Forward	GGACCATCGATGTGCCTGC	Zhang et al., 2019
GhPR5·Rev	Reverse	TCAATGCAAAGGTTGGGGTG	Zhang et al., 2019
GhPAL·Fw	Forward	CAATGGACAATGCTCGTTTGGCTAT	Aadil et al., 2020
GhPAL·Rev	Reverse	CACGGTGTTCTTCACTGTGCTCCTC	Aadil et al., 2020
GhHSP17.6·Fw	Forward	GAGCGAAAGCGTGAGAAAGAG	In this study
GhHSP17.6·Rev	Reverse	GGCAATGCGAACTTCCTCATAAAC	In this study
GhGRX480·Fw	Forward	GCCAGGAAGGGTTGTTGTATG	In this study
GhGRX480·Rev	Reverse	AGCCTCATCCTCCTCATCAATC	In this study
GhCYP81D11·Fw	Forward	GGCCACCTTCACTTGCTAATAA	In this study
GhCYP81D11·Rev	Reverse	CGTGAACCCAAGCGAAGAGAA	In this study
GhGST6·Fw	Forward	GCCTTCACGAGAAAGGTACTGA	In this study
GhGST6·Rev	Reverse	AAGCTGGAACTTGACCGAATG	In this study
GhGST8·Fw	Forward	GGGATACCATACGAGTACAGAGAA	In this study
GhGST8·Rev	Reverse	ACCTGAATGACCGACTCACAAA	In this study
GhMYC2·Fw	Forward	TCAATCAAGAAACCCTTCAACAGC	Hu et al., 2018

GhMYC2·Rev	Reverse	TTGGACTCCCCTTTCCCTTTATCT	Hu et al., 2018
GhLOX2·Fw	Forward	TTTTACTCCTACTGTGCTTCCCTTCA	Zhu et al., 2021
GhLOX2·Rev	Reverse	CCATGCCAACTCCGATTTTTCTC	Zhu et al., 2021
GhOPR3·Fw	Forward	GCTTACGGGCAAACCGAATC	Zhu et al., 2021
GhOPR3·Rev	Reverse	AGGCGGCCGTAAGATACAAG	Zhu et al., 2021
GhGST1·Fw	Forward	GAGGAAACTTGGAAGCATAATCT	Li et al., 2019
GhGST1·Rev	Reverse	TTTCATATACTCGCAAGCTTCG	Li et al., 2019
GhGST2·Fw	Forward	AAGAAGCTTGTGAGTGTCTAAAAAT	Li et al., 2019
GhGST2·Rev	Reverse	TCCACTGACAACACCTCCAAT	Li et al., 2019
GhGST3·Fw	Forward	GAAGAGGTGAAGGTTTTTGGAGC	Li et al., 2019
GhGST3·Rev	Reverse	ACTGGGACTTTCTTATGAACCGAG	Li et al., 2019
GhTGA7·Fw	Forward	GCTAACCAATCGCAAACCCT	In this study
GhTGA7·Rev	Reverse	AAATCGCCACTTTGTCCACC	In this study
GhUBQ7·Fw	Forward	AGGCATTCCACCTGACCAAC	Zhu et al., 2021
GhUBQ7·Rev	Reverse	CAGCGAGCTTGACCTTCTTC	Zhu et al., 2021

CHAPTER 3: A CIRCADIAN CLOCK RD29A IS AN ESTERASE, RELAYING AN OPDA SIGNAL IN PRIMING PLANT DROUGHT TOLERANCE

Note: This chapter is a manuscript that we are submitting to the journal as a Brief Communication. Hence, I am formatting the following section accordingly for submission.

3.1. ABSTRACT

Drought is a critical limiting factor for crop production, with efforts to combat its effects through breeding and engineering of drought-responsive genes (DRGs) often hampered by adverse impacts on plant growth and yield. Our recent research identified two DRGs, *Response to Desiccation (RD)29A* and *RD29B*, induced by the rhizobacterium *Paenibacillus polymyxa* CR1, which primes drought tolerance and enhances growth. Since their discovery, these genes have been used as molecular markers to monitor drought-response pathways across different plant species, but their activity and physiological roles have remained unknown. In the present study, we finally characterized that *RD29A* is an esterase/hydrolase enzyme ***i***) of which expression is driven by the circadian rhythm in both optimal and stress conditions, ***ii***) relaying *RD29B* activity and plant defense hormone (esp., 12-oxo-phytodienoic acid) signaling to regulate the temporal expression of drought-responsive genes in ***iii***) priming plant growth-promoting rhizobacteria (PGPR)-induced systemic tolerance (IST) and activating defense (acclimation) responses in plants against drought stress. Contrary to previous hypotheses, *RD29s* are functionally distinct, with *RD29B* being a constitutive gene acting upstream of *RD29A*, regulating its expression and circadian rhythm and upregulated by salt stress, unlike *RD29A*, which is downregulated. Transient gene expression analysis showed that the circadian rhythmic overexpression of *RD29A* could genetically replicate the PGPR-mediated IST across plants, upgrading drought resilience without the usually accompanied growth penalty across the plant species. This research offers new pathways for engineering drought-tolerant crops without compromising growth by mimicking rhizobacterium-induced stress tolerance. Future work exploring RD29A's substrates and RD29B's potential activity will help better understand plant growth and defense coordination across various plant species.

3.2. INTRODUCTION, RESULTS AND DISCUSSION

Drought is the most destructive and costliest environmental stress on crop productions. Thus, decades-long studies have identified a large pool of drought-responsive genes (DRGs) and transcription factors (TFs) that control an array of DRG expressions. Unfortunately, efforts to genetically engineer drought-tolerant plants modifying those TFs and/or DRGs appear to be at a standstill since their ectopic expressions suppress plant growth and development. Such transgenic plants can activate abscisic acid (ABA) signaling and/or iron transfer systems, causing stomatal closure to prevent water loss, which, however, also reduces CO_2 uptake, suppressing photosynthesis and growth under optimal conditions, thereby reducing yield (Farooq et al., 2009). Hence, our recent studies have been exploiting innovations to engineer plants with induced systemic tolerance (IST), activated by plant growth-promoting rhizobacteria (PGPR), provide, throughout the plant, enhanced tolerance to various abiotic constraints without compromising growth under both standard and stress conditions (Liu et al., 2020; 2023).

To investigate the mode and utility of IST, we ***i***) identified *Paenibacillus polymyxa* CR1, capable of sensitizing IST and concurrently increasing root growth in plants, and ***ii***) determined that this PGPR distinctively induces the expression of two DRGs, *Response to Desiccation* (*RD*)*29A* and *RD29B*, before drought stress (Liu et al., 2020). In that context, *RD29* KO (*rd29*) plants impaired IST and elevated susceptibility to drought without growth penalty (Liu et al., 2023). *RD29*s were originally isolated as drought- and cold-inducible genes and have long been used as key defense/stress-related markers across different plant species (Jia et al., 2012). However, little is known about their roles, activities, and mechanisms in plant growth and defenses. They are proposed to be functionally redundant (Msanne et al., 2011), but our results illuminated the differential role and function of *RD29*s as each coordinates a unique subset of stress-regulating TFs and downstream DRGs. Besides, *rd29a* conferred enhanced tolerance to increasing NaCl concentrations compared to WT and *rd29b*, indicating that *RD29A* −but not *RD29B*− is a negative regulator of salinity responses, and both *RD29*s actuate their own metabolic pathways, which in part intertwined to ward off stresses effectively (Liu et al., 2023).

Thus far, only studies on *RD29s* have been limited to the characterization and feasibility of their cis-elements in the temporal overexpression of DRGs to practice drought-tolerant plants (Jia et al., 2012). Their promoter region consists of one or more DRE (drought-responsive element) and ABRE (ABA-responsive element) motifs. Despite sharing cis-elements, our qRT-PCR analyses discerned disparate level and pattern expressions of *RD29*s. *RD29A* is a highly abundant circadian clock gene (**Figs 3.1A** and **3.2-3.4**) expressed significantly greater than *RD29B* (~45 to 400 folds, **Fig 3.5**). In a resting state, *RD29A* expressions were diurnally oscillated with a peak in the afternoon (~3pm) under 12-hour light:dark (LD) cycles, as well as free-running conditions (constant light, LL). To this extent, an IST stimulus and environmental changes did not cause the phase resetting of *RD29A* (**Fig 3.1B**, left). *P. polymyxa* CR1 and drought upregulated, whereas excess NaCl downregulated *RD29A* expressions, which nonetheless kept the same exact diurnal oscillation as its basal expressions. However, *rd29b* attenuated *RD29A* expressions, as well as dysregulated its circadian rhythmic inductions in both standard and stress states (**Fig 3.1B**, right), indicating that *RD29B* is positioned upstream and controls the circadian rhythm and magnitude of *RD29A* expressions.

On the other hand, *RD29B* appeared to be a constitutive gene showing a steady-state expression under LD and LL conditions (**Fig 3.1A**), which is upregulated by not only drought and *P. polymyxa* CR1, but also −unlike *RD29A*− salt treatments (**Fig 3.1C** vs. **B**), further supporting its distinct, *RD29A*-independent, role in plant defenses against salt stress (Liu et al., 2023). Besides, *rd29a* caused little change in its level/pattern expressions and inductions (**Fig 3.1C** right vs. left), depicting no reciprocal effect of *RD29A* toward *RD29B* transcriptions.

Our results suggest the important role of *RD29A* and its circadian rhythmic upregulations in developing PGPR-mediated IST by facilitating cellular multitasking, enabling plants to simultaneously run 'growth and defense machinery' through the time-sharing of limited resources to each operation one by one. To further substantiate this hypothesis, we ***i***) qRT-PCR searched and identified a candidate strong circadian promoter, the 5' flanking region of *COld Regulated (COR)15A,* that exhibits a robust circadian expression rhythm and also peaks at ~3pm (like *RD29A*, **Fig 3.1D**) and ***ii***)

prepared a series of plant transformation constructs harboring *RD29*s under the control of native (pRD29A and pRD29B), strong circadian (pCOR15A) and strong constitutive (p35S) promoters for transient expression screenings in tomato cv MicroTom (MT) and *Nicotiana benthamiana* (**Figs 3.1E** and **3.6**). As anticipated, the agroinfiltration of pCOR15A:*RD29A* in MT showed a noticeable drought tolerance improvement (**Fig 3.1E**). In *N. benthamiana*, *RD29A* overexpression by both native and COR15A promoters showed higher efficacy compared to an empty vector (EV) control and p35S (**Fig 3.6**). These validate the feasibility of *RD29A* and its circadian overexpressions in engineering IST and resolving adverse effects on normal growth from the constant overexpression of DRGs in transgenic plants. Similarly, the overexpression of another circadian DRG, *DREB1A,* driven by p35S improved drought tolerance but hindered plant growth, whereas using pRD29A displayed enhanced stress tolerance with minimal growth impact (Jia et al., 2012).

However, no information −to our best knowledge− is available for "how RD29s work." In fact, our in-silico searches using InterPro, MOTIF, Pfam, ProDom, and ScanProsite did not detect any known functional domain/motif in RD29s (Liu et al., 2023). Hence, to explore the yet-unknown biochemical activities of RD29s, we employed the API ZYM system. API ZYM is a semi-quantitative assay designed to determine 19 enzymatic activities colorimetrically. Incubation of RD29A, but not RD29B, proteins led to colored reactions of a substrate at 2-naphthyl butyrate (**Table 3.1**), illuminating that RD29A is an esterase/hydrolase. To scrutinize the detection, the catalytic capacity of RD29s was assessed toward artificial substrates *para*-nitrophenyl (*p*NP)-acetate (C2) and *p*NP-butyrate (C4). The steady-state kinetic parameters ($K_{M(app)}$ and k_{cat}) of RD29A were determined to be 1.0 µM and 4.67 s^{-1}, as well as 1.1 µM and 77.21 s^{-1}, respectively (**Figs 3.1F** and **G**), whereas RD29B exhibited little if any activity. In addition, neither RD29 was able to metabolize *p*NP-hexanoate (data not shown), indicating a limiting activity of RD29A toward longer fatty acid chains (≥C6). Together, our assays uncovered −for the first time− that RD29A is an enzyme capable of splitting esters into an acid and an alcohol with water, i.e., hydrolysis, known to play a key role in plant development and stress tolerance (Bornscheuer, 2002). Note, however, that our following in-silico and manual analyses still could not pinpoint a typical enzymatic motif of esterase, catalytic triad, from

the sequence of RD29A, suggesting it is a noncanonical esterase/hydrolase; a future study is needed to explore its cellular substrates and target pathways.

A previous study described that a phytodefense hormone, jasmonic acid-isoleucine (JA-Ile), controls level increases in *RD29A* mRNA during drought (de Ollas et al., 2015). However, JA-Ile is proposed to be a negative regulator (contrary to *RD29A*), reducing crop yield under drought and not induced by drought (Savchenko et al., 2014; Kim et al., 2009). To delineate a potential link between hormone signals and *RD29A* in imparting drought tolerance, we tested but observed WT-like drought responses in mutant plants lacking JA-Ile accumulations (*jar1*), as did *npr1* disrupting salicylic acid (SA) signaling (**Fig 3.1H**), indicating JA-Ile and SA are not involved directly in plant drought defenses. Instead, we observed enhanced drought susceptibility in *cyp20-3* and *Δtrx*, mutants lacking 12-oxo-phytodienoic acid (OPDA, a primary precursor of jasmonates) signaling (Liu and Park, 2021). In agreement, drought (Savchenoko et al., 2014) and IST-inducing PGPR (*P. polymyxa* CR1, **Fig 3.7**) activated OPDA, but not JA-Ile, signaling in leaf tissues, highlighting an intrinsic activity of OPDA signaling in plant drought tolerance and IST. Henceforth, to resolve if OPDA signaling activates *RD29A*, we monitored its differential expressions in WT following OPDA, MeSA, and SA treats. Indeed, only OPDA increased level *RD29A* transcripts (**Fig 3.1I**, top), which was again compromised in *cyp20-3* but not in *jar1* (**Fig 3.8A**, left), elaborating that CYP20-3/OPDA signaling conveys a message of water deficiency to activate *RD29A*. It is, however, independent of *RD29B*, which was not induced by OPDA (**Fig 3.1I**, bottom).

Several investigations elucidated that CYP20-3/OPDA signaling controls TGA TFs (Liu and Park, 2021). It is, in fact, evident that the promoter region of *RD29A* contains an ideal palindromic TGA TF binding site, which is absent in *RD29B* (**Fig 3.8B**). On the contrary, CYP20-3/OPDA signaling suppressed *RD29B* expressions as it is upregulated by OPDA in *cyp20-3* (**Fig 3.8A**, right). The impairment of OPDA signaling may elevate ABA signaling that upregulates *RD29B* expressions (Jia et al., 2012; Savchenko et al., 2014), highlighting the coordinate/synergistic activity of OPDA and ABA in orchestrating IST and local/basal responses toward drought stress.

As eluded, *RD29*A has long been considered a ubiquitous DRG and a marker to monitor stress-response pathways throughout plant species. In the present study, we

characterize −for the first time− that *RD29A* is a circadian clock gene and acts as an esterase/hydrolase enzyme. Despite an earlier hypothesis, *RD29A* are functionally and mechanistically distinctive from *RD29B*, although both are responsive to drought and IST-inducing PGPR, *P. polymyxa* CR1. *RD29B* is a constitutive gene positioned upstream and controls *RD29A*-dependent/independent defense responses. *RD29A* then relays CYP20-3/OPDA signaling to drive the temporal expression of DRGs in priming IST and activating defense (acclimation) responses toward drought stress in plants without the usually accompanied growth penalty. Hence, the circadian rhythmic overexpression of *RD29A* genetically replicates the PGPR-mediated IST in plants, providing a novel avenue for engineering drought-tolerant crops without compromising growth. The future work toward exploring target substrates of RD29A and possible activity of RD29B will further decipher plant mechanisms that coordinate growth and defenses and IST development across different plant varieties.

3.3. MATERIALS AND METHODS

3.3.1. Plant materials and growth conditions

Plants were grown in a chamber with a light intensity of ~120 $\mu E \cdot m^{-2} \cdot s^{-1}$ at 22°C and 60-80 % relative humidity. *Arabidopsis thaliana* wild type (WT) and mutants (*rd29a, rd29b, cyp20-3, jar1, npr1* and Δ*trx*) in Columbia (Col-0) background were grown with a 12-hour light/dark cycle, while *Nicotiana benthamiana* and *Solanum Lycopersicum* cv. Micro Tom (MT) were grown under a 16-hour:8-hour light:dark cycle.

3.3.2. Preparation of recombinant proteins

The full coding sequence of *RD29A* and *RD29B* was PCR cloned from cDNA and PCR subclone (U15808 from the Arabidopsis Biological Resource Center) into pET28a (Novagen) using primers with restriction enzymes, *BamH*I and *Nde*I (**Table 3.3**). Each recombinant protein was then expressed in *E. coli* BL21 (DE3) at 37 °C by 100 mM isopropyl ß-D-1-thiogalactopyranoside for 5 hr and purified via the nickel (Ni) affinity-purification. Briefly, cell pellets were resuspended in lysis buffer (50 mM Tris-HCl, pH 8.0, 150 mM NaCl) and disrupted by sonication. The resulting lysate was clarified by centrifugation at 4 °C. The supernatant was loaded onto the HisPur™ Ni-NTA resin

(ThermoFisher) and eluted in a lysis buffer containing increasing concentrations of imidazole (60 to 500 mM). Purified recombinant proteins were dialyzed by the SnakeSkin tubing (ThermoFisher) against lysis buffer and re-subjected to the cobalt agarose beads (GoldBio) for the 2nd round purification, eluted in lysis buffer containing 250 mM imidazole.

3.3.3. API® ZYM assay

As per the guideline of manufacturer (bioMérieux), supernatants (65 µL with 25 µg RD29A or 50 µg RD29B) were dispensed into 20 microcupules. Sterile water was added to the plastic outer cover to create a humid atmosphere. The API ZYM strips were covered and incubated at 37°C for 4 h. After that, one drop (30 µL) of the commercial reagents ZYM A and ZYM B was added to all microcupules to develop chromogenic substrates. Color reactions were read after 5 min.

3.3.4. Enzymatic assay

The esterase activities were determined colorimetrically by measuring the liberation of *para*-nitrophenol (*p*NP) from *p*NP-acetate (C2), -butyrate (C4), and -hexanoate (C6) as described in Park et al. (2008) with a slight modification. Briefly, the standard 1-mL reaction mixture consisted of 0 to 4 mM substrate in 50 mM potassium phosphate buffer, pH 7.0. The reaction was allowed to proceed for 15 min at 24°C, and the amount of *p*NP was measured at 420 nm (1 unit = $nM \cdot min^{-1} \cdot ng^{-1}$). Steady-state *K*M(app) values were determined by an initial velocity experiment. Kinetic parameters were calculated to fit untransformed data to $v=k_{cat}[S]/(K_M + [S])$ using Microsoft Excel.

3.3.5. Preparation and soil inoculation of PGPR

A PGPR strain, *P. polymyxa* CR1, was cultured as previously described (Liu et al., 2020). Briefly, it was grown in liquid LB medium at 30°C for 16 h with constant agitation and collected by centrifugation. The bacterial pellet was resuspended, washed twice with sterile ddH_2O, and adjusted to an inoculum concentration of 10^8 $cfu \cdot mL^{-1}$. The inoculum (8 mL) was then syringe-infiltrated into soils around the roots of 3-wk-old WT Arabidopsis (Col-0) plants.

3.3.6. Stress treatments

For salt treatment, 4-wk-old WT Arabidopsis (Col-0) plants were sprayed with 100 mM of NaCl, while drought stress was applied to 2-wk-old WT and mutant Arabidopsis (Col-0) plants by depriving water for 10 d before taking photographs and measuring the photo-synthesis efficacy.

3.3.7. Photosynthesis Measurements

The data collection for chlorophyll fluorescence-based photo-synthetic traits, the total non-photochemical exciton quenching (NPQt, Tietz et al., 2017), and quantum efficiency for photosystem II photochemistry (ΦII, Kuhlgert et al., 2016) were conducted on two leaves from each of the five plants, using the hand-held MultispeQ device (Kuhlgert et al., 2016), and uploaded to the PhotosynQ platform "http;//www.photosynq.org" according to the manufacturer's instructions.

3.3.8. Semiquantitative and quantitative RT-PCR

Total leaf RNA was isolated using TRIzol reagent (Invitrogen) and the Direct-zol RNA Kit (Zymo Research) following manufacturer protocols. RNA qualities were checked via agarose gel electrophoresis and NanoDrop spectrophotometry (A_{260}/A_{280} > 1.8, and A_{260}/A_{230} > 2.0, Udvardi et al., 2008). RT reactions utilized oligo(dT) reverse primer and qScript reverse transcriptase (Quantabio). Semi-quantitative RT-PCR was performed with 2 µL cDNA with Q5® High-Fidelity 2X Master Mix (New England BioLabs) at an annealing temperature of 55°C for primer pairs (**Table 3.2**) for 34 cycles. On the other hand, quantitative RT-PCR employed PerfeCT® SYBR® Green Fast Mix® Reaction Mixes (QuantaBio) in the CFX96 Touch™ PCR system (Bio-Rad) with 40 cycles, using gene-specific primer sets (**Table 3.2**). The annealing temperature for the primer pairs was 53 ^{o}C. To determine the relative abundance of target transcripts, the sample cDNA was assessed with housekeeping genes, *POLYUBIQUITIN-C (UBC*, Czechowski et al., 2005), and the average threshold cycle (i.e., Ct) was normalized to that of *UBC* where $-\Delta Ct = (Ct_{,gene} - Ct_{,UBC})$.

3.3.9. Plant transient-gene expression assay

To generate plant transformation constructs, the promoter regions of *RD29A* (~1.5 kb), *RD29B* (~0.6 kb) and *COR15A* (~1.0 kb), as well as 35S CaMV (~0.3 kb, Ramegowda et al., 2014) were PCR amplified using primers carrying *BamH*I, *Kpn*I and/or *Sac*I restriction sites (**Table 3.3**) and cloned into a binary vector pCAMBIA1300. In subsequent, (g)DNA sequence of *RD29A* and *RD29B,* including 3'- flanking regions (315 and 127 bp, respectively), was PCR amplified by primers carrying *BamH*I and *Pst*I restriction sites (**Table 3.3**) and cloned into the prepared pCAMBIA1300 harboring 4 different promoter regions to produce pRD29A:*RD29A,* pRD29B:*gRD29A,* pCOR15A:*gRD29A,* p35S:*gRD29B,* pRD29A:*gRD29B,* pRD29B:*gRD29B,* pCOR15A:*gRD29B* and p35S:*gRD29B*. The constructs were electro-porated into *Agrobacterium tumefaciens* LBA4404 and then grown in LB media with 20 µM acetosyringone, which were then resuspended in 10 M MES buffer (pH 5.6) containing 10 mM $MgCl_2$ and 150 µM acetosyringone by OD_{600} of 0.8. Each bacterial culture was incubated at room temperature for 2 hr and infiltrated into the underside of intact 6-wk-old leaves of *N. benthamiana* and *S. Lycopersicum* cv. MT using a 1 ml needleless syringe (Norkunas et al., 2018).

3.4. REFERENCES

Bornscheuer, U.T. (2002). Microbial carboxyl esterases: classification, properties and application in biocatalysis. FEMS microbiology reviews, 26(1), 73-81.

Czechowski, T., Stitt, M., Altmann, T., Udvardi, M.K., & Scheible, W.R. (2005). Genome-wide identification and testing of superior reference genes for transcript normalization in Arabidopsis. Plant physiology, 139(1), 5-17.

de Ollas, C., Arbona, V., & GóMez-Cadenas, A. (2015). Jasmonoyl isoleucine accumulation is needed for abscisic acid build-up in roots of Arabidopsis under water stress conditions. Plant, Cell & Environment, 38(10), 2157-2170.

Epple, P., Apel, K., & Bohlmann, H. (1995). An *Arabidopsis thaliana thionin* gene is inducible via a signal transduction pathway different from that for pathogenesis-related proteins. Plant physiology, 109(3), 813-820.

Farooq, M., Wahid, A., Kobayashi, N.S.M.A., Fujita, D.B.S.M.A., & Basra, S.M. (2009). Plant drought stress: effects, mechanisms and management. Sustainable agriculture, 153-188.

Harb, A., Krishnan, A., Ambavaram, M.M., & Pereira, A. (2010). Molecular and physiological analysis of drought stress in Arabidopsis reveals early responses leading to acclimation in plant growth. Plant physiology, 154(3), 1254-1271.

Jia, H., Zhang, S., Ruan, M., Wang, Y., & Wang, C. (2012). Analysis and application of *RD29* genes in abiotic stress response. Acta Physiologiae Plantarum, 34, 1239-1250.

Kim, E.H., Kim, Y.S., Park, S.H., Koo, Y.J., Choi, Y.D., Chung, Y.Y., Lee, I.J., & Kim, J.K. (2009). Methyl jasmonate reduces grain yield by mediating stress signals to alter spikelet development in rice. Plant Physiology, 149(4), 1751-1760.

Kuhlgert, S., Austic, G., Zegarac, R., Osei-Bonsu, I., Hoh, D., Chilvers, M.I., Roth, M.G., Bi, K., TerAvest, D., Weebadde, P., & Kramer, D.M. (2016). MultispeQ Beta: a tool for large-scale plant phenotyping connected to the open PhotosynQ network. Royal Society open science, 3(10), 160592.

Liu, W., & Park, S.W. (2021). 12-oxo-Phytodienoic acid: a fuse and/or switch of plant growth and defense responses? Frontiers in Plant Science, 12, 724079.

Liu, W., Sikora, E., & Park, S.W. (2020). Plant growth-promoting rhizobacterium, *Paenibacillus polymyxa* CR1, upregulates dehydration-responsive genes, *RD29A* and *RD29B*, during priming drought tolerance in arabidopsis. Plant Physiology and Biochemistry, 156, 146-154.

Liu, W., Thapa, P., & Park, S.W. (2023). *RD29A* and *RD29B* rearrange genetic and epigenetic markers in priming systemic defense responses against drought and salinity. Plant Science, 337, 111895.

Msanne, J., Lin, J., Stone, J.M., & Awada, T. (2011). Characterization of abiotic stress-responsive *Arabidopsis thaliana RD29A* and *RD29B* genes and evaluation of transgenes. Planta, 234, 97-107.

Mueller, S., Hilbert, B., Dueckershoff, K., Roitsch, T., Krischke, M., Mueller, M.J., & Berger, S. (2008). General detoxification and stress responses are mediated by

oxidized lipids through TGA transcription factors in Arabidopsis. The Plant Cell, 20(3), 768-785.

Norkunas, K., Harding, R., Dale, J., & Dugdale, B. (2018). Improving agroinfiltration-based transient gene expression in *Nicotiana benthamiana*. Plant methods, 14, 1-14.

Park, S.W., Liu, P.P., Forouhar, F., Vlot, A.C., Tong, L., Tietjen, K., & Klessig, D.F. (2009). Use of a synthetic salicylic acid analog to investigate the roles of methyl salicylate and its esterases in plant disease resistance. Journal of Biological Chemistry, 284(11), 7307-7317.

Qin, X.F., Holuigue, L., Horvath, D.M., & Chua, N.H. (1994). Immediate early transcription activation by salicylic acid via the cauliflower mosaic virus as-1 element. The Plant Cell, 6(6), 863-874.

Ramegowda, V., Basu, S., Krishnan, A., & Pereira, A. (2014). Rice *GROWTH UNDER DROUGHT KINASE* is required for drought tolerance and grain yield under normal and drought stress conditions. Plant physiology, 166(3), 1634-1645.

Savchenko, T., Kolla, V.A., Wang, C.Q., Nasafi, Z., Hicks, D.R., Phadungchob, B., Chehab, W.E., Brandizzi, F., Froehlich, J., & Dehesh, K. (2014). Functional convergence of oxylipin and abscisic acid pathways controls stomatal closure in response to drought. Plant Physiology, 164(3), 1151-1160.

Tietz, S., Hall, C.C., Cruz, J.A., & Kramer, D.M. (2017). NPQ (T): a chlorophyll fluorescence parameter for rapid estimation and imaging of non-photochemical quenching of excitons in photosystem-II-associated antenna complexes (Vol. 40, No. 8, pp. 1243-1255).

Udvardi, M.K., Czechowski, T., & Scheible, W.R. (2008). Eleven golden rules of quantitative RT-PCR. The Plant Cell, 20(7), 1736-1737.

Wang, H., Wang, J., Jiang, J., Chen, S., Guan, Z., Liao, Y., & Chen, F. (2014). Reference genes for normalizing transcription in diploid and tetraploid Arabidopsis. Scientific reports, 4(1), 6781.

Yamaguchi-Shinozaki, K., & Shinozaki, K. (1993). Arabidopsis DNA encoding two desiccation-responsive *rd29* genes. Plant physiology, 101(3), 1119.

Yamaguchi-Shinozaki, K., & Shinozaki, K. (1993). Characterization of the expression of a desiccation-responsive *rd29* gene of *Arabidopsis thaliana* and analysis of its promoter in transgenic plants. Molecular and General Genetics MGG, 236, 331-340.

Yamaguchi-Shinozaki, K., & Shinozaki, K. (1994). A novel cis-acting element in an Arabidopsis gene is involved in responsiveness to drought, low-temperature, or high-salt stress. The Plant Cell, 6(2), 251-264.

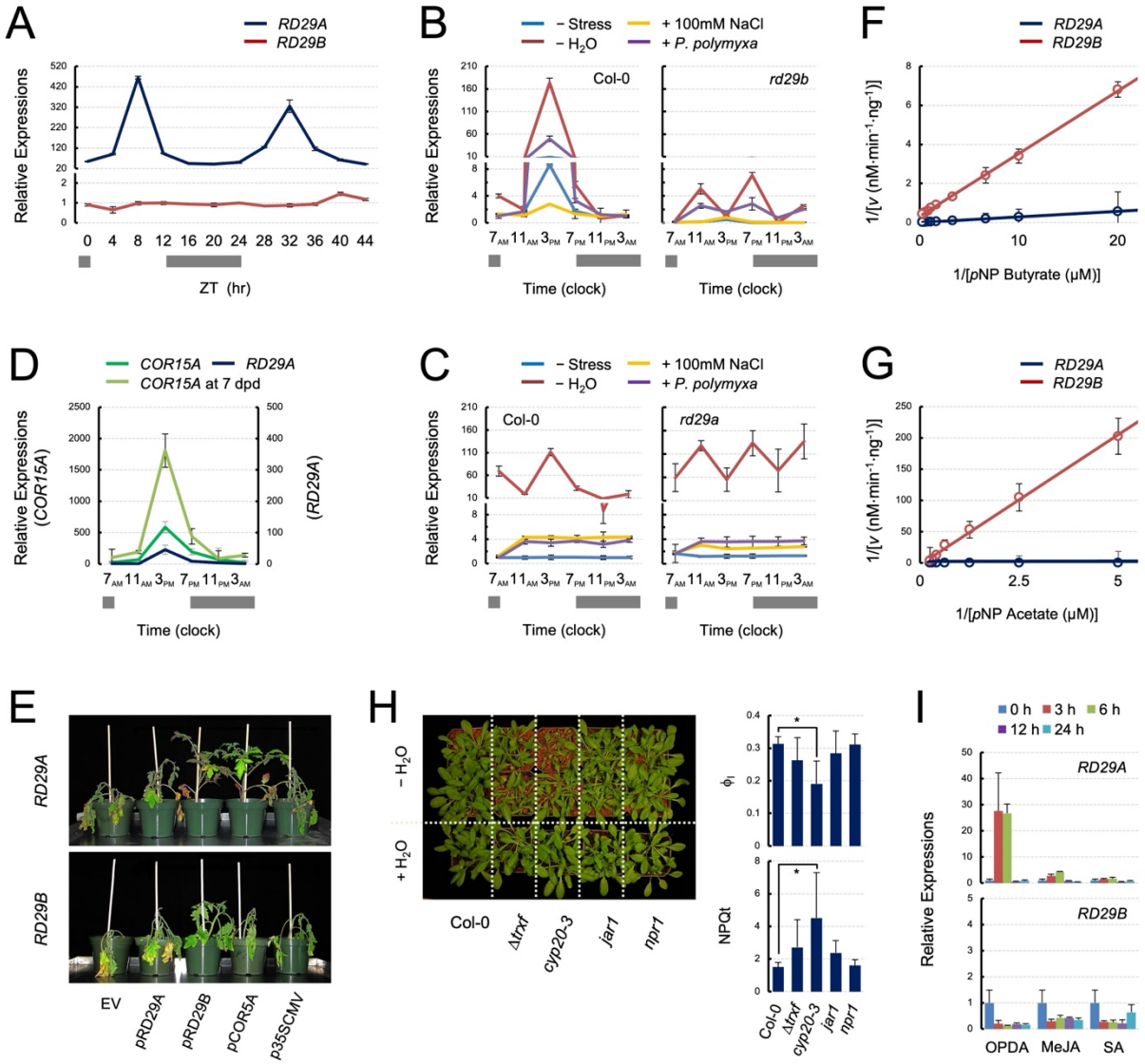

Figure 3.1. A circadian clock RD29A is an esterase/hydrolase enzyme, conveying CYP20-3/OPDA signaling in priming plant drought resilience.

*(**A-D**)* Time-resolved qRT-PCR analyses of *RD29A, RD29B* (***A-D***) and/or *COR15A* (***D***) in WT (Col-0) and/or KO mutant (*rd29a* and *rd29b*) plants grown under 12-hour light/dark conditions (***A-D***) and transferred to continuous light (***A***). 3-wk-old plants were treated with water (- stress), salt (+ 100mM NaCl), drought (- H_2O) or PGPR (+ *P. polymyxa*) for 1 or 7-d before harvesting leaves every 4- or 6-h for a day. ZT, Zeitgeber time. Grey bars indicate the dark cycle. (***E)*** A representative effect of the transient overexpression of *RD29s* in WT (MT) toward drought. Tomato leaves, 3-wk old, were syringe-infiltrated with *A. tumefaciens* harboring *RD29A* and *RD29B* under the control of native (pRD29s), strong

circadian (pAtCOR15A) and strong constitutive (p35S) promoters. Plants were photographed 20-d after drought stress. (***F, G***) Lineweaver-Burk plots for the esterase activity of RD29A using *p*NP butyrate (***F***) and acetate (***G***) as substrates, measured spectrophotometrically at OD_{420} nm. (***H***) A representative effect of WT (Col-0) and KO mutant (Δ*trx*, *cyp20-3*, *jar1,* and *npr1*) plants toward drought (***left***, a photograph was taken at 12-d). In parallel, their photosynthetic efficacy (ΦII, ***right top***) and nonphotochemical quenching (NPQt, ***right bottom***) values were measured at 10-d (means ± SD; *n*=10). Statistical analyses were conducted using the Tukey-Kramer honestly significant difference test on all pairs (P < 0·05). (***I***) Time-resolved qRT-PCR analyses of *RD29A* and *RD29B* in WT Arabidopsis after 75 μM OPDA, MeJA, and SA treatments. Total RNAs were prepared from leaves at 0, 3, 6, 12, and 24 h following hormone treatments. (***A-D, I***) Fold changes (means ± SD; *n*=3) were made relative to *POLYUBIQUTIN* (*UBC*) expressions.

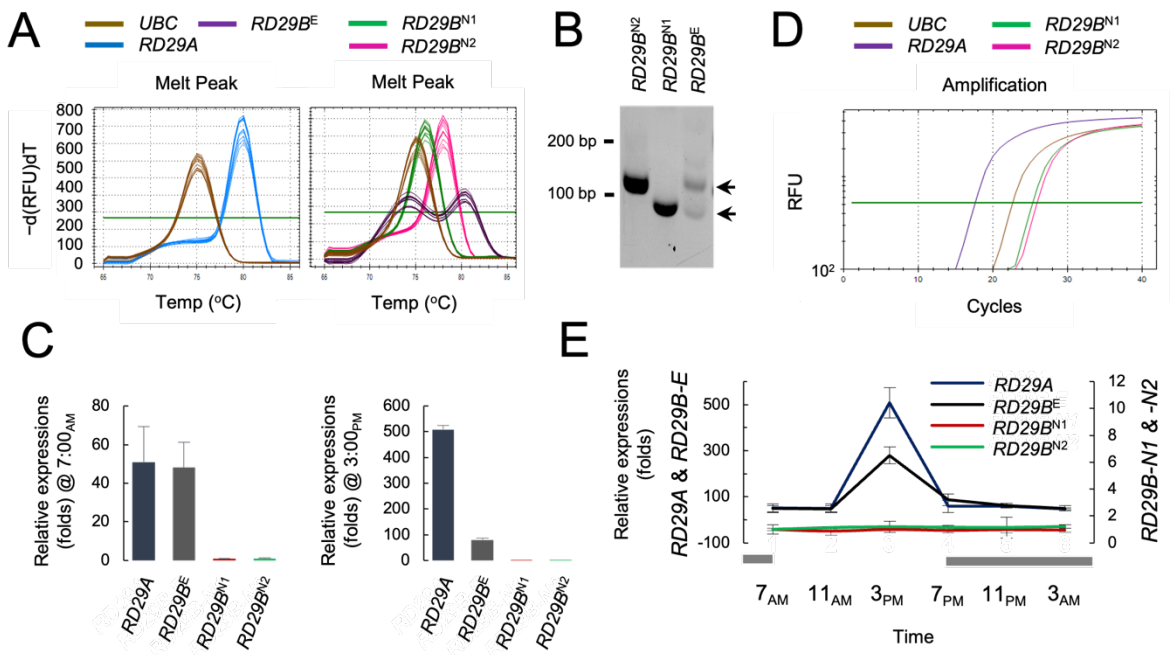

Figure 3.2. The level transcript of *RD29A* is >50-folds higher than that of *RD29B*. Thus far, most studies, including ours, reported that the level transcripts of *RD29A* and *RD29B* in the resting state are comparable (Yanaguchi-Shinozaki et al., 1993a,b; 1994; Harb et al., 2010; Liu et al., 2020). However, we −in this study− found rather difficulty (unlike *RD29A*) in PCR amplifying the full coding sequence of *RD29B* from total RNA prepared from leaf tissues grown under standard and drought conditions. In the end, our qRT-PCR uncovered that a primer set used for *RD29B* amplifications in the earlier study (Liu et al., 2020, referred to as *RD29B*^{E}, Fig 3.3A and Table 3.2) produced off-target amplicons (two peaks from purple curves in *right*, (***A***) representing 134 and 89 bp amplicons (see arrows, *B*) which were likely amplified from *RD29B* (134 bp) and *RD29A* (89 bp) cDNAs, respectively (Fig 3.3). Hence, two new specific primer sets for *RD29B* (N1, green curves and N2, pink curves; *A*) were designed (Fig 3.4 and Table 3.2), which specifically amplify 73 bp and 128 bp products, respectively (***B***). (***C***) Transcript quantification by qRT-PCR of *RD29A* and *RD29B* (by *RD29B*^{E}, *RD29B*^{N1} and *RD29B*^{N2}) at 7:00AM and 3:00PM in WT (Col-0) plants. Values were normalized to the expression of *POLYUBIQUITIN-C* (*UBC*, means ± SD; *n* = 3). *RD29B* expression analysis using *RD29B*^{N1} and *RD29B*^{N2} specific primer sets revealed that *RD29B* is expressed at levels 45 to 400 times lower than *RD29A*. (***D***) A representative amplification graph of *UBC*,

RD29A, and *RD29B* (by *RD29B*^{N1} and *RD29B*^{N2}) at 3:00PM in WT (Col-0) plants. The amount of *RD29A* cDNA from the sample represented in the purple curve is 32 times (5 Cq) higher, whereas *RD29B* cDNA shown in green and pink curves are ~8 times (3 Cq) lower than the amount of a reference (*UBC*) cDNA, one of top 10 richest reference genes (Czechowski et al., 2005; Wang et al., 2014). (***E***) Time-resolved qRT-PCR analyses of *RD29A* and *RD29B* (by *RD29B*^{E}, *RD29B*^{N1} and *RD29B*^{N2}) in WT (Col-0) plants grown under 12-hour light/dark conditions. Grey bars beneath a graph indicate the dark period. Total RNAs were prepared from leaves every 4 h, and values were normalized to the expression of the *UBC* gene (means ± SD; n = 6).

A

RD29B^{E}_F: 5′-ACG AGC AAG ACC CAG AAG TT
RD29B^{E}_R: 5′-CAT CGG AGG AGA TTG TTC C

B

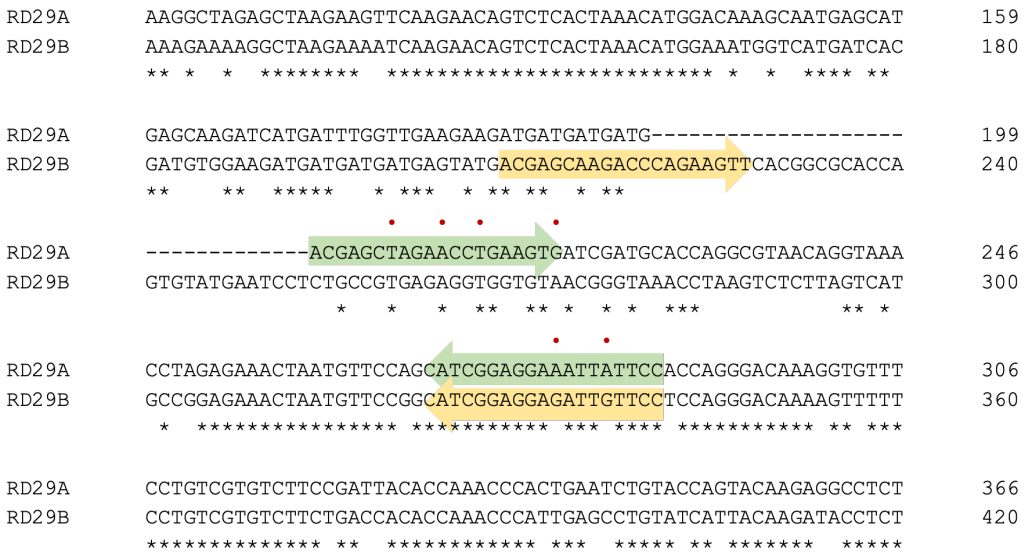

Figure 3.3. The predicted non-specific target of RD29BE qRT-PCR primers in RD29A mRNA.

The predicted non-specific target of *RD29B*^{E} qRT-PCR primers in *RD29A* mRNA. (***A***) The sequence of a set (F, forward and R, reverse) of *RD29B*^{E} qRT-PCR primers used in the earlier study (Liu et al., 2020). (***B***) The target sequences of *RD29B*^{E} in *RD29A* (green arrows, 89 bp) and *RD29B* (yellow arrows, 134 bp) mRNA, as observed in Fig 3.2B. The red dots indicate mismatched nucleotides between *RD29B*^{E} primers and *RD29A* mRNA.

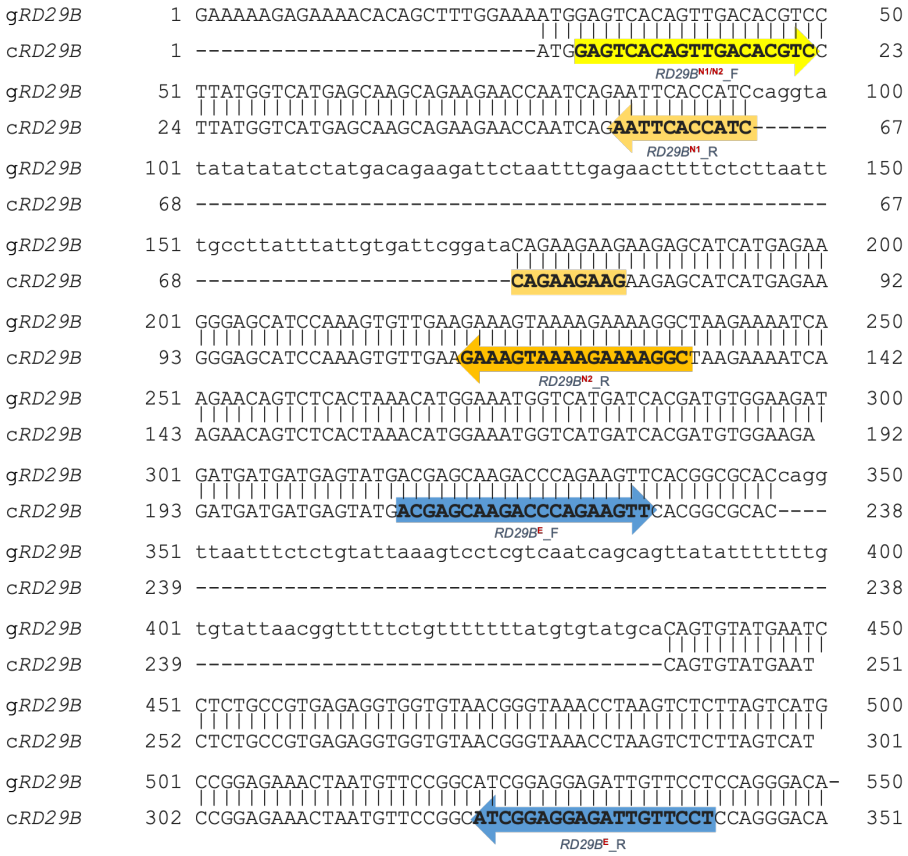

Figure 3.4. Sequential positions of qRT-PCR primer set for *RD29B*.

The forward (F) and reverse (R) positions of three primer sets (*RD29B*^{E}, *RD29B*^{N1} and *RD29B*^{N2}) are indicated by arrows onto the sequence alignment of 5'-region genomic DNA (g) and coding sequence (c) of *RD29B*. Note that the reverse primer for *RD29B*^{N1} contains an exon^exon junction.

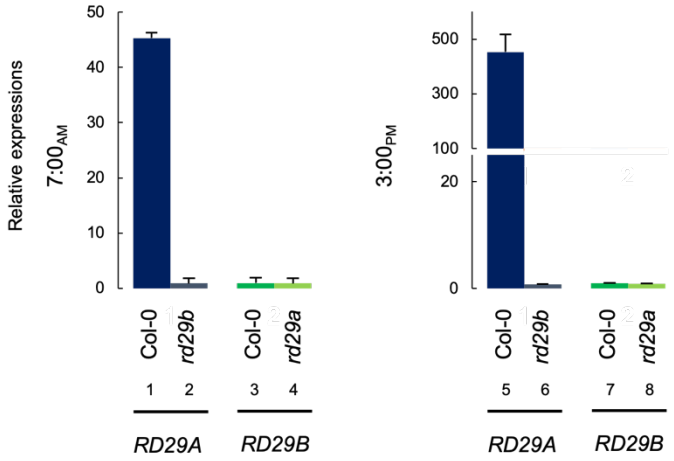

Figure 3.5. *RD29B* is an upstream regulator of *RD29A*, governing the upregulation of *RD29A*.

qRT-PCR quantification of *RD29A* and *RD29B* (average of *RD29B*^{N1} and *RD29B*^{N2}) transcripts at 7:00 AM and 3:00PM in WT (Col-0) and mutant *rd29a* and *rd29b* plants. The mutant Arabidopsis knocking out *RD29B* (*rd29b*) attenuated *RD29A* expressions, ~45 (lane 2 vs. 1) and ~450 (lane 6 vs. 5) folds at 7:00 AM and 3:00PM, respectively. In contrast, the KO mutation of *RD29A* (*rd29a*) caused little, if any, effect in *RD29B* expressions (lanes 4 vs. 3, and 8 vs. 7).

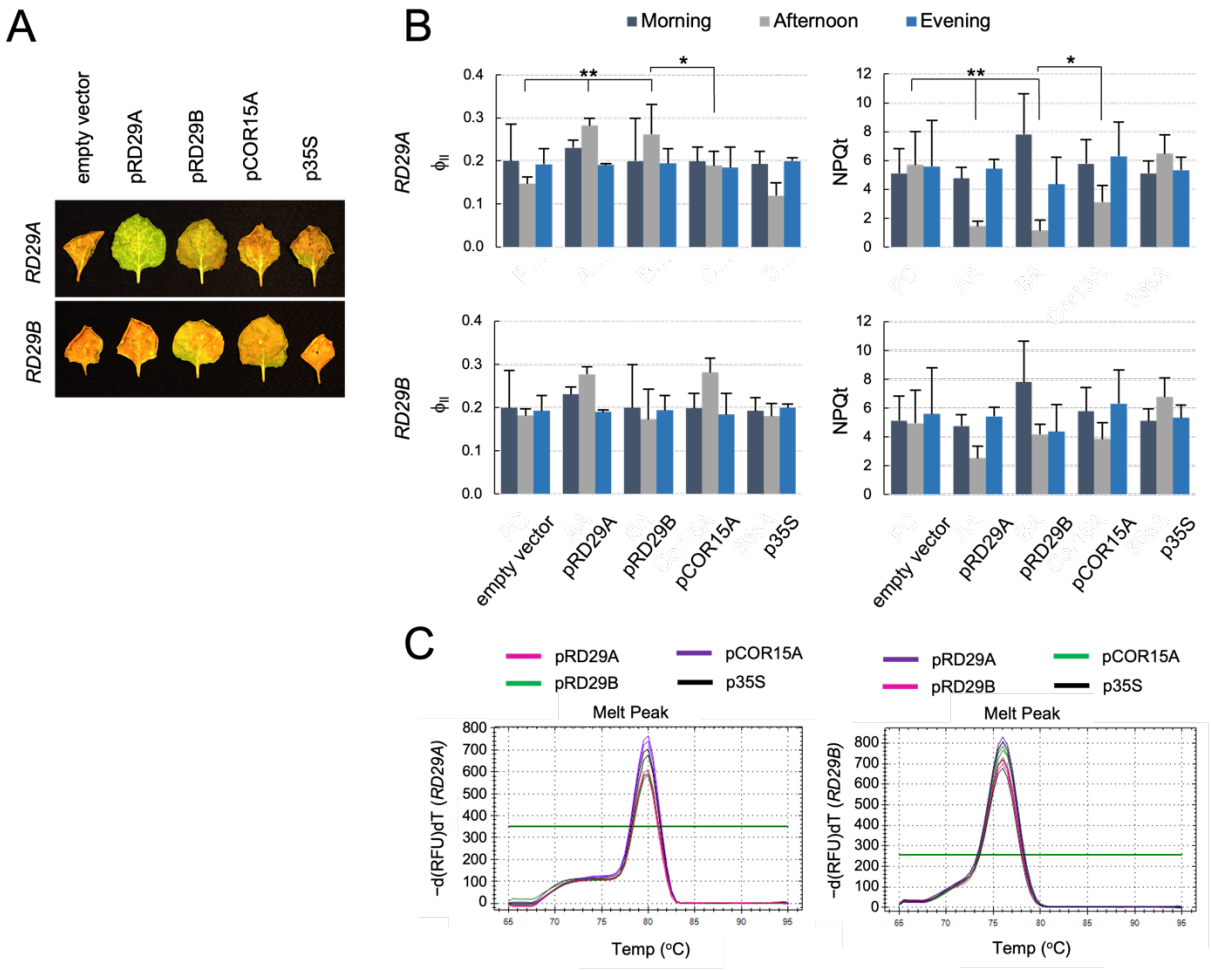

Figure 3.6. Transient overexpression of *RD29A* enhances drought tolerance in *N. benthamiana* leaves.

(***A***) Representative responses of *N. benthamiana* leaves agroinfiltrated with *RD29*s towards drought. A set of empty and plant transformation constructs (pCAMBIA) harboring Arabidopsis *RD29A* or *RD29B* under the control of native (pRD29A and pRD29B), strong circadian (pCOR15A) or strong constitutive (p35S) promoters were generated and transformed into *A. tumefaciens* LBA4404, which were then syringe-infiltrated into *N. benthamiana* leaves. After stopping watering, photographs were taken at 15 d. (***B***) Transient overexpression of *RD29A* under circadian rhythmic promoters improved plant photosynthesis efficacy under drought. The asterisks indicate statistically significant differences (*p ≤0.05, **p ≤0.01, the student's t-test). ΦII (photosystem II quantum yield) and NPQt (total nonphoto-chemical quenching) values were measured in the morning (8AM), afternoon (2PM), and evening (8PM) in WT (Col-0) transiently

overexpressing empty and plant transformation constructs at 10 d-post drought treatment (means ± SD; *n* = 10). (***C***) Transient overexpression of Arabidopsis *RD29s* in *N. benthami-ana.* Total RNAs were prepared from leaves at 10 d-post drought treatment or agroinfiltration. This RNA was then used for qRT-PCR to generate melt peak curves demonstrating the overexpression of *A. thaliana RD29A* (*Left*) and *AtRD29B* (*right*) in transient transgenic *N. benthamiana* leaves.

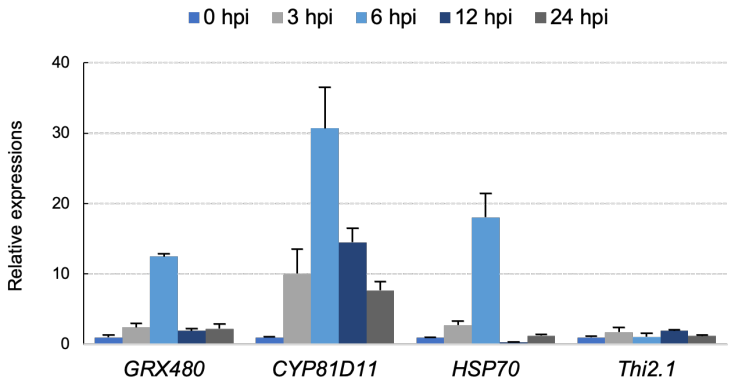

Figure 3.7. Soil applications of P. polymyxa activate OPDA signaling in Arabidopsis leaves.

Time-resolved qRT-PCR analyses of OPDA-responsive genes (Mueller et al., 2008) such as *GLUTAREDO-XIN 480* (*GRX480*), *CYTOCHROME P450* (*CYP81D11*) and *HEAT SHOCK PROTEIN 70* (*HSP70*) and a JA-Ile responsive gene (Epple et al., 1995) *THIONIN* (*Thi2.1*) after the treatment of *P. polymyxa* CR1 into soils around WT Arabidopsis roots. Total RNAs were prepared from leaves at 0, 3, 6, 12, and 24 h-post PGPR inoculations (hpi; mean ± SD, *n*=3*),* and values were normalized to the expression of *UBC*.

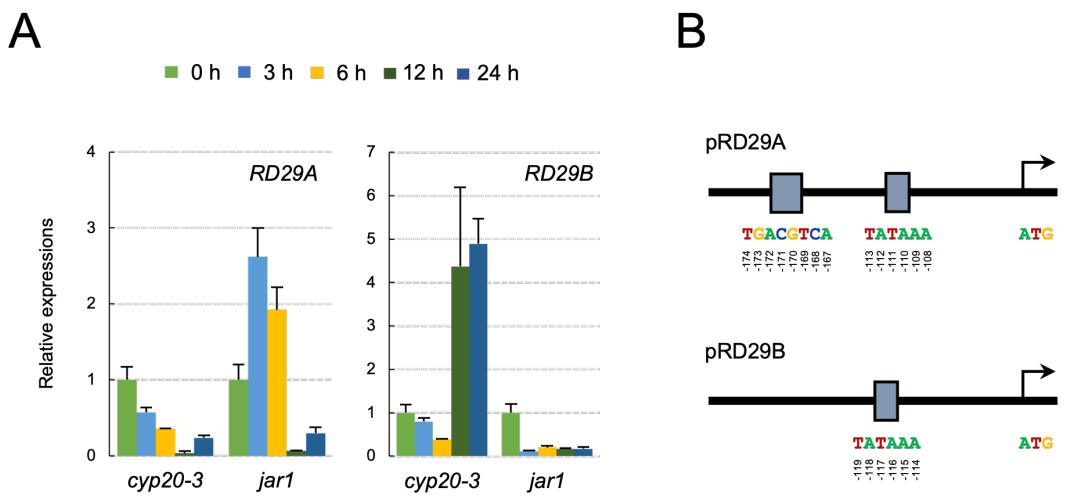

Figure 3.8. CYP20-3/OPDA signaling binds and controls TGA TFs to upregulate *RD29A* and downregulate *RD29B* expression.

(***A***) Time-resolved qRT-PCR analyses of *RD29A* (*left*) and *RD29B* (*right*) in *cyp20-3* and *jar1* after OPDA treatment. Total RNAs were prepared from leaves at 0, 3, 6, 12, and 24 h following OPDA treatments (mean ± SD; *n* = 3), and values were normalized to the expression of *UBC*. (***B***) Region schematics of cis-elements of *RD29*s. An *RD29A* promotor contains an ideal palindromic TGA-TF binding site (TGACGTCA; Qin et al., 1994) near the TATA (TATAAA) box, whereas the *RD29B* promoter lacks this TGA-binding site.

Table 3.1. Semi-quantitative, API® ZYM, probing the enzymatic activity of RD29A and RD29B.

Enzymatic activities	RD29A	RD29B
Control	-	-
Alkaline phosphatase	-	-
Esterase (C4)	+	-
Esterase Lipase (C8)	-	-
Lipase	-	-
Leucine arylamidase	-	-
Valine arylamidase	-	-
Crystine arylamidase	-	-
Trypsin	-	-
α-chymotrypsin	-	-
Acid phosphatase	-	-
Naphthol-AS-BI-phosphohydrolase	-	-
α-galactosidase	-	-
β-galactosidase	-	-
β-glycuronidase	-	-
α-glucosidase	-	-
β-glucosidase	-	-
N-acetyl-β-glucosaminidase	-	-
α-mannosidase	-	-
β-fucosidase	-	-

Table 3.2. Oligonucleotide used for qRT-PCR.

Genes	Directions	Sequence (5'-3')
UBC	Forward	CTGCGACTCAGGGAATCTTCTAA
At5g25760	Reverse	TTGTGCCATTGAATTGAACCC
COR15A	Forward	CAGATGGTGAGAAAGCGAAA
At2g42540	Reverse	CCCTACTTTGTGGCATCCTT
RD29A	Forward	ATCGATGCACCAGGCGTAA
At5g52310	Reverse	TGCATCGTGTCCGTAAGAGG
RD29B^{E}	Forward	ACGAGCAAGACCCAGAAGTT
At5g52300	Reverse	AGGAACAATCTCCTCCGATG
RD29B^{N1}	Forward	GAGTCACAGTTGACACGTC
At5g52300	Reverse	CTTCTTCTGGATGGTGAATT
RD29B^{N2}	Forward	GAGTCACAGTTGACACGTC
At5g52300	Reverse	GCCTTTTCTTTTACTTTC

Table 3.3. Oligonucleotide used for cloning PCR.

Genes	Directions	Sequence (5'-3')
*RD29A_Nde*I	Forward	TCGATCCATATGATGGATCAAACAGAGGAACCAC
*RD29A_BamH*I	Reverse	GATCTGGGATCCTTAAAGCTCCTTCTGCACCGG
*RD29B_Nde*I	Forward	TCGATCCATATGGAGTCACAGTTGACACGTCC
*RD29B_BamH*I	Reverse	GATCTGGGATCCTCAGTTCCCAGAATCTTGAACTC
*gRD29A_BamH*I	Forward	ATATATGGATCCATGGATCAAACAGAGGAACCA
*gRD29A_Pst*I	Reverse	ATATATCTGCAGAATATGCTCTCATCCTAGAAAT
*gRD29B_BamH*I	Forward	ATATATGGATCCATGGAGTCACAGTTGACACG
*gRD29B_Pst*I	Reverse	ATATATCTGCAGTCTTATCCAAAAAAGCAAATATTT
p35S_*Kpn*I	Forward	ATATTAGGTACCACATCAATCCACTTGCTTTG
p35S_*BamH*I	Reverse	ATATTAGGATCCCCATGGAGTCAAAGATTC
pCOR15A_*Sac*I	Forward	GAGCTCTAGATCTTGTCCGTTGAATT
pCOR15A_*Kpn*I	Reverse	GGTACCAGATGTGAGAATAAAAAGAAG
pRD29A_*Kpn*I	Forward	GCTATCGGTACCAGATTTGGGGTTTTGCTTTTG
pRD29A_*BamH*I	Reverse	GCTATCGGATCCTCCAAAGATTTTTTTCTTTCC
pRD29B_*Kpn*I	Forward	GCTATCGGTACCCGTAATTTTCTAGATCCGTCTTGG
pRD29B_*BamH*I	Reverse	GCTATCGGATCCTCCAAAGCTGTGTTTTCTC

CHAPTER 4: CYCLOPHILIN 20-3, AN OPDA RECEPTOR, COORDINATES PLANT ROOT HAIR GROWTH AND RESISTANCE AGAINST PARASITIC NEMATODES

4.1. ABSTRACT

Plant parasitic nematodes (PPN) are the major threat to agriculturally important crops, resulting in substantial yield losses and economic repercussions. However, the mode and apparatus of plant responses against PPN remain largely elusive. Here, we describe a vital role of cyclophilin 20-3 (CYP20-3), a receptor of 12-oxo-phytodienoic acid (OPDA) signal, in constitutive plant resistance against PPN attacks. To define a present working model whether plant roots deploy hypersensitive response (HR) to restrict PPN populations, we co-imaged 'real-time' interactions of a proposed HR system, hypersensitive cotton LONREN-1 vs. *Rotylenchulus reniformis*. However, root imaging did not reveal any clear HR patterns. Instead, it highlighted a negative relationship between PPN infections and larger root/root hair growth. The latter was then identified to couple with the spatial expression of *peptidyl-prolyl isomerases* such as *CYP20-3*. To substantiate these findings further, we employed a reverse generic approach using a model plant Arabidopsis. Indeed, knockout *cyp20-3* mutants exhibited significant defects in the root hair formation and also enhanced susceptibility to PPN, *Meloidogyne hapla*, challenges. Moreover, *M. hapla* induced OPDA productions and signaling in Arabidopsis roots, but did not affect other jasmonate (jasmonic acid-isoleucine, JA-Ile) and salicylic acid (SA) synthesis and marker gene expression. In parallel, mutant and transgenic plants blocking the accumulation of JA-Ile and SA demonstrated WT-level root/root hair growth and galling formations. Thus, we conclude that CYP20-3-dependent OPDA signaling is a key plant defense metabolic pathway, fortifying protective barriers and conferring innate resistance against PPN.

4.2. INTRODUCTION

Plant parasitic nematodes (PPN) constitute a formidable threat to the global agriculture and inflict the annual damage of ~$ 173 billion, affecting >12 % of crop productions worldwide, with the looming specter of global climate changes projected to

exacerbate their deleterious impact in the foreseeable future (Elling et al. 2013; Khanal et al. 2023). Ubiquitous in nature, PPNs imperil the most staple and cash crops (Bernard et al. 2017). Presently, the management of PPNs heavily relies on various chemical agents, notwithstanding the associated risks due to their potentially hazardous and toxic properties and their economic costs exceeding their utility (Pires et al. 2022). This overreliance on chemical control measures is compounded by the scarcity of resilient plant varieties, stemming from an incomplete understanding of intricate mechanisms governing plant-PPN interactions (Li et al. 2015; Starr et al. 2007).

It is, therefore, of great interest to decipher how plants can defend themselves against PPN. A current working model describes that plant resistance (R) genes recognize avirulence (Avr) effectors released from the PPN stylet during infections. The R-Avr interaction then activates the stereotypical effector-triggered immunity (ETI) and triggers programmed cell death (PCD) at the invasion sites, also called hypersensitive response (HR, Sato et al. 2019). Consistent with this scenario, an electron microscopy (EM) imaging of potato roots infected with the cyst nematode *Globodera rostochiensis* Ro1 detected a layer of dead cells surrounding the syncytium (Rice et al. 1985). Several histological examinations have periodically followed the similar observation of necrotic cells near PPN infection sites in different root systems (Grundler et al. 1997; Agudelo et al. 2005; Anthony et al. 2005; Khallouk et al. 2011; Cabasan et al. 2014) including a wild cotton species *G. longicalyx* (Agudelo et al. 2005). These studies −as a matter of course− hypothesized that those dead cells are the result of HR, especially since their EM images revealed the sign of reactive oxygen species (ROS) accumulations aligned with PPN infection routes (Waetzig et al. 1999; Pegard et al. 2004; Melillo et al. 2006, 2011; Simonetti et al. 2009). Of note, the oxidative bursts, involving the rapid and robust production of ROS as a part of early plant responses to pathogens, was once considered as a chemical signature of HR due to its cellular toxicity. However, the electrophile was turned out to be less likely a direct cause of PCD/HR (Jones and Dang 2006; Peng et al. 2018; Huang et al. 2019), making it inconclusive if the cell death observed during PPN infections is ***i***) an example of HR or ***ii***) damage associated-cell lysis (Williamson and Kumar 2006). Besides, most EM analyses employed lengthy and extensive fixation steps that potentially cause cellular damages and physiological alterations (Santana et al.

2015). Never-the-less, PPN-induced cell necrosis was detected chiefly at >7-14 d-post inoculations (dpi, Rice et al. 1985; Grundler et al. 1997; Agudelo et al. 2005; Anthony et al. 2005; Khallouk et al. 2011; Cabasan et al. 2014), which was considerably slower than the typical, foliar HR (Mur et al. 2008). This suggests that root HR may be biochemically and biologically unique, or perhaps ineffective. Alternatively, the cell death could be a disease condition or symptom. Indeed, there has yet been no study −to the best of our knowledge− that identified a complete set of R-gene-(guardee/decoy)-Avr effector proteins for any incompatible plant-PPN interaction that can confer ETI.

On the other hand, a number of studies have exploited the role of phytodefense hormones such as salicylic acid (SA) and jasmonates [12-oxo-phytodienoic acid (OPDA) and jasmonic acid-isoleucine (JA-Ile)] in plant PPN responses. These however have yielded so far inconclusive, rather contradictory, results. In plant-microbe interactions, ETI mainly triggers SA signaling and in turn activates HR (Jones and Dangl 2006). Indeed, early studies concurred that PPN resistant plants employ SA signaling, upregulating the expression of SA-producing and -responsive genes. Moreover, SA soil treatments stimulated plant defenses against PPN (Uehara et al. 2010; Molinari et al. 2014). However, later studies argued that plant roots do not induce SA accumulation or maker gene expression; instead, triggered jasmonate accumulations and -responsive gene expressions (Kammerhofer et al. 2015). Moreover, plant root treatments with MeJA and JA demonstrated enhanced resistance capacity against different PPN (Fan et al. 2015; Hu et al. 2017). Note that SA and jasmonate signaling are mutually antagonistic (Li et al. 2019). Then again, conflicting results showed that jasmonates are a negative defense regulators enhancing disease susceptibility toward PPN (Ithal et al. 2007a,b; Bhattarai et al. 2008; Nahar et al. 2011; Damiani et al. 2012). In the end, a generic approach attested that neither jasmonates nor SA function(s) in plant-PPN interactions (Gao et al. 2008). Upon the infection of PPN, maize and Arabidopsis mutants disrupted *LIPOXYGENASE 3* (*LOX3*) exhibited significantly increased susceptibility, although showed elevated (or WT-level) jasmonate and SA levels post PPN infections.

Alternatively, recent mutant surveys reconstituted that OPDA, instead of JA-Ile and SA, signaling confers plant PPN resistance, demonstrated as a mutant Arabidopsis lacking OPDA signaling (*cyp20-3*) impaired PPN defense responses (Gleason et al.

2016). However, a role of OPDA-dependent defense activations against PPN is still unclear. The same study also measured increased PPN susceptibility in jasmonate biosynthesis mutants (*fad3/7/8* and *dde2*), and WT-like PPN resistance in *opr3*, partially arresting conversion of OPDA to JA, and *coi1* (*coronatine insensitive 1*, a receptor of JA-Ile). Caveats are that ***i***) *coi1* impedes not only the perception of JA-Ile but also stress-induced jasmonate (e.g., OPDA and JA-Ile) biosynthesis (Feys et al. 1994; Chung et al. 2008; Park et al. 2013) and ***ii***) *opr3* still accumulates substantial amounts of JA-Ile (Chini et al. 2018), together −in fact− further supporting an earlier hypothesis (Gao et al. 2008) disputing any role of jasmonates in plant PPN resistance. The cause for contradictory results between *coi1* and *fad3/7/8* and *dde2* is not understood, but it may result from ***A***) the potential, residual accumulations of jasmonates in *coi1* and/or ***B***) the direct effect of MeJA and/or JA toward PPN, as their supplements in plant growth media suppressed PPN infections (Gleason et al. 2016). Further investigations must clarify the nature of jasmonates toward PPN.

Therefore, it is important to resolve the role of PTI, ETI, phytohormones, and/or HR in plant-PPN interactions. Henceforth, the current study utilized confocal microscopy and monitored the real-time interaction between *Rotylenchulus reniformis* and hypersensitive cotton germplasm LONREN-1 with a minimal cell fixation process (Sikkens et al. 2011; Bell et al. 2014). This attempt, however, showed no PPN-associated PCD reactions in LONREN-1 but −instead− discerned that the resistant cotton germplasm BABREN-713 (Bell et al. 2015) grows denser root hairs than LONREN-1, as well as SureGrow747 (SG747, McCarty 2017), a susceptible cotton germplasm. In line with this scenario, we identified that one of BABREN-714 root-specific genes is *cyclophilin 20-3* (*CYP20-3*), an OPDA signal receptor upregulated on inoculation by PPN. Indeed, its T-DNA insertion KO mutant (*cyp20-3*) impairs proper root hair growth and, in turn, enhances susceptibility toward PPN infections. In comparison, the mutant and transgenic plant lacking JA-Ile or SA biosynthesis has normal root hair growth and maintains WT-like PPN defense responses. This suggests a unique insight into plant-PPN interactions, namely that OPDA is a critical phytodefense hormone coordinating inducible and preformed plant defense activations against PPN but is unlikely to be able to activate HR.

4.3. RESULTS AND DISCUSSION

4.3.1. LONREN-1 roots do not display *R. reniformis*-associated cell necrosis

PPNs are eukaryotic animals that exhibit overall low genomic variability among species and even genera (Montarry et al. 2021), proposing that their ***i***) Avr-R interactions and ***ii***) defense mechanisms are durable and conserved. Hence, if HR is −in fact− an effective/true plant defense machinery against PPN, its cellular components and modes could assist developing a broad-spectrum PPN management strategy across various crops. In this study, to assess if PPN triggers HR through their infection routes, we employed confocal laser-scanning microscopy and traced 'real-time' interactions between *R. reniformis* and LONREN-1 roots. LONREN-1 is hypersensitive germplasm that ***A***) contains a resistance QTL, *Ren*^{lon}, from *G. Longicalyx* (Bell et al. 2014; Grover et al. 2020), and ***B***) manifested necrosis in root cells upon *R. reniformis* infections (Li et al. 2015; Sikkens et al. 2011) similar to its parent line, *G. longicalyx* (Agudelo et al. 2005; Bhandari et al. 2015). To minimize physical damages caused during fixation processes, we only briefly stained samples, *R. reniformis*-infected LONREN-1 roots, with a PI solution before placing them on the stage. We then used two channels, 488 nm (FTIC) and 562 nm (TRITC), to sequentially picture the green autofluorescence of *R. reniformis* (**Fig 4.1A,** left) and the living cell membrane of LONREN-1 roots (**Fig 4.1**, right). Note that PI is not membrane-permeable, making it capable of differentiating dead and intact cells based on membrane integrity (Crowley et al. 2016).

Unexpectedly, confocal imaging assays did not support PPN-mediated HR activations. As shown in **Figures 4.2 and 4.3**, the thin optical sectioning near and above an invaded *R. reniformis* showed the prolonged intact cell membrane and nucleus of LONREN-1 roots around/at its infection sites. Moreover, root cells remained alive until *R. reniformis* was grown to an adult female stage, showing no sign of cell mortality even ≥ ~1 wk after infections (**Fig 4.3B**). To substantiate these observations further, we used a cell-permeable H_2O_2-specific probe (DCFDA) to screen if *R. reniformis* infections prompt the biphasic ROS bursts, a well described molecular fingerprint of defense responses (e.g., ETI, Jones and Dang 2006; Zurbriggen et al. 2010; Fosu-Nyarko and Jones 2016; Gillet et al. 2017; Peng et al. 2018). However, LONREN-1 roots again produced little −if any− H_2O_2 during *R. reniformis* infections (**Fig 4.4**, lower panel) compared to control

plants; susceptible SG747 (McCarty 2017) and another resistant BARBREN-713, harboring a resistance QTL, Renbarb2, from *G. barbadense* GB-713 (Bell et al. 2015). A caveat was that BARBREN-713 and SG747 roots ***i***) showed H_2O_2 productions throughout in an apparently random pattern (**Fig 4.4**), unlike defense-associated H_2O_2 bursts, which should occur prevalently around infection sites (Torres et al. 2006), and ***ii***) exhibited no cell death symptom at the site of *R. reniformis* infections (**Fig 4.5**). Together, these results suggest that hypersensitive responses previously reported in LONREN-1 were less likely true PCD/HR but rather necrotic symptoms.

4.3.2. A negative correlation exists between PPN infections and plant root hair growth

While probing cell death and H_2O_2 bursts in three cotton varieties' roots (**Fig 4.4**), it became apparent that a resistant BARBREN-713 develops a dense growth of root hairs all along the lateral root (Upper Panel). In contrast, LONREN-1 showed fewer root hairs, whereas a susceptible SG747 formed little −if any− root hair growth, linking a potential correlation between plant root hair growth and PPN resistance. To test our observations, we examined the growth of 10 different commercial cotton cultivars in the field infested with *R. reniformis* and their root hair formations (**Fig 4.6**). At ~40 d post *R. reniformis* inoculations (dpi), plant growth parameters such as heights and root/shoot weights were measured and compared with their survival rates, revealing that a PhytoGen (PHY)443 is the most resistant while a DeltaPine1646 is the most susceptible (**Fig 4.6A**). PHY443 manifested survival rates up to > 60 % while conveying a noticeable growth enhancement. Its shoot and root weights were noticeably heavier than other cultivars, though there was no significant difference. We then further looked closely at their root hair growth across the tip, elongation and differentiation zones, using brightfield microscopy, and categorized them into five classes (**Fig 4.6B**). As expected, PHY443 grew elongated and the most densely populated root hairs supporting a possible role of elevated root mass and denser/extended root hairs in heighten plant resilience against PPN challenges.

Previously, Usery et al. (2005) put forward a negative correlation between the population density of PPN and larger root systems. All 52 cotton cultivars tested in their greenhouse assays revealed that Stonevile4793 and SG521 exhibiting a greater root

volume are provisionally tolerant than others toward PPN infestations. In agreement, mutant maize disrupting *LIPOXYGENASE 3* displayed shorter root lengths and conferred enhanced susceptibility to PPN (Gao et al. 2008). Likewise, a mutant Arabidopsis line (*brassinazole resistant1-1D*) with an anomalous root architecture and smaller root lengths attracted more PPN (Warmerdam et al. 2018). Conversely, Lotus plants overexpressing *CYTOKININ OXIDASE* grew significantly more lateral roots and were highly resistant to PPN infections (Lohar et al. 2004). Indeed, PPN invoked cytoskeletal responses and induced root hair waviness via PPN signals capable of acting from a distance. Hence, mutant plants lacking the ability to perceive these signals exhibited increased PPN infections, underscoring the crucial role of root hair responses in plant susceptibility to nematodes (Weerasinghe et al. 2005). To further substantiate this hypothesis, we conducted a similar field test with *M. incognita* in 7 cotton cultivars. We again found that PHY443 and PHY332 are the most resistant, whereas PHY340 and NG4938, growing a lower number of root hairs (**Fig 4.6B**), are the most susceptible to *M. incognita* infections (**Fig 4.7**). Similar results were obtained when we evaluated soybean varieties, where we discovered that the amount of resistance is directly proportional to the number of root hairs (**Table 4.1**). Collectively, these findings underscore the potential importance of root hairs/mass in enhancing a plant's ability to withstand infections caused by PPN.

4.3.3. CYP20-3, a receptor of OPDA signal, is critical for proper root hair growth

Moving forward, a system biology approach was employed to identify plant PPN defense genes spatially associated with roots/root hairs by reassessing our previous transcriptome data which measured transcript abundance in BARBREN-713, LONREN-1 and SG747 roots (Li et al. 2015). We subtracted a list of genes expressed in LONREN-1 and SG747 from those in BARBREN-713 roots, and discerned that several *PEPTIDYL-PROLYL ISOMERASES* including *CYP20-3* are expressed distinctively in BARBREN-713 roots. *CYP20-3* is a receptor of OPDA, actuating and finetuning defense (adaptive) responses against an array of biotic and abiotic constraints, as well as growth processes (Dos Santo and Park 2019; Liu and Park 2021). OPDA induced under stresses binds CYP20-3 to stimulate sulfur assimilation, which switches on cysteine (Cys) biosynthesis and leads to increased thiol (e.g., glutathione, GSH) levels. The enhanced reduction

capacity then S-glutathionylates and activates 2-Cys Peroxiredoxin A, a critical H_2O_2-scavenger that safeguards a linear flow of electrons during photosynthesis while coordinating retrograde directional, nuclear defense gene expressions (Park et al. 2013; Cheong et al. 2017; Liu et al. 2020; Adhikari and Park 2023).

Next, to validate a role of *CYP20-3* in root hair growth, we adapted reverse genetic analyses using its KO mutant *cyp20-3* generated from a model plant *Arabidopsis* (Domingues-Solis et al. 2008). In agreement with the *in-silico* finding, an optical microscope imaging exhibited that *cyp20-3* lacks root hair formation (**Fig 4.8A**, Liu and Park 2021). The result infers a possible function of OPDA signaling in root hair growth. We thus retrospectively examined if other jasmonate and/or defense hormones besides OPDA (e.g., JA-Ile and SA) are also involved in root morphogenesis by monitoring *jar1* mutant and *NahG* transgenic Arabidopsis, deficient in the accumulation of JA-Ile and SA, respectively (Delaney et al. 1994; Staswick et al. 2002). However, *jar1* and *NahG* grew WT-like root hairs (**Fig 4.8A**) and exhibited no apparent difference in overall root architecture (**Table 4.2**). In comparison, *cyp20-3* has again a smaller root system, characterized by decreases in total root length of ~ 40 % compared to WT Col-0, *jar1* and *NahG* (**Table 4.2**).

4.3.4. OPDA, but not JA-Ile and SA, signaling plays a critical role in plant PPN resistance.

Our findings prompted a closer examination of phytodefense hormone activities in plant PPN responses, with a particular focus on OPDA and its receptor CYP20-3. Toward that, we re-evaluated the defense capacity of *cyp20-3* against *M. hapla* infections, which expectedly validated an earlier result (Gleason et al. 2016) exhibiting a significantly greater number of total galls and gall numbers per mg-root formations (**Fig 4.8B**). Now, to further scrutinize the findings, we counted the number of gall formations also in *jar1* and *NahG* following *M. hapla* inoculations, confirming that they confer WT-like resistance (**Fig 4.8B**). The results clearly underpinned that ***i***) the induction/accumulation of JA-Ile or SA is not necessary for PPN defenses, instead clearly underlying ***i***) the importance of OPDA signaling and root architecture and root hair growth in perhaps fortifying plant resilience against PPN invasions. It is worth noting that −unlike most other root/root hair

defective mutants− *cyp20-3* (vs. WT Col-0) showed little abnormality/deficiency in the growth of aerial parts (**Fig 4.9**, Domingues-Solis et al. 2008; Park et al. 2013), uniquely qualifying it to use/assess the function of root/root hairs against plant defense responses.

To further delineate the activity of OPDA in the activation of PPN defense mechanisms, we probed the differential expression of OPDA, JA-Ile, and SA-producing and signaling marker genes in WT Col-0 at 15 d-post *M. hapla* inoculations (dpi). Surprisingly, PPN set off the upregulation of *ALLENE OXIDE CYCLASE 1* (*AOC1* synthesizing OPDA) expressions but induced little change in the level transcripts of *OPDA REDUCTASE 3* (*OPR3* converting OPDA to JA) and *ISOCHORISMATE SYNTHASE 1* (*ICS1* synthesizing SA) (**Fig 4.10A**), implying that plants resisting infections to PPN accumulated OPDA, but not likely JA, JA-Ile and SA. In line with this scenario, PPN activated exclusively OPDA signaling (**Fig 4.10B**), which was determined by the increased expressions of OPDA responsive genes such as *GLUTAREDOXIN 480* (*GRX480*) and *CYTOCHROME P450* (*CYP81D11*) (Mueller et al. 2008). In contrast, we observed the decreased level expression of JA-Ile responsive genes *THIONIN* (*Thi2.1*), *VEGETATIVE STORAGE PROTEIN* (*VSP1*) and *DEFENSIN* (*PDF1.2*), as well as the slight increases in SA responsive gene *NONINDUCIBLE IMMUNITY-INTERACTING* (*NIMIN2*) (Epple et al. 1995; Penninckx et al. 1998; Guerineau et al. 2003; Hermann et al. 2013). These results further support the notion that SA and JA are not major contributors to PPN defense responses and alternatively suggest that OPDA signaling plays a crucial role in fostering plant resistance against PPN attacks. Hence, it is important to re-evaluate previous results and conduct hormone quantifications to explore the detailed role of defense hormones in plant root-PPN interactions.

4.4. CONCLUSION

As an initial step to delineate how plant roots defend themselves against PPN infections, we attempted to validate the PPN-associated HR in cotton roots, which has been proposed as a prominent resistance apparatus against PPN infections (Agudelo et al. 2005; Rice et al. 1985). However, our confocal microscope imaging of invading *R. reniformis* into host cotton root cells illuminated no distinctive cell death around PPN-infected root tissues, speculating that HR may not be a master plan of plants. We thus

asked, “What make(s) plants resistance or tolerance against PPN?” As one of the potential hints, we observed that the resistant cotton germplasm BARBREN-713 grows thicker and denser root hairs all along the secondary roots, compared with the hypersensitive LONREN-1 and susceptible SG747 cotton germplasms. In agreement, our new field trials with commercial cotton cultivars validated a negative correlation between PPN infections and plant root hair growth.

Interestingly, a receptor of OPDA, CYP20-3 ***i***) belongs to a family of PPIases that are distinctively upregulated in PPN-resisting BARBREN-713 roots and ***ii***) determines both plant root hair growth and PPN resistance. In contrast, mutant/transgenic plants disrupting JA-Ile and SA accumulations conferred WT-like resistance to PPN. In addition, PPN infections induce OPDA, and not SA or JA-Ile, productions and signaling in roots, collectively highlighting a crucial role of OPDA in facilitating the constitutive defense barriers of plants against PPN. In accordance with these, *NahG* and *npr1-1 (nonexpressor of pathogenesis-related protein1-1*, impairing SA signaling*)* plants demonstrated resistance levels equivalent to WT against PPN in rice and Arabidopsis plants (Fujimoto et al. 2011; Nahar et al. 2011). Furthermore, the mutation of jasmonate-producing enzymes, *13-LOX* and *AOC1* (−OPDA and −JA-Ile), resulted in increased plant susceptibility to PPN (Kammerhofer et al. 2015; Nahar et al. 2011; Ozalvo et al. 2014). However, *jar1* KO mutants, which arrest conversion of JA to JA-Ile, conferred WT-like PPN resistance (**Fig 4.8B**), further underpinning a critical role of OPDA signaling in plant defense responses against PPN in the absence of JA-Ile.

CYP20-3 is a key regulator of sulfur assimilations under environmental stresses, relaying an OPDA signal to stimulate Cys biosynthesis (Dominguez-Solis et al. 2008; Park et al. 2013). Cys is the first organic compound with reduced sulfur produced by plants (Takahashi et al. 2011) and has a vital role in detoxifying cyanide and plant immunity, which is crucial for plant’s response to pathogens and development of root hairs (Romero et al. 2014). As a result of the lack of Cys availability, *cyp20-3* may not be able to produce root hair properly, which in turn increases susceptibility toward PPN. Hence, the present study indicates that CYP20-3 is a vital cellular component in plant constitutive resistance that assists root differentiation and/or root hair growth, potentializing plants’ defense capacity against PPN. The CYP20-3-dependent set-up of defense barriers may not

require OPDA signaling, as it likely is shaped prior to PPN infections. However, the CYP20-3-mediated PPN resistance may be further explained by the induced defense responses upon the accumulation of OPDA induced by PPN infections, as it regulates cellular sulfur, Cys, and redox homeostasis. The finer relationships between OPDA, CYP20-3, cyanide, root hair growth, and related defense gene expressions must be explored to better delineate plant-PPN interactions in future work.

4.5. MATERIALS AND METHODS

4.5.1. Plant growth conditions

Cotton germplasms (LONREN-1, BARBREN-713 and SG747) and Arabidopsis WT (Col-0) and mutant (*jar1*, *cyp20-3* and *NahG*) plants were grown and cultivated in a growth chamber under a 12-hour light/dark cycle and 60-80 % relative humidity at 30 ^{o}C and 22 ^{o}C, respectively. Cotton seeds were first germinated in a water-dampen germination paper (Ahlstrom-Munksjö) inside the Ziploc bag and transferred to either 500 cm^3 polystyrene pots or 20 mL centrifuge tubes filled with sandy soils (80 % sand, 10 % silt and 10 % clay), procured from Plant Science Research Center, Auburn Uni. (Gattoni et al. 2023). Then, they were subjected to 12 hr pasteurization at 88°C, followed by 24 hr of cooling before repeating the process. In contrast, Arabidopsis seed sterilization was done for 5 minutes with 70 % ethanol before being placed on half-strength MS Gelrite®-agar (Research Products Interactional) plates.

4.5.2. PPN preparations

R. reniformis (the same genotype as Sikkens et al. 2011) and *Meloidogyne incognita* were cultured on, and collected from cotton roots as described earlier (Liu et al. 2019), while *M. hapla* was cultured on tomato roots following the same procedure as *M. incognita.* Briefly, after 60 d of nematode inoculations in the greenhouse, cotton roots were washed and placed in 0.625 % NaOCl, then agitated for 4 min on a rotary shaker at 120 rpm to extract PPN eggs (Hussey and Barker 1973). Eggs were washed with tap water, filtered through sieves (75 µm over 25 µm), removing debris, and then subjected to sucrose centrifugation at 240 g-force for 1 min (Jenkins 1964). They were incubated on a slide warmer at 30°C for 6-7 d for hatching. After seven days, second-stage juveniles

(J2) were counted at ×40 magnification using the TMS inverted phase contrast microscope (Nikon).

4.5.3. PPN inoculations

For cotton infections, seedlings were moved to 50 mL centrifuge tubes filled with sandy soil containing approximately 2000 *R. reniformis* or *M. incognita*. They were then placed in a growth chamber with a 12-hour light/dark for two weeks for microscopy analysis.

M. hapla was cultured and extracted for Arabidopsis infections, as described for *M. incognita.* Eggs were hatched and collected at the J2 stage by being strained through a 25 µm pore sieve. The J2 *M. hapla* was surface sterilized using 0.5 % $HgCl_2$ and then 0.7 % streptomycin. After 5 min incubations, each solution was vacuum-filtered and 5 times water-washed by the Büchner funnel. The sterile J2 *M. hapla* was then transferred to a 50 mL centrifuge tube, of which 10 µL was used to determine the approximate number of nematodes. Two-wk-old *A. thaliana* MS Gelrite®-agar plates were inoculated with ~120 sterile PPN per a plant. Each plate was then wrapped with aluminum foil to simulate low light conditions and placed in a 12-hour light/dark growth chamber until 15 dpi. Root galls were then counted under the SZ51 stereoscopic zoom microscope (Olympus), and roots were subsequently cut and weighed to calculate root galls per mg weight.

4.5.4. Confocal microscopy imaging of plant-PPN interactions

Cotton roots, healthy and infected, were collected by rinsing off soil and then immersed for 5 min in a 10 µg/mL solution of propidium iodide (PI). Cotton roots were then examined with the A1R-MP laser scanning confocal microscope (Nikon) using a 561.5 nm excitation wavelength with the tetramethyl rhodamine isothiocyanate (TRITC) filter set, which excites PI in root cells, emitting a red color (passbands of 610 to 650 nm). The autofluorescence of PPN was detected at a 488 nm excitation wavelength with the fluorescein isothiocyanate (FITC) filter set, emitting a green color (passbands of 505 to 525 nm). A real-time image of *R. reniformis* infections in cotton roots was attained for each cotton germplasm by simultaneously imaging at 488 and 561.5 nm.

To monitor H_2O_2 bursts, cotton roots were exposed to 2,7-dichlorofluorescin diacetate (DCFDA, 50 μM) for 30 min before PI staining. The ROS production is detectable using the same filter set and settings as PPN autofluorescence.

4.5.5. Field Evaluation of Tolerance

Field experiments were carried out as described previously (Usery et al. 2005) in the Gulf Coast Research & Extension Center (GCREC) and the Tennessee Valley Regional Research & Extension Center (TVREC), which are naturally infested with *R. reniformis* and *M. incognita*, respectively. TVREC soil was categorized as silt loam (23.7 % sand, 53.7 % silt and 22.5 % clay, pH 6.5) and GCREC soil as a sandy loam (59 % sand, 31 % silt and 10 % clay). Plots consisting of two rows (each 7.62 m long with row spacing of 101 cm) were cultivated with minimum tillage in all years. Field sites are carefully managed to prevent soil, seed, or foliar-borne pathogens infestation. The tests were organized into paired plots using a randomized complete block design, each replicated five times, allowing for a direct correlation between plant susceptibility to nematodes and plant survival percentage. Each field trial was repeated over two years.

Data was analyzed using the PROC GLIMMIX procedure (statistical analysis system's general linear model). The analysis of variance was conducted with varieties as the main factor. Means were separated using Tukey Kramer LS-means test at $P \leq 0.05$. Student panels were produced to determine the normality of the residuals. There were no significant interactions between the two repeats of the cotton variety tests, thus data were pooled into a single data set for a total of ten replications, and means were distinguished with Tukey Kramer test ($P \leq 0.05$).

4.5.6. Arabidopsis root hair analysis

To determine the root growth and architecture of Arabidopsis, the root system was measured for length, diameter, surface area, volume, projected area, and number of tips by using the WinRhizo Arabidopsis version 5.0 (Regent Instruments, Inc., Canada). Roots from 2-wk-old Arabidopsis WT Col-0 and mutants grown on MS media were evenly placed in a water layer within 25 cm by 20 cm transparent acrylic trays. They were then scanned

at 800 dots per linear inch using the expression 10000XL scanner (Epson), and the calibration grid was used as a reference scale for the analysis.

4.5.7. Quantitative RT-PCR

Total root RNA of 3−4-wk-old Arabidopsis was prepared using TRIzol reagent (Invitrogen) and the Direct-zol RNA Kit (Zymo Research) according to the manufacturer's instructions. RNA qualities were examined by agarose gel electrophoresis and NanoDrop (A_{260}/A_{280}>1.8 and A_{260}/A_{230}>2.0, Udvardi et al. 2008). RT reactions were performed using an oligo(dT) reverse primer and a qScript reverse transcriptase (QuantaBio). Quantitative PCR was performed with the PerfeCT® SYBR® Green Fast Mix® Reaction Mixes (QuantaBio) in the CFX96 Touch™ (Bio-Rad) PCR system cycled 40 times using gene-specific primer sets (**Table 4.3**). The annealing temperature for the primer pairs was 53 °C. To determine the relative abundance of target transcripts, the sample cDNA was assessed with a housekeeping gene, *POLYUBIQUITIN-C* (*UBC*, Czechowski et al. 2005), and the average threshold cycle (i.e., Ct) was normalized to that of *UBC* as $2^{-\Delta Ct}$ where $-\Delta Ct = (Ct_{,gene} - Ct_{,UBC})$.

4.6. REFERENCES

Adhikari, A., & Park, S.W. (2023). Reduced GSH Acts as a Metabolic Cue of OPDA Signaling in Coregulating Photosynthesis and Defense Activation under Stress. Plants, 12(21), 3745.

Agudelo, P., Robbins, R.T., Stewart, J.M., Bell, A., & Robinson, A.F. (2005). Histological observations of *Rotylenchulus reniformis* on *Gossypium longicalyx* and interspecific cotton hybrids. Journal of nematology, 37(4), 444.

Anthony, F., Topart, P., Martinez, A., Silva, M., & Nicole, M. (2005). Hypersensitive-like reaction conferred by the *Mex-1* resistance gene against *Meloidogyne exigua* in coffee. Plant Pathology, 54(4), 476-482.

Balint-Kurti, P. (2019). The plant hypersensitive response: concepts, control and consequences. Molecular plant pathology, 20(8), 1163-1178.

Bell, A.A., Forest Robinson, A., Quintana, J., Dighe, N.D., Menz, M.A., Stelly, D.M., Zheng, X., Jones, J.E., Overstreet, C., Burris, E., Cantrell, R.G., & Nichols, R.L.

(2014). Registration of LONREN-1 and LONREN-2 germplasm lines of upland cotton resistant to reniform nematode. Journal of Plant Registrations, 8(2), 187-190.

Bell, A.A., Robinson, A.F., Quintana, J., Duke, S.E., Starr, J.L., Stelly, D.M., Zheng, X., Prom, S., Saladino, V., Gutiérrez, O.A., Stetina, S.R., & Nichols, R.L. (2015). Registration of BARBREN-713 germplasm line of upland cotton resistant to reniform and root-knot nematodes. Journal of Plant Registrations, 9(1), 89-93.

Bernard, G.C., Egnin, M., & Bonsi, C. (2017). The impact of plant-parasitic nematodes on agriculture and methods of control. Nematology-concepts, diagnosis and control, 1, 121-151.

Bhandari, B., Myers, G.O., Indest, M.O., & Overstreet, C. (2015). Response of five resistant cotton genotypes to isolates of *Rotylenchulus reniformis* collected from reniform nematode infested fields of Louisiana. Nematropica, 45(2), 252-262.

Bhattarai, K.K., Xie, Q.G., Mantelin, S., Bishnoi, U., Girke, T., Navarre, D.A., & Kaloshian, I. (2008). Tomato susceptibility to root-knot nematodes requires an intact jasmonic acid signaling pathway. Molecular plant-microbe interactions, 21(9), 1205-1214.

Cabasan, M.T.N., Kumar, A., Bellafiore, S., & De Waele, D. (2014). Histopathology of the rice root-knot nematode, *Meloidogyne graminicola,* on *Oryza sativa* and *O. glaberrima*. Nematology, 16(1), 73-81.

Cheong, H., Barbosa dos Santos, I., Liu, W., Gosse, H.N., & Park, S.W. (2017). Cyclophilin 20–3 is positioned as a regulatory hub between light-dependent redox and 12-oxo-phytodienoic acid signaling. Plant signaling & behavior, 12(9), e1362520.

Chini, A., Monte, I., Zamarreño, A.M., Hamberg, M., Lassueur, S., Reymond, P., Weiss, S., Sintzi, A., Schaller, A., Porzel, A., García-Mina, J.M., & Solano, R. (2018). An OPR3-independent pathway uses 4, 5-didehydrojasmonate for jasmonate synthesis. Nature chemical biology, 14(2), 171-178.

Chung, H.S., Koo, A. J., Gao, X., Jayanty, S., Thines, B., Jones, A.D., & Howe, G.A. (2008). Regulation and function of Arabidopsis JASMONATE ZIM-domain genes in response to wounding and herbivory. Plant physiology, 146(3), 952-964.

Crowley, L.C., Scott, A.P., Marfell, B.J., Boughaba, J.A., Chojnowski, G., & Waterhouse, N.J. (2016). Measuring cell death by propidium iodide uptake and flow cytometry. Cold Spring Harbor Protocols, 2016(7), pdb-prot087163.

Czechowski, T., Stitt, M., Altmann, T., Udvardi, M.K., & Scheible, W.R. (2005). Genome-wide identification and testing of superior reference genes for transcript normalization in Arabidopsis. Plant physiology, 139(1), 5-17.

Damiani, I., Baldacci-Cresp, F., Hopkins, J., Andrio, E., Balzergue, S., Lecomte, P., Puppo, A., Abad, P., Favery, B., & Hérouart, D. (2012). Plant genes involved in harbouring symbiotic rhizobia or pathogenic nematodes. New Phytologist, 194(2), 511-522.

Delaney, T.P., Uknes, S., Vernooij, B., Friedrich, L., Weymann, K., Negrotto, D., Gaffney, T., Gut-Rella, M., Kessmann, H., Ward, E., & Ryals, J. (1994). A central role of salicylic acid in plant disease resistance. Science, 266(5188), 1247-1250.

Dominguez-Solis, J.R., He, Z., Lima, A., Ting, J., Buchanan, B.B., & Luan, S. (2008). A cyclophilin links redox and light signals to cysteine biosynthesis and stress responses in chloroplasts. Proceedings of the National Academy of Sciences, 105(42), 16386-16391.

Barbosa dos Santos, I., & Park, S.W. (2019). Versatility of cyclophilins in plant growth and survival: a case study in Arabidopsis. Biomolecules, 9(1), 20.

Elling, A.A. (2013). Major emerging problems with minor *Meloidogyne* species. Phytopathology, 103(11), 1092-1102.

Epple, P., Apel, K., & Bohlmann, H. (1995). An *Arabidopsis thaliana thionin* gene is inducible via a signal transduction pathway different from that for pathogenesis-related proteins. Plant physiology, 109(3), 813-820.

Fan, J.W., Hu, C.L., Zhang, L.N., Li, Z.L., Zhao, F.K., & Wang, S.H. (2015). Jasmonic acid mediates tomato's response to root knot nematodes. Journal of Plant Growth Regulation, 34, 196-205.

Feys, B.J., Benedetti, C.E., Penfold, C.N., & Turner, J.G. (1994). Arabidopsis mutants selected for resistance to the phytotoxin coronatine are male sterile, insensitive to methyl jasmonate, and resistant to a bacterial pathogen. The Plant Cell, 6(5), 751-759.

Fosu-Nyarko, J., & Jones, M.G. (2016). Advances in understanding the molecular mechanisms of root lesion nematode host interactions. Annual Review of Phytopathology, 54, 253-278.

Fujimoto, T., Tomitaka, Y., Abe, H., Tsuda, S., Futai, K., & Mizukubo, T. (2011). Jasmonic acid signaling pathway of *Arabidopsis thaliana* is important for root-knot nematode invasion. Nematological Research (Japanese Journal of Nematology), 41 (1), 9-17.

Gao, X., Starr, J., Göbel, C., Engelberth, J., Feussner, I., Tumlinson, J., & Kolomiets, M. (2008). Maize *9-lipoxygenase ZmLOX3* controls development, root-specific expression of defense genes, and resistance to root-knot nematodes. Molecular plant-microbe interactions, 21(1), 98-109.

Gattoni, K.M., Park, S.W., & Lawrence, K.S. (2023). Evaluation of the mechanism of action of *Bacillus* spp. to manage *Meloidogyne incognita* with split root assay, RT-qPCR and qPCR. Frontiers in Plant Science, 13, 1079109.

Gillet, F.X., Bournaud, C., Antonino de Souza Júnior, J.D., & Grossi-de-Sa, M.F. (2017). Plant-parasitic nematodes: towards understanding molecular players in stress responses. Annals of Botany, 119(5), 775-789.

Gleason, C., Leelarasamee, N., Meldau, D., & Feussner, I. (2016). OPDA has key role in regulating plant susceptibility to the root-knot nematode Meloidogyne hapla in Arabidopsis. Frontiers in plant science, 7, 1565.

Grover, C.E., Pan, M., Yuan, D., Arick, M.A., Hu, G., Brase, L., Stelly, D.M., Lu, Z., Schmitz, R.J., Peterson, D.G., Wendel, J.F., & Udall, J.A. (2020). The *Gossypium longicalyx* genome as a resource for cotton breeding and evolution. G3: Genes, Genomes, Genetics, 10(5), 1457-1467.

Grundler, F.M.W., Sobczak, M., & Lange, S. (1997). Defence responses of *Arabidopsis thaliana* during invasion and feeding site induction by the plant–parasitic nematode *Heterodera* glycines. Physiological and Molecular Plant Pathology, 50(6), 419-429.

Guerineau, F., Benjdia, M., & Zhou, D.X. (2003). A jasmonate-responsive element within the *A. thaliana vsp1* promoter. Journal of experimental botany, 54(385), 1153-1162.

Hermann, M., Maier, F., Masroor, A., Hirth, S., Pfitzner, A.J., & Pfitzner, U.M. (2013). The Arabidopsis NIMIN proteins affect *NPR1* differentially. Frontiers in Plant Science, 4, 88.

Hu, Y., You, J., Li, C., Hua, C., & Wang, C. (2017). Exogenous application of methyl jasmonate induces defence against *Meloidogyne hapla* in soybean. Nematology, 19(3), 293-304.

Huang, H., Ullah, F., Zhou, D. X., Yi, M., & Zhao, Y. (2019). Mechanisms of ROS regulation of plant development and stress responses. Frontiers in plant science, 10, 800.

Hussey, R.S., & Barker, K.R. (1973). A comparison of methods of collecting inocula of *Meloidogyne* spp., including a new technique. Plant dis. rep. 57, 1025-1028.

Ithal, N., Recknor, J., Nettleton, D., Hearne, L., Maier, T., Baum, T.J., & Mitchum, M.G. (2007). Parallel genome-wide expression profiling of host and pathogen during soybean cyst nematode infection of soybean. Molecular plant-microbe interactions, 20(3), 293-305.

Ithal, N., Recknor, J., Nettleton, D., Maier, T., Baum, T.J., & Mitchum, M.G. (2007). Developmental transcript profiling of cyst nematode feeding cells in soybean roots. Molecular Plant-Microbe Interactions, 20(5), 510-525.

Jenkins, W.R.B. (1964). A rapid centrifugal-flotation technique for separating nematodes from soil. Plant Dis. Rep. 48, 692.

Jones, J.D., & Dangl, J.L. (2006). The plant immune system. nature, 444(7117), 323-329.

Kammerhofer, N., Radakovic, Z., Regis, J. M., Dobrev, P., Vankova, R., Grundler, F.M., Siddique, S., Hofmann, J., & Wieczorek, K. (2015). Role of stress-related hormones in plant defence during early infection of the cyst nematode *Heterodera schachtii* in Arabidopsis. New Phytologist, 207(3), 778-789.

Khallouk, S., Voisin, R., Van Ghelder, C., Engler, G., Amiri, S., & Esmenjaud, D. (2011). Histological mechanisms of the resistance conferred by the *Ma* gene against *Meloidogyne incognita* in *Prunus* spp. Phytopathology, 101(8), 945-951.

Khanal, C., & Land, J. (2023). Study on two nematode species suggests climate change will inflict greater crop damage. Scientific Reports, 13(1), 14185.

Li, J., Zou, C., Xu, J., Ji, X., Niu, X., Yang, J., Huang, X., & Zhang, K.Q. (2015). Molecular mechanisms of nematode-nematophagous microbe interactions: basis for biological control of plant-parasitic nematodes. Annual review of phytopathology, 53, 67-95.

Li, N., Han, X., Feng, D., Yuan, D., & Huang, L.J. (2019). Signaling crosstalk between salicylic acid and ethylene/jasmonate in plant defense: do we understand what they are whispering? International journal of molecular sciences, 20(3), 671.

Li, R., Rashotte, A.M., Singh, N.K., Lawrence, K.S., Weaver, D.B., & Locy, R.D. (2015). Transcriptome analysis of cotton (*Gossypium hirsutum* L.) genotypes that are susceptible, resistant, and hypersensitive to reniform nematode (*Rotylenchulus reniformis*). PLoS One, 10(11), e0143261.

Liu, W., Dos Santos, I.B., Moye, A., & Park, S.W. (2020). CYP20-3 deglutathionylates 2-CysPRX A and suppresses peroxide detoxification during heat stress. Life Science Alliance, 3(9).

Liu, W., Jones, A.L., Gosse, H.N., Lawrence, K.S., & Park, S.W. (2019). Validation of the chemotaxis of plant parasitic nematodes toward host root exudates. Journal of Nematology, 51(1), 1-10.

Liu, W., & Park, S.W. (2018). Underground mystery: Interactions between plant roots and parasitic nematodes. Current plant biology, 15, 25-29.

Liu, W., & Park, S.W. (2021). 12-oxo-Phytodienoic acid: a fuse and/or switch of plant growth and defense responses? Frontiers in Plant Science, 12, 724079.

Lohar, D.P., Schaff, J.E., Laskey, J.G., Kieber, J.J., Bilyeu, K.D., & Bird, D.M. (2004). Cytokinins play opposite roles in lateral root formation, and nematode and rhizobial symbioses. The Plant Journal, 38(2), 203-214.

López-Orenes, A., Alba, J.M., Kant, M.R., Calderón, A.A., & Ferrer, M.A. (2020). OPDA and ABA accumulation in Pb-stressed *Zygophyllum fabago* can be primed by salicylic acid and coincides with organ-specific differences in accumulation of phenolics. Plant Physiology and Biochemistry, 154, 612-621.

McCarty Jr, J.C., Jenkins, J.N., Wubben, M.J., Hayes, R.W., Callahan, F.E., & Deng, D. (2017). Registration of six germplasm lines of cotton with resistance to the root-knot and reniform nematodes. Journal of Plant Registrations, 11(2), 168-171.

Melillo, M.T., Leonetti, P., Leone, A., Veronico, P., & Bleve-Zacheo, T. (2011). ROS and NO production in compatible and incompatible tomato-*Meloidogyne incognita* interactions. European Journal of Plant Pathology, 130, 489-502.

Melillo, M.T., Leonetti, P., Bongiovanni, M., Castagnone-Sereno, P., & Bleve-Zacheo, T. (2006). Modulation of reactive oxygen species activities and H2O2 accumulation during compatible and incompatible tomato–root-knot nematode interactions. New Phytologist, 170(3), 501-512.

Molinari, S., Fanelli, E., & Leonetti, P. (2014). Expression of tomato salicylic acid (SA)-responsive pathogenesis-related genes in *Mi-1*-mediated and SA-induced resistance to root-knot nematodes. Molecular plant pathology, 15(3), 255-264.

Montarry, J., Mimee, B., Danchin, E.G., Koutsovoulos, G.D., Ste-Croix, D.T., & Grenier, E. (2021). Recent advances in population genomics of plant-parasitic nematodes. Phytopathology®, 111(1), 40-48.

Mueller, S., Hilbert, B., Dueckershoff, K., Roitsch, T., Krischke, M., Mueller, M.J., & Berger, S. (2008). General detoxification and stress responses are mediated by oxidized lipids through TGA transcription factors in Arabidopsis. The Plant Cell, 20(3), 768-785.

Mur, L.A., Kenton, P., Lloyd, A.J., Ougham, H., & Prats, E. (2008). The hypersensitive response; the centenary is upon us but how much do we know? Journal of experimental Botany, 59(3), 501-520.

Nahar, K., Kyndt, T., De Vleesschauwer, D., Höfte, M., & Gheysen, G. (2011). The jasmonate pathway is a key player in systemically induced defense against root knot nematodes in rice. Plant physiology, 157(1), 305-316.

Ozalvo, R., Cabrera, J., Escobar, C., Christensen, S.A., Borrego, E.J., Kolomiets, M.V., Castresana, C., Iberkleid, I., & Brown Horowitz, S. (2014). Two closely related members of Arabidopsis *13-lipoxygenases (13-LOXs), LOX3* and *LOX4*, reveal distinct functions in response to plant-parasitic nematode infection. Molecular plant pathology, 15(4), 319-332.

Park, S.W., Li, W., Viehhauser, A., He, B., Kim, S., Nilsson, A.K., Andersson, M.X., Kittle, J.D., Ambavaram, M.M., Luan, S., Esker, A.R., Tholl, D., Cimini, D., Ellerström, M., Coaker, G., Mitchell, T.K., Pereira, A., Dietz, K.J., & Lawrence, C.B. (2013).

Cyclophilin 20-3 relays a 12-oxo-phytodienoic acid signal during stress responsive regulation of cellular redox homeostasis. Proceedings of the National Academy of Sciences, 110(23), 9559-9564.

Pegard, A., Brizzard, G., Fazari, A., Soucaze, O., Abad, P., & Djian-Caporalino, C. (2005). Histological characterization of resistance to different root-knot nematode species related to phenolics accumulation in *Capsicum annuum*. Phytopathology, 95(2), 158-165.

Peng, Y., van Wersch, R., & Zhang, Y. (2018). Convergent and divergent signaling in PAMP-triggered immunity and effector-triggered immunity. Molecular plant-microbe interactions, 31(4), 403-409.

Penninckx, I.A., Thomma, B.P., Buchala, A., Métraux, J.P., & Broekaert, W.F. (1998). Concomitant activation of jasmonate and ethylene response pathways is required for induction of a plant defensin gene in Arabidopsis. The Plant Cell, 10(12), 2103-2113.

Pires, D., Vicente, C.S., Menéndez, E., Faria, J.M., Rusinque, L., Camacho, M.J., & Inácio, M.L. (2022). The fight against plant-parasitic nematodes: Current status of bacterial and fungal biocontrol agents. Pathogens, 11(10), 1178.

Rice, S.L., Leadbeater, B.S.C., & Stone, A.R. (1985). Changes in cell structure in roots of resistant potatoes parasitized by potato cyst-nematodes. I. Potatoes with resistance gene *H1* derived from *Solanum tuberosum* ssp. andigena. Physiological Plant Pathology, 27(2), 219-234.

Romero, L.C., Aroca, MÁ., Laureano-Marín, A. M., Moreno, I., García, I., & Gotor, C. (2014). Cysteine and cysteine-related signaling pathways in *Arabidopsis thaliana*. Molecular plant, 7(2), 264-276.

Santana, B.P., Nedel, F., Perelló Ferrúa, C., e Silva, RM., da Silva, A. F., Demarco, F.F., & Lenin Villarreal Carreño, N. (2015). Comparing different methods to fix and to dehydrate cells on alginate hydrogel scaffolds using scanning electron microscopy. Microscopy research and technique, 78(7), 553-561.

Sato, K., Kadota, Y., & Shirasu, K. (2019). Plant immune responses to parasitic nematodes. Frontiers in plant science, 10, 479663.

Sikkens, R.B., Weaver, D.B., Lawrence, K.S., Moore, S.R., & Van Santen, E. (2011). LONREN upland cotton germplasm response to *Rotylenchulus reniformis* inoculum level. Nematropica, 68-74.

Simonetti, E., Veronico, P., Melillo, M.T., Delibes, Á., Andrés, M.F., & López-Braña, I. (2009). Analysis of class III peroxidase genes expressed in roots of resistant and susceptible wheat lines infected by *Heterodera avenae.* Molecular plant-microbe interactions, 22(9), 1081-1092.

Starr, J.L., Koenning, S.R., Kirkpatrick, T.L., Robinson, A.F., Roberts, P.A., & Nichols, R.L. (2007). The future of nematode management in cotton. Journal of Nematology, 39(4), 283.

Staswick, PE., Tiryaki, I., & Rowe, M. L. (2002). Jasmonate response locus *JAR1* and several related Arabidopsis genes encode enzymes of the firefly luciferase superfamily that show activity on jasmonic, salicylic, and indole-3-acetic acids in an assay for adenylation. The Plant Cell, 14(6), 1405-1415.

Takahashi, H., Kopriva, S., Giordano, M., Saito, K., & Hell, R. (2011). Sulfur assimilation in photosynthetic organisms: molecular functions and regulations of transporters and assimilatory enzymes. Annual review of plant biology, 62, 157-184.

Torres, M.A., Jones, J.D., & Dangl, J.L. (2006). Reactive oxygen species signaling in response to pathogens. Plant physiology, 141(2), 373-378.

Udvardi, M.K., Czechowski, T., & Scheible, W.R. (2008). Eleven golden rules of quantitative RT-PCR. The Plant Cell, 20(7), 1736-1737.

Uehara, T., Sugiyama, S., Matsuura, H., Arie, T., & Masuta, C. (2010). Resistant and susceptible responses in tomato to cyst nematode are differentially regulated by salicylic acid. Plant and cell physiology, 51(9), 1524-1536.

Usery Jr, S.R., Lawrence, K.S., Lawrence, G.W., & Burmester, C.H. (2005). Evaluation of cotton cultivars for resistance and tolerance to Rotylenchulus reniformis. Nematropica, 121-134.

Waetzig, G., Sobczak, M., & Grundler, F. (1999). Localization of hydrogen peroxide during the defence response of *Arabidopsis thaliana* against the plant-parasitic nematode *Heterodera glycines*. Nematology, 1(7), 681-686.

Warmerdam, S., Sterken, M.G., van Schaik, C., Oortwijn, M.E., Sukarta, O.C., Lozano-Torres, J.L., Dicke, M., Helder, J., Kammenga, J.E., Goverse, A. & Smant, G. (2018). Genome-wide association mapping of the architecture of susceptibility to the root-knot nematode *Meloidogyne incognita* in *Arabidopsis thaliana*. New Phytologist, 218(2), 724-737.

Weerasinghe, R.R., Bird, D.M., & Allen, N.S. (2005). Root-knot nematodes and bacterial Nod factors elicit common signal transduction events in *Lotus japonicus*. Proceedings of the National Academy of Sciences, 102(8), 3147-3152.

Williamson, V.M., & Kumar, A. (2006). Nematode resistance in plants: the battle underground. TRENDS in Genetics, 22(7), 396-403.

Zhu, C., Gan, L., Shen, Z., & Xia, K. (2006). Interactions between jasmonates and ethylene in the regulation of root hair development in Arabidopsis. Journal of experimental botany, 57(6), 1299-1308.

Zurbriggen, M.D., Carrillo, N., & Hajirezaei, M.R. (2010). ROS signaling in the hypersensitive response: when, where and what for? Plant signaling & behavior, 5(4), 393-396.

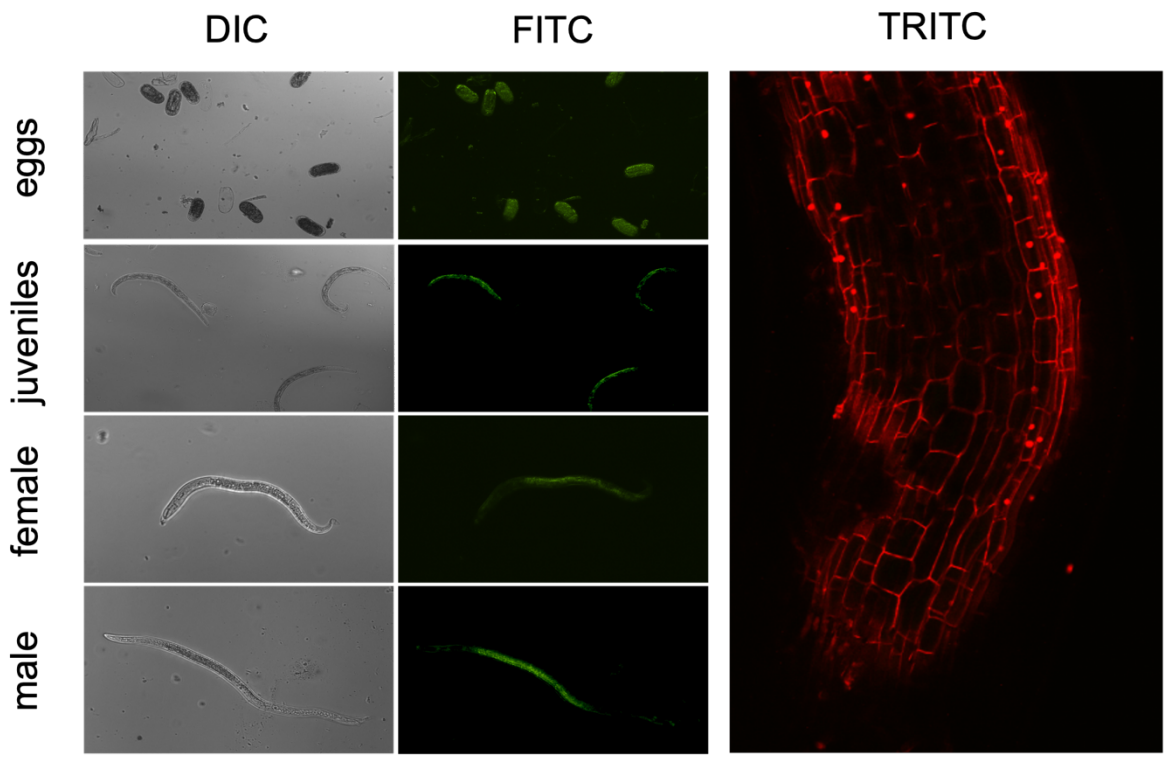

Figure 4.1. *R. reniformis* emits autofluorescence.

The laser scanning confocal microscopy images of (***A***) autofluorescence signals in the different growth stages of *R. reniformis*, and (***B***) LPNREN-1 roots stained with 1 mg/L PI solution. To validate if autofluorescence is an intrinsic feature of *R. reniformis*, both male and female nematodes spanning different developmental stages from eggs to maturity were subjected to extensive washing processes before the imaging. The persistence of green autofluorescence indicates that this trait was inherent to *R. reniformis* themselves rather than being a byproduct of the surrounding soil. DIC, bright field; FTIC, fluorescein isothiocyanate at 488-nm; TRITC, tetramethylrhodamine isothiocyanate at 561.5-nm.c

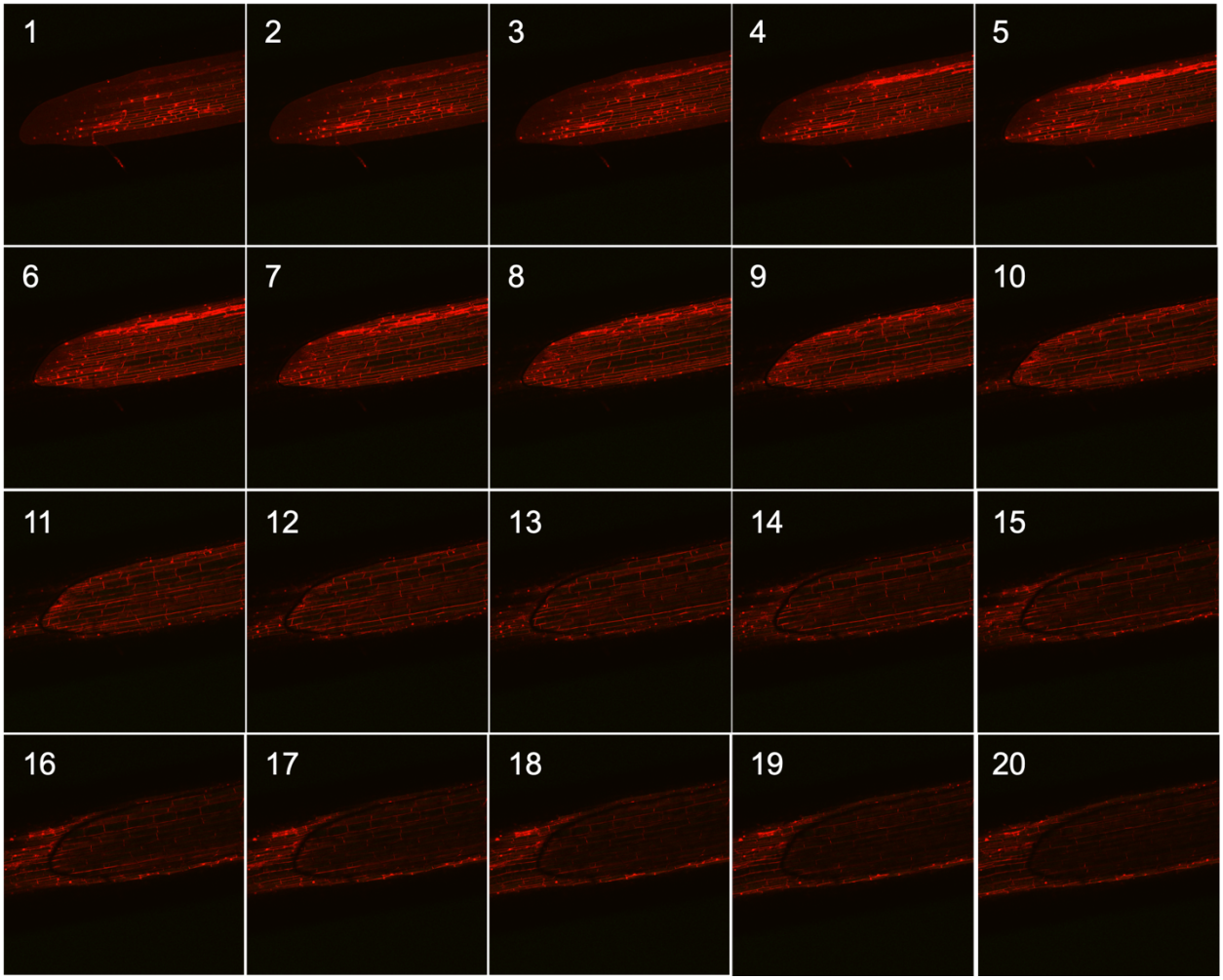

Figure 4.2. A typical stack of optical sections (often termed a z-series) through LONREN-1 root using 562-nm (red fluorescence) laser system.

An arrow indicates *R. reniformis* progressing root infections.

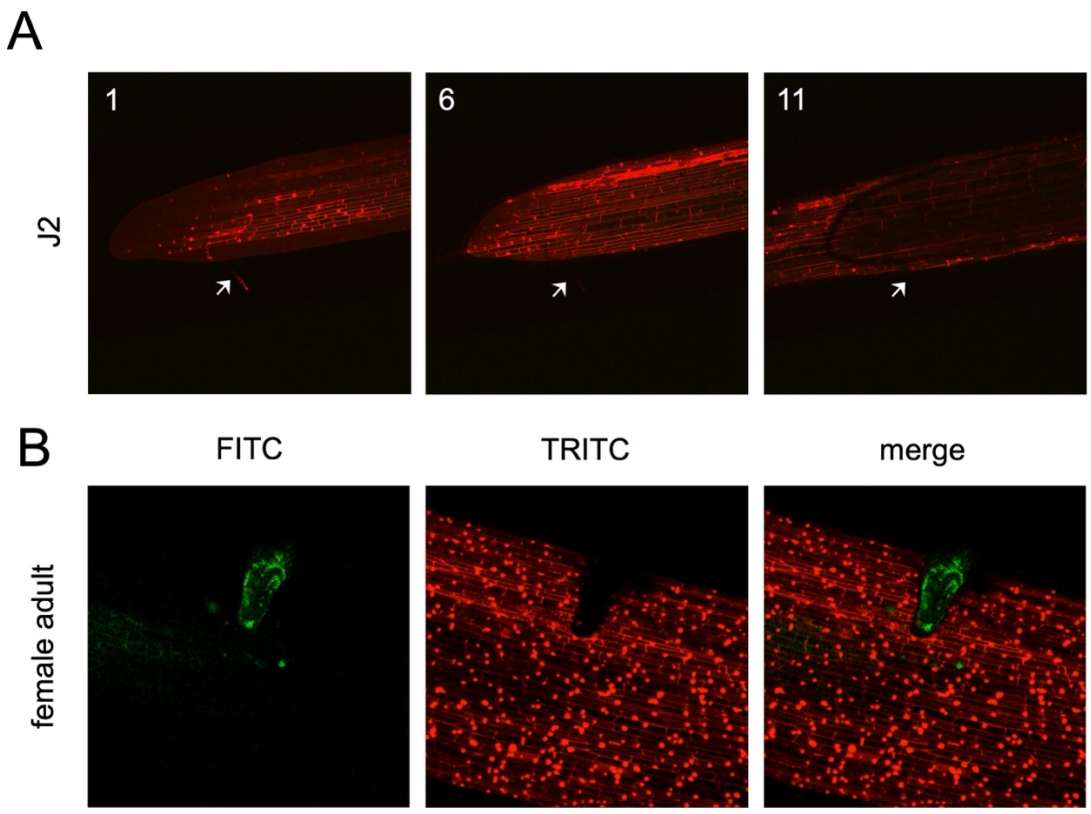

Figure 4.3. *R. reniformis* infections do not trigger PCD/HR in LONREN-1 roots.
Laser scanning confocal microscopy images of the infection progress by (***A***) J1 and (***B***) female adult stage *R. reniformis* PPN through LONREN-1 roots. For (***A***), the exemplary stack (#1, 6, and 11 from **Fig 4.2**) of optical sections through *R. reniformis*-infected LONREN-1 roots under TRITC. An arrow indicates *R. reniformis* progressing root infections. For (***A*** and ***B***) FTIC, green fluorescein isothiocyanate at 488 nm; TRITC, red tetramethylrhodamine isothiocyanate at 561.5 nm.

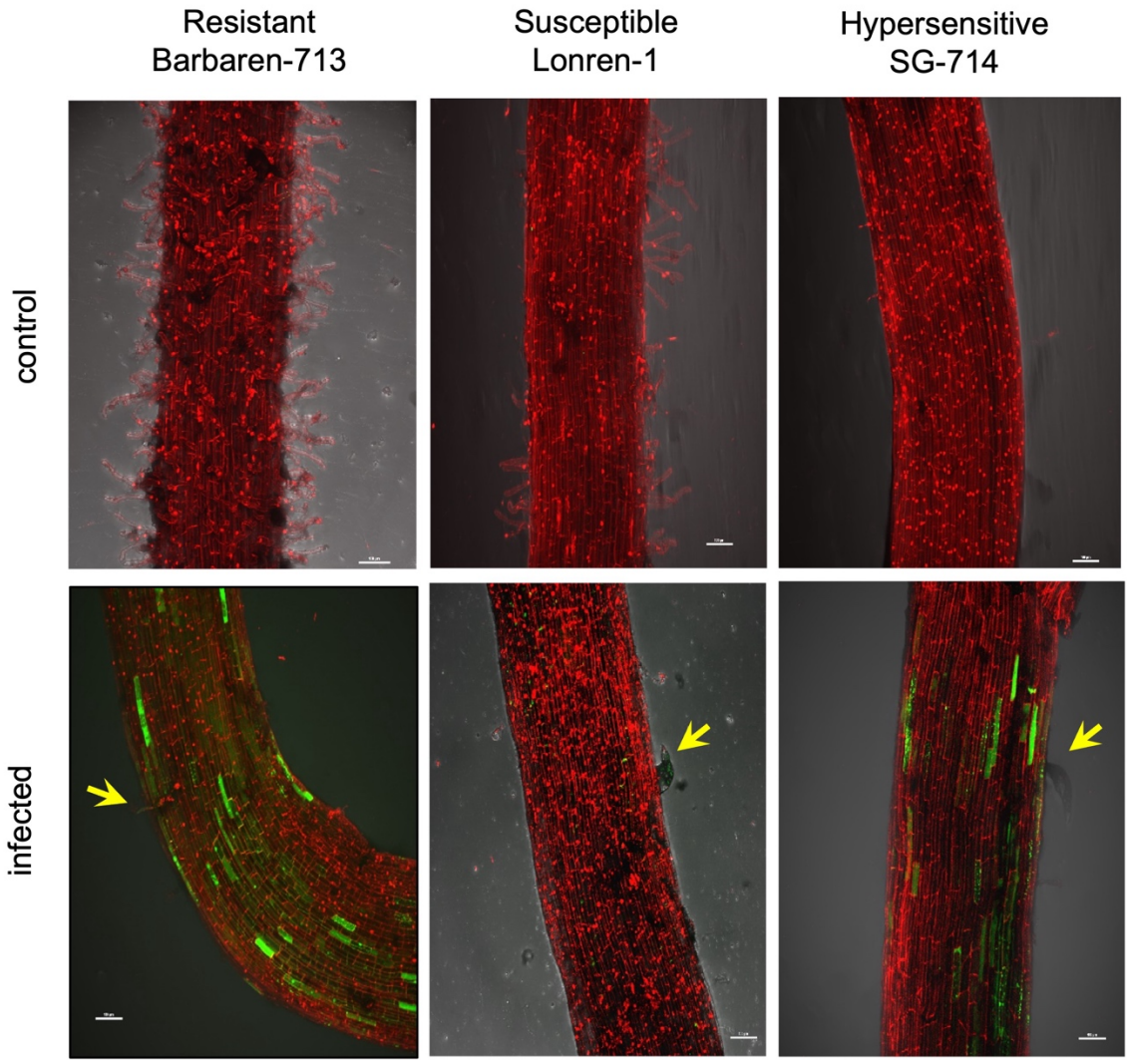

Figure 4.4. *R. reniformis* infections trigger H2O2 bursts in BARBREN-713 and SG747, but not LONREN-1, in a random pattern.

Root tissues were visualized under confocal microscopy after staining with PI (red) and H_2DCFDA (green). Yellow arrows indicate root-infected *R. reniformis*.

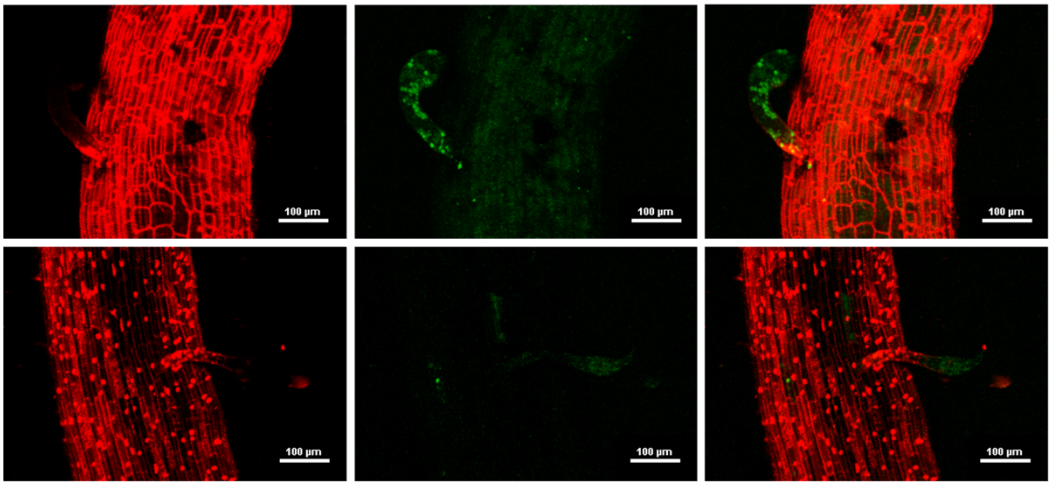

Figure 4.5. Real-time interactions between cotton roots and *R. reniformis*.
Roots of Barbaren-713 (top) and SG-714 (bottom) infected with *R. reniformis* were subjected to a scanning confocal microscopy after staining with a PI solution (red). TRITC at 561.5 nm; FTIC at 488 nm.

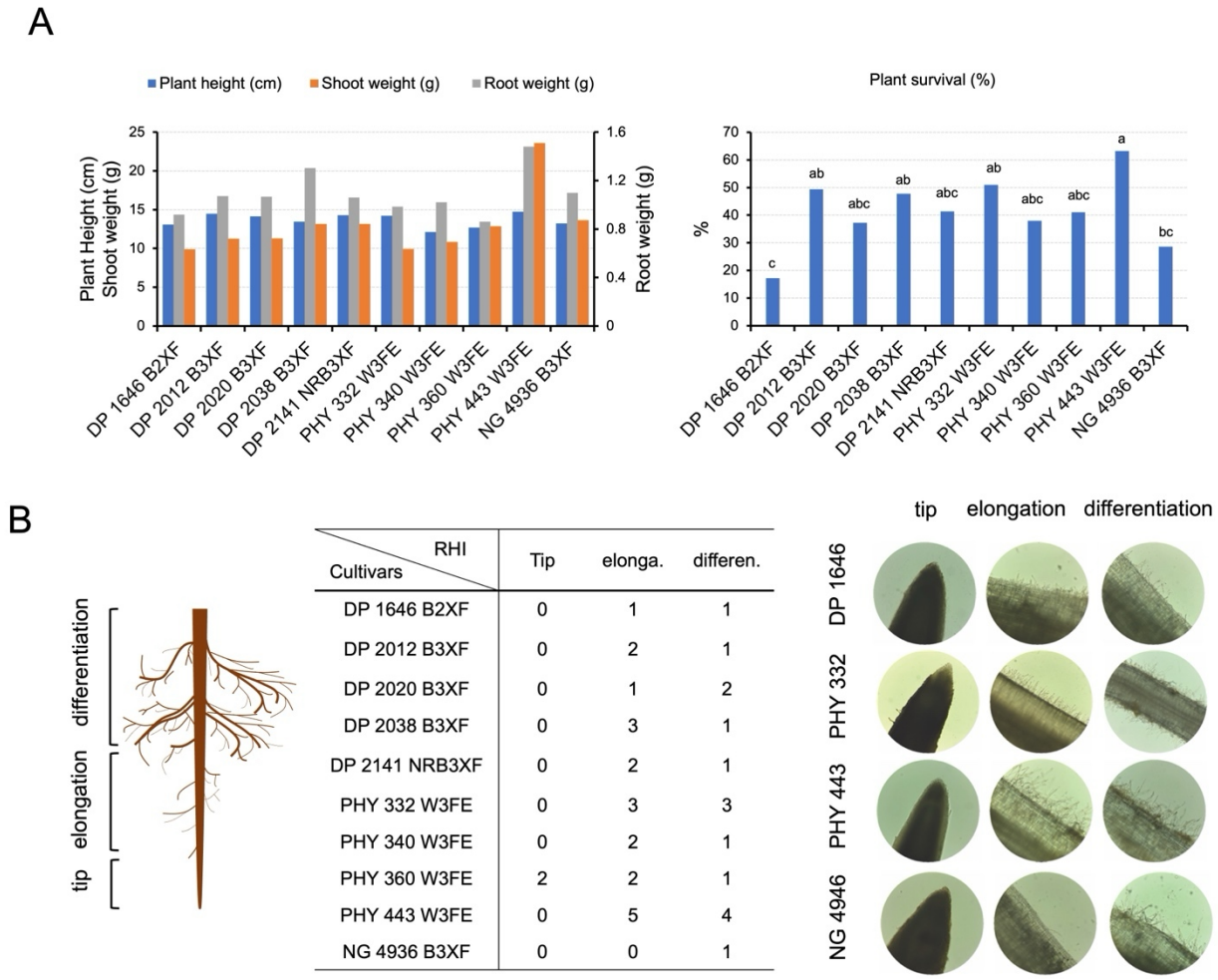

Figure 4.6. Root hair growth and development facilitate cotton defense responses against *R. reniformis* infections.

(***A***) Measurement of plant growth parameters- Plant height, shoot and root fresh weight (left), and survival rates (right) against *R. reniformis* infections. Ten commercial cotton varieties (n = 5) were grown in *R. reniformis*-infested soils in a randomized complete block design and harvested at 40 days for the measurement. Different letters indicate statistically significant differences between cultivars (Tukey–Kramer HSD test on all pairs; α = 0.05). (***B***) Root hair growth of ten cotton commercial varieties was quantified over three different sections (i.e., tip, elongation, and differentiation regions; see left schematic) 40 days after planting and expressed as the Root Hair Index (RHI), ranked on the scale of 0-5, with 0 = no root hair and 5 = maximum root hair. Representative pictures

of root hairs with relatively high RHI (PHY 443) and comparatively low RHI (DP 1646 and NG 4936).

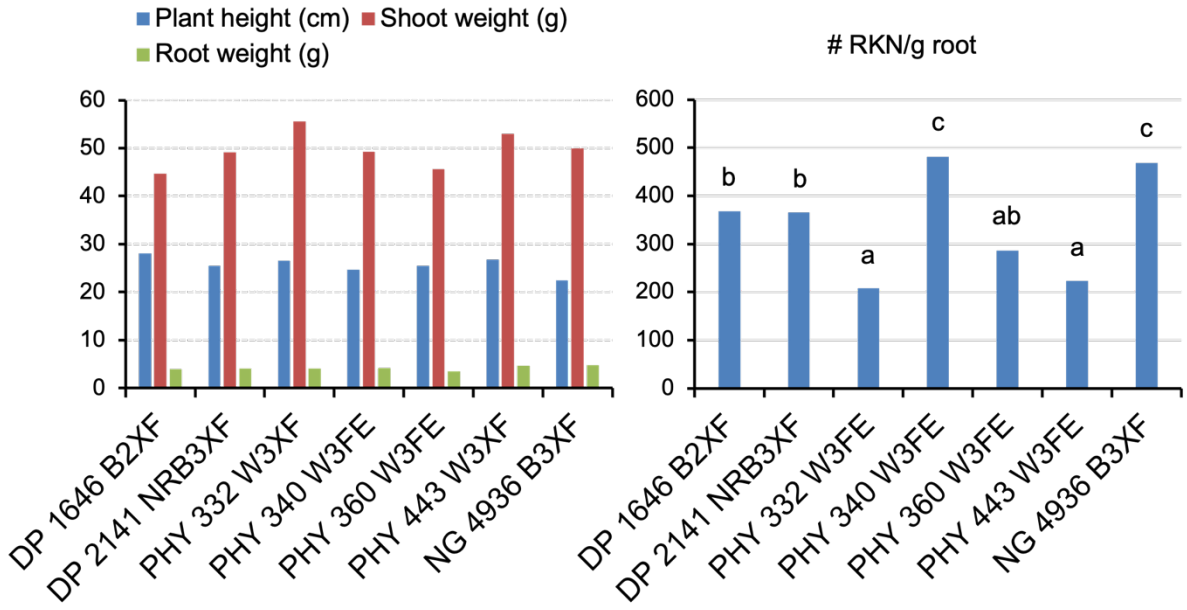

Figure 4.7. Measurement of plant growth parameters (left) and the number of M. incognita grown in cotton roots (right).

Seven commercial cotton varieties were grown on *M. incognita*-infested soils in a randomized complete block design and harvested at 40 days for the measurement. Different letters and asterisks indicate statistically significant differences between cultivars (Tukey–Kramer honestly significant difference test on all pairs; $\alpha = 0.05$).

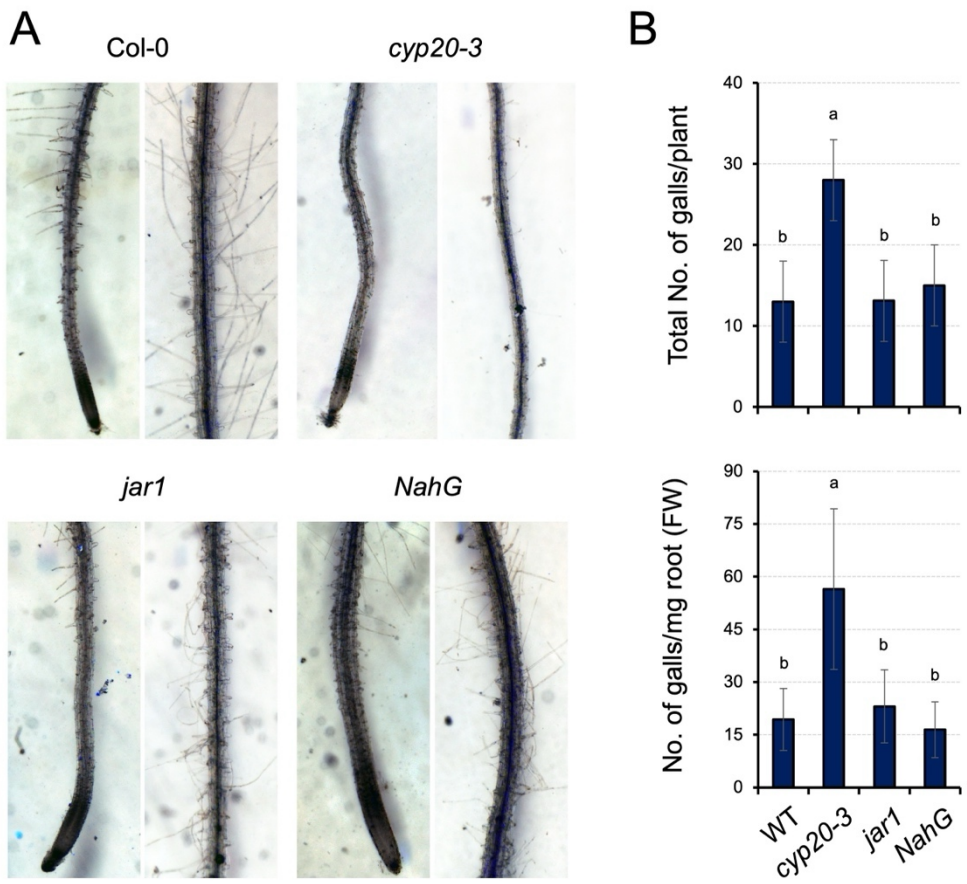

Figure 4.8. OPDA signaling mutant *cyp20-3* impedes root hair development and shows enhanced susceptibility to *M. halpa.*

(***A***) Representative pictures of root hairs of WT (Col-0), T-DNA insertion KO Arabidopsis mutants *cyp20-3* and *jar1*, and *NahG* transgenic Arabidopsis plants. (***B***) 2-wk-old seedlings grown on MS media were subjected to inoculation with 120 *M. hapla* J2 nematodes per plant, and the number of galls and number of galls per milligram of fresh weight of 10 biological replicates of each mutant plant was assessed at 15 dpi. The extent of gall formation in each mutant was compared to that in the Col-0 control group. Different letters within each category denote significant differences between the treatments, as determined by Tukey's HSD test with a significance level of $\alpha = 0.05$.

Figure 4.9. Aerial phenotypes of Arabidopsis WT Col-0, mutant (cyp20-3 and jar1), and transgenic (NahG) plants.

They display little, if any, difference in growth and development. A representative picture was taken at 3-wk post germinations.

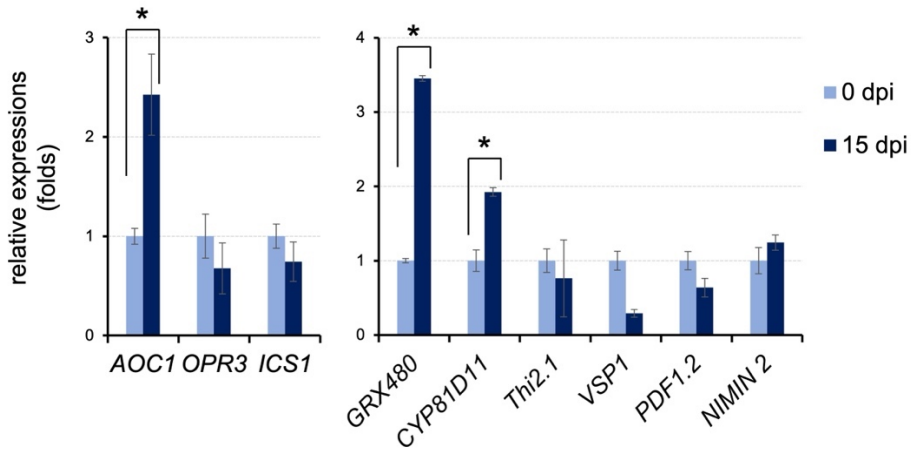

Figure 4.10. Nematode infection induces OPDA biosynthesis and signaling

qRT-PCR analyses of jasmonate (*AOC1*), JA *(OPR3*) and SA (*ICS1*) biosynthesis genes (**Left**), as well as OPDA responsive (*CYP81D11* and *GRX480*), JA (*Thi2.1, VSP1* and *PDF1.2*) and SA (*NIMIN2*)-responsive genes (**Right**). The WT Col-0 Arabidopsis, grown under a 12-h day cycle in MS media, was inoculated with 120 *M. hapla* J2 per plant. Root samples were then collected at 15 d post inoculations (dpi), and total mRNAs were extracted. Values were normalized to the expression of *POLYUBIQUITIN* (mean ± SD; *n*=3).

Table 4.1. Root hair growth survey of various soybean cultivars.

Responses to *R. reniformis*	**Cultivars**	**RHI**		
		Tip	**Elongation**	**Differentiation**
Tolerance	Forrest	1	5	5
Resistance	Peking	2	2	5
Resistance	Cloud	1	3	4
Resistance	PI 88788	1	2	4
Moderate	Hartwig	1	3	3
Moderate	PI 89772	0	2	3
Moderate	PI 209332	0	2	2
Moderate	PI 90763	2	2	2
Susceptible	Williams82	1	1	3

Table 4.2. Evaluations of root architecture as measured by total root length, root projected and surface areas, average root diameter, and total numbers of tips, forks, and crossings.

Genotype	Length cm	Projected Area cm^2	Surface Area cm^2	Average ø mm	Root Volume cm^3	Tips	Forks	Crossings
Col-0	15.14	0.198	0.622	0.128	0.002	84	53.8	13.2
cyp20-3	9.19*	0.126	0.364	0.123	0.001	66	32.1	4.4
jar1	13.66	0.171	0.545	0.126	0.002	78	48.4	10.8
NahG	12.19	0.169	0.502	0.124	0.002	73	41.7	6.2

Asterisks (*) indicate statistically significant differences.

Table 4.3. Oligonucleotides used for RT-PCR.

Name	Direction	Sequence, 5' to 3'
GRX480 At1g28480	Forward	TGA TTG TGA TTG GAC GGA GA
	Reverse	TAA ACC GCC GGT AAC TTC AC
CYP18D11 At3g28740	Forward	TCT CAA CAT G^GG TTT GTG AA
	Reverse	AAG TAT C^AT AAC AAG TAT GA
Thi2.1 At1g72260	Forward	CT^C AGC TGA TGC TAC CAA TGA GC
	Reverse	GCT CCA TTC ACA ATT TCA CTT GC
VSP1 At5g24780	Forward	GGA CTT GCC CTA AAG AAC GA
	Reverse	GTG TTC TCG GTC CCA TAT CC
PDF1.2 At5g44420	Forward	GCT GCT TTC G^AC GCA CCG GC
	Reverse	TTA ACA TGG GAC GTA ACA GAT AC
OPR3 At2g06050	Forward	CAC ATG ACG GCG GCA CAA GG
	Reverse	TCA GAG GCG GGA AAA AGG A
ICS1 *At1g74710*	Forward	GAA CTC AAA TCT CAA CCT CC
	Reverse	ACT GCG ACG AGA GAA GAA AC
NIMIN2 At3g25882	Forward	AAC AAC TCT TTG AAG AAA G
	Reverse	CTC CGT AAT ATC TTG AAA AAC
UBC At5g25760	Forward	CTG CGA CTC AG^G GAA TCT TCT AA
	Reverse	TTG TGC CAT TGA ATT GAA CCC

^ Position of an exon-exon junction